Universidade Federal do Rio Grande do Sul

Centro de Biotecnologia

Programa de Pós-Graduação em Biologia Celular e Molecular

Dissertação de Mestrado

Desenvolvimento e caracterização de duas linhagens celulares de adenocarcinoma de pulmão com níveis clinicamente relevantes de resistência à cisplatina

Carolina Lumertz Martello

Porto Alegre, janeiro de 2018

Universidade Federal do Rio Grande do Sul

Centro de Biotecnologia

Programa de Pós-Graduação em Biologia Celular e Molecular

Desenvolvimento e caracterização de duas linhagens celulares de adenocarcinoma de pulmão com níveis clinicamente relevantes de resistência à cisplatina

Dissertação submetida ao Programa de Pós-Graduação em Biologia Celular e Molecular do Centro de Biotecnologia da UFRGS como requisito parcial para a obtenção do título de Mestre.

Carolina Lumertz Martello

Profa. Dra. Karina Mariante Monteiro – Orientador

Porto Alegre, janeiro de 2018

Este trabalho foi desenvolvido no Laboratório de Genômica Estrutural e Funcional do Centro de Biotecnologia da Universidade Federal do Rio Grande do Sul (CBiot/UFRGS), e contou com o apoio financeiro do Conselho Nacional de Desenvolvimento Científico e Tecnológico (CNPq) e da Fundação de Amparo à Pesquisa do Estado do Rio Grande do Sul (FAPERGS).

Tu verdad, no: la Verdad.

Y ven conmigo a buscarla.

La tuya, guárdatela.

- Antonio Machado,

Proverbios y cantares.

ÍNDICE

ABREVIATURAS, SÍMBOLOS E UNIDADES

A549: linhagem celular imortalizada de adenocarcinoma de pulmão humano

A549/CDDP: linhagem celular de adecarcinoma de pulmão humano com resistência adquirida à cisplatina

A549/CDDP$_{CT}$: linhagem celular de adenocarcinoma de pulmão humano com resistência adquirida à cisplatina mimetizando o tratamento clínico

EMT: transição epitélio-mesenquimal (de *epithelial–mesenchymal transition*)

ER: retículo endoplasmático (de *endoplasmic reticulum*)

FASP: preparação de amostra de auxiliada por filtro (de *filter-aided sample preparation*)

GI$_{50}$: concentração necessária para inibir 50% do crescimento celular

GO: ontologia (de *gene ontology*)

GTP: guanosina trifosfato

h: hora

INCA: Instituto Nacional do Câncer

kDa: kilodalton(s)

min: minuto(s)

ml: mililitro(s)

mM: milimolar

MMR: reparo de pareamentos errados de DNA (de *DNA mismatch repair*)

NER: reparo por excisão de nucleotídeos do DNA (de *DNA nucleotide excision repair*)

NSCLC: câncer de pulmão de células não pequenas (de *non-small cell lung cancer*)

ºC: grau Celsius

PBS: salina tamponada com fosfato (de *phosphate-buffered saline*).

PE: eficiência de plaqueamento (de *plating efficiency*)

pGL3: plasmídeo GL3

ROS: espécies reativas de oxigênio (de *reactive oxygen species*)

SCLC: câncer de pulmão de células pequenas (de *small cell lung cancer*)

SD: desvio padrão (de *standard deviation*)

SF: fração sobrevivente (de *surviving fraction*)

SRB: sulforodamina B

μM: micromolar

LISTA DE FIGURAS E TABELAS

1. INTRODUÇÃO

2. *Development and characterization of two A549 human lung cancer cell sublines with clinically relevant levels of cisplatin resistance*

2.1. Figuras

2.2. Tabelas

RESUMO

O câncer de pulmão é um dos principais responsáveis pelas mortes causadas por câncer no mundo, principalmente o câncer de pulmão de células não pequenas (NSCLC). A cisplatina é o quimioterápico mais comumente utilizado para tratamento de NSCLC. Contudo, a resistência à cisplatina e a consequente recorrência do tumor são obstáculos frequentes desse tratamento. Com o objetivo de investigar os mecanismos moleculares envolvidos na resistência à cisplatina em NSCLC, foram desenvolvidas duas sublinhagens a partir da linhagem humana de adenocarcinoma de pulmão A549 com níveis clinicamente relevantes de resistência à cisplatina, A549/$CDDP_{CT}$ e A549/CDDP. As duas sublinhagens foram analisadas comparativamente por análises celulares e proteômica. As células A549/CDDP apresentaram menor proliferação e maior capacidade de reparo a danos no DNA quando comparadas com as células A549 e A549/$CDDP_{CT}$. As análises de proteômica e ontologia das células resistentes à cisplatina revelaram o enriquecimento de proteínas relacionadas ao reparo de DNA, resposta ao estresse de retículo endoplasmático, regulação do processo apoptótico, dentre outros mecanismos potencialmente envolvidos na resistência à droga. A549/$CDDP_{CT}$ apresentou mudanças morfológicas já identificadas em células resistentes à cisplatina, perfil de proteínas ribossomais exclusivo, além de potencial evasão de danos do estresse oxidativo ocasionado pela cisplatina. A549/CDDP apresentou diversas proteínas enriquecidas relacionadas à organização do citoesqueleto, além de morfologia alongada (fibroblasto-*like*), sugestiva de uma possível transição epitélio-mesenquimal. Dessa forma, A549/$CDDP_{CT}$ e A549/CDDP apresentaram conjuntos únicos de mecanismos de resistência, mostrando-se valiosos modelos celulares clinicamente relevantes para futuros estudos dos mecanismos moleculares da resistência à cisplatina.

ABSTRACT

Lung cancer, a major responsible by cancer death in the world, have platinum-based chemotherapy as first-line therapy for patients with advanced non-small cell lung cancer (NSCLC), being cisplatin the most frequently used drug. However, cisplatin resistance and consequent tumor recurrence remain an obstacle to treatment. In order to investigate the molecular pathways involved with cisplatin resistance in NSCLC, we developed two human lung adenocarcinoma A549 sublines with clinically relevant levels, A549/$CDDP_{CT}$ and A549/CDDP. Both sublines were analyzing by cellular characterization and protein expression modulation. A549/CDDP cells presented lower proliferation and increased cisplatin DNA damage repair when compared to A549 and A549/$CDDP_{CT}$. Proteomic and gene ontology analyses provided evidences of DNA repair proteins, endoplasmatic reticulum stress response, apoptotic process response, as others mechanisms potentially related to cisplatin resistance. A549/$CDDP_{CT}$ presented morphological changes already observed in cisplatin resistant cells, exclusive ribosomal profile as well as potential oxidative stress evasion. A549/CDDP presented fibroblast-like morphology and enriched proteins related to cytoskeletal organization, as a possible epithelial-mesenchymal transition (EMT). Therefore, A549/$CDDP_{CT}$ and A549/CDDP presented two unique sets of resistance mechanisms, standing as valuable clinically relevant cellular models to further investigations of drug resistance molecular mechanisms.

1. INTRODUÇÃO

1.1. Câncer

Câncer é uma malignidade de distribuição mundial, afetando países desenvolvidos e subdesenvolvidos (TORRE et al., 2015). A crescente incidência de câncer e consequente falecimento dos pacientes se dá tanto pelo maior envelhecimento da população quanto pelos hábitos pouco saudáveis cada vez mais adotados. Dados globais de 2012 apontam 14,1 milhões de casos de câncer e 8,2 milhões de mortes derivadas da doença. Isso torna o câncer a segunda principal causa de morte no mundo, sendo doenças cardíacas a primeira causa. Entre essas ocorrências, o câncer de pulmão é um dos líderes de causa de morte por câncer no mundo.

1.1.1. Câncer de pulmão

O câncer de pulmão é classificado em duas categorias principais, o câncer de células pequenas e o de células não pequenas. Segundo dados da *American Cancer Society* (AMERICAN CANCER SOCIETY, https://www.cancer.org/content/dam/CRC/PDF/Public/8708.00.pdf), o câncer de pulmão de células pequenas representa 10 a 15% dos casos. O câncer de pulmão de células não pequenas representa 80 a 85% dos casos, sendo dividido em outras três subcategorias: adenocarcinoma, carcinoma de células escamosas e carcinoma de grandes células. O tumor de origem glandular é denominado adenocarcinoma e representa a grande parcela de 40% dos casos de câncer de pulmão.

A incidência de pacientes diagnosticados com câncer de pulmão representam 13% dos casos mundiais de câncer, apresentando uma estimativa de 1,8 milhões de casos em 2012 (TORRE et al., 2015). O câncer de pulmão é o segundo maior responsável por mortes causadas por câncer no mundo, sendo a primeira causa para homens e a segunda para mulheres (GLOBOCAN, http://globocan.iarc.fr) (Figura 1). No Brasil, dados do Instituto Nacional do Câncer (INCA) (INSTITUTO NACIONAL DO CÂNCER, (INCA, http://www2.inca.gov.br/wps/wcm/connect/tiposdecancer/site/home/pulmao/definicao) apontam o câncer de pulmão como o segundo mais prevalente em ambos os sexos, apenas atrás de câncer de mama para mulheres e câncer de próstata para homens, com 28 mil novos casos estimados em 2016. Óbitos por câncer de pulmão no Brasil acompanham a distribuição global, tendo dados do Sistema de Informação sobre

Mortalidade de 2013 apontado o câncer de pulmão como responsável por 24 mil mortes, sendo 14 mil de homens e 9 mil de mulheres.

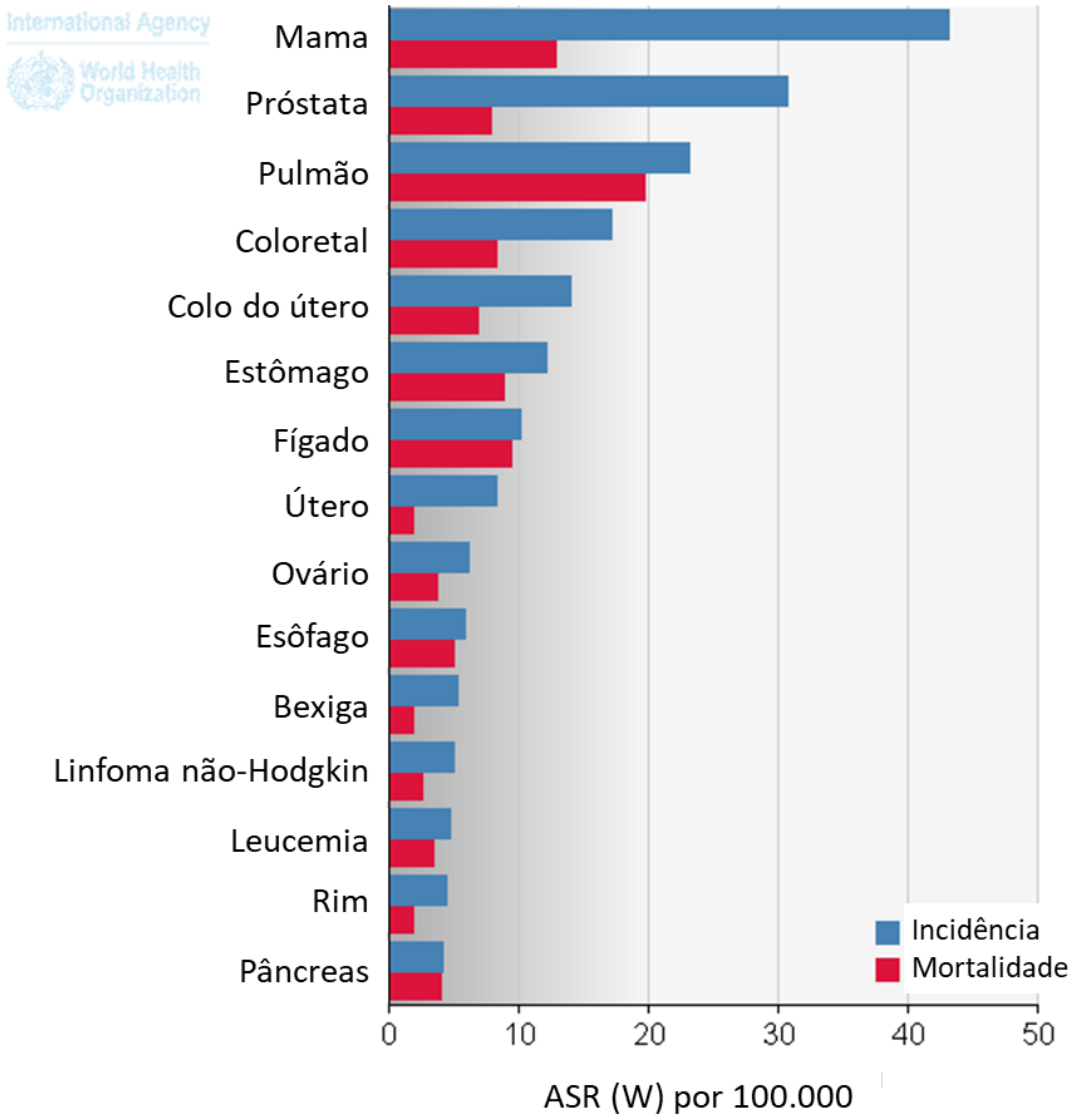

Figura 1: Incidência e mortalidade do câncer na população mundial. Adaptado de http://globocan.iarc.fr/Pages/fact_sheets_population.aspx (acesso em 18/12/2017).

A incidência de câncer de pulmão está diretamente relacionada ao tabagismo, sendo essa a principal causa desse tipo de câncer (TORRE et al., 2015). A distribuição de casos de câncer de pulmão segue a mesma distribuição da epidemia do tabaco de cada país. Países nos quais a epidemia do tabaco está em recessão apresentam uma queda da incidência de câncer de pulmão. Da mesma forma, países que estão no auge da epidemia tem expectativa de aumentar os casos de câncer de pulmão nas próximas

décadas. Além disso, a poluição do ar e o contato com substâncias carcinogênicas também são causas menos frequentes de câncer de pulmão.

Fica evidente, portanto, que a prevenção contra o tabagismo se mostra a forma mais eficiente de prevenir o desenvolvimento de câncer de pulmão. A prevenção pode ser realizada por campanhas para evitar o início do tabagismo e aumentar a desistência do hábito entre fumantes. No Brasil, o Ministério da Saúde por meio do INCA desenvolve uma campanha antitabagista desde 1980. Iniciativas como aumento do valor do produto, implementação de contrapropaganda e proibição de tabagismo em áreas fechadas são formas de prevenir o hábito. Essas iniciativas levaram a uma redução de 30% no número de fumantes nos últimos 9 anos, segundo levantamento do Sistema Único de Saúde (SISTEMA ÚNICO DE SAÚDE, http://portalarquivos2.saude.gov.br/images/pdf/2015/maio/28/apresentacao-tabaco.pdf). Campanhas nacionais como estas são de extrema importância para o combate ao desenvolvimento do câncer de pulmão, levando a uma redução da incidência e consequente diminuição de óbitos por câncer.

O diagnóstico do câncer de pulmão é realizado através de raios-X do tórax seguido de tomografia computadorizada. Contudo, o diagnóstico se torna difícil por poder se desenvolver em qualquer região do pulmão, apresentar múltiplos aspectos clínicos e patológicos e não possuir sintomas definidos. Dessa forma, o diagnóstico muitas vezes é confirmado em estágios avançados do câncer, quando os sintomas ficam mais evidentes (DESANTIS et al., 2014). Um estudo realizado pelo *The National Lung Screening Trial Research Team* demonstrou que a tomografia computadorizada de baixa dosagem poderia reverter essa situação pela detecção de câncer de pulmão em estágios iniciais (THE NATIONAL LUNG SCREENING TRIAL RESEARCH TEAM, 2011). Contudo, esse estudo apresentou uma alta incidência de resultados falsos positivos. Dessa forma, o diagnóstico precoce de câncer de pulmão continua a ser um empecilho para a correta detecção e início do tratamento contra o câncer.

O tratamento para pacientes com câncer de pulmão varia de acordo com o tipo e o estágio do tumor. De acordo com a *American Cancer Society* (AMERICAN CANCER SOCIETY, https://www.cancer.org/cancer/non-small-cell-lung-cancer/treating.html), os tratamentos incluem cirurgia, radioterapia, quimioterapia, ablação por radiofrequência, terapia alvo oncológica e imunoterapia, não sendo

incomum a combinação de mais de um tipo de tratamento no combate ao câncer. Pacientes com câncer de pulmão de células pequenas normalmente são tratados com quimioterapia ou radioterapia (DESANTIS et al., 2014). Pacientes com câncer de pulmão de células não pequenas recebem tratamentos específicos, de acordo com o estágio em que se encontra o tumor. Aqueles com diagnóstico de tumores em estágios iniciais normalmente são submetidos à cirurgia e uma parcela desses recebe quimio ou radioterapia após a cirurgia. Contudo, pacientes com diagnóstico de câncer de pulmão avançado costumam ser tratados com quimioterapia, radioterapia ou a combinação dos dois. As drogas quimioterápicas mais comuns para o tratamento do câncer de pulmão de células não pequenas são a carboplatina e a cisplatina.

1.2. O uso da cisplatina no tratamento do câncer

A cisplatina foi sintetizada pela primeira vez por Michel Peyrone em 1845, tendo sua estrutura identificada em 1893 por Alfred Werner. Contudo, foi apenas na década de 1960 que a cisplatina começou a ser investigada como potencial quimioterápico (ROSENBERG et al., 1969). Compostos inorgânicos de platina, incluindo cisplatina, inibiam a mitose ou interferiam nos cromossomos das células que mantinham a divisão. A comprovação da cisplatina como quimioterápico após testes clínicos levou a sua liberação para comercialização em 1977. Atualmente, a cisplatina é uma droga amplamente utilizada contra diversos tipos de câncer e costuma ser a linha de tratamento inicial e mais efetiva.

Desde então, a cisplatina tem sido amplamente utilizada como tratamento para uma ampla variedade de tipos de câncer, como câncer de cabeça e pescoço, de mama, de cérebro e de pulmão (DASARI; TCHOUNWOU, 2014). A administração da droga se dá principalmente por infusão intravenosa, com doses específicas para cada tipo de câncer, normalmente em um intervalo de 3 a 4 semanas (THE INTERNATIONAL ADJUVANT LUNG CANCER TRIAL COLLABORATIVE GROUP, 2004). A platina se espalha pelo corpo, se concentrando principalmente no fígado, próstata e rins, seguindo em menores doses para a bexiga, os músculos, os testículos e o pâncreas, baixas concentrações atingem o intestino, as glândulas adrenais, o coração, o pulmão e o cérebro (STEWART et al., 1982).

Em nível molecular, a cisplatina é composta por um átomo de platina ligado a dois átomos de cloro e duas moléculas de amônia (Figura 2) (DASARI;

TCHOUNWOU, 2014). Em contato com a água, a cisplatina assume a sua forma tóxica, perdendo seus átomos de cloro e se tornado positivamente carregada (SIDDIK, 2003). Em sua forma ativa, a cisplatina se liga as bases nucleotídicas do DNA, criando adutos intra- e inter-cadeias (Figura 3). Essa interferência no DNA desencadeia uma inibição da replicação, transcrição e divisão celular, podendo levar a apoptose.

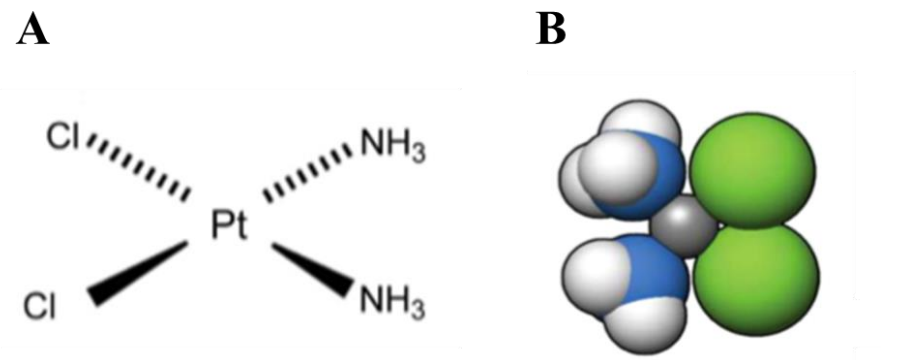

Figura 2: Estrutura da cisplatina. Estrutura química (A) e molecular computacional (B) da cisplatina. Adaptado de Dasari & Tchounwou (2014).

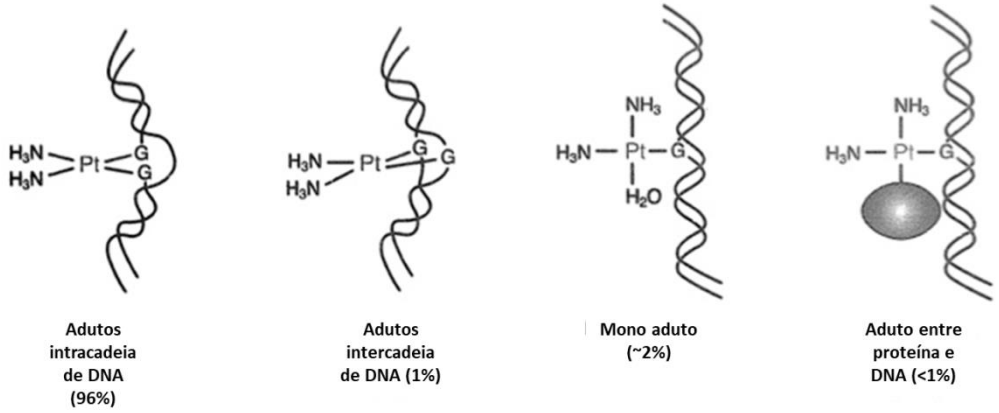

Figura 3: Interações da cisplatina com o DNA. Possíveis interações da cisplatina com o DNA e a frequência com que ocorrem. Adaptado de http://www.conconilab.ca/wp-content/uploads/2013/05/image-cisplatin-3.jpg (acesso em 18/10/2017).

Após a exposição das células à cisplatina e consequente interação da droga com o DNA, diversas vias de sinalização podem ser desencadeadas como resposta ao dano. A pausa da célula nos pontos de checagem do ciclo celular pode ser desencadeada normalmente para tentativa de reparo do DNA, mas caso a extensão dos danos seja

muito grave a célula ativa as vias de apoptose, levando a morte celular (SIDDIK, 2003). A ativação da apoptose se dá por intermédio da proteína supressora de tumor p53, que por sua vez é ativada por proteínas quinases, sendo todo o processo uma resposta aos danos que a cisplatina causa ao DNA. Além disso, a cisplatina pode levar a morte celular por aumentar o estresse oxidativo ou desregular a homeostase do cálcio (DASARI; TCHOUNWOU, 2014).

Contudo, a resistência das células tumorais à cisplatina se apresenta como um efeito recorrente no tratamento contra diversos tipos de câncer (DASARI; TCHOUNWOU, 2014). A resistência pode ser intrínseca, quando o paciente já apresenta resistência e o tratamento inicial não será efetivo nessas células (KÖBERLE et al., 2010). Ou a resistência pode ser adquirida, por exposição à droga ao longo do tratamento, resultando na diminuição da sua eficiência. A resistência à cisplatina, por ser um problema grave no tratamento de diversos tipos de câncer, tem sido amplamente estudada e foi descrita como tendo aspecto multifatorial. Os mecanismos moleculares que caracterizam a resistência à cisplatina incluem diminuição no influxo da droga para o meio intracelular, aumento no efluxo da droga para fora da célula, diminuição da toxicidade da cisplatina por conjugação a moléculas contendo tiol, aumento no reparo ao dano no DNA causado pela cisplatina e mudanças nas vias de sinalização para evitar apoptose ou outros tipos de morte celular (SIDDIK, 2003). Esses mecanismos podem atuar sozinhos ou combinados para caracterizar resistência do tumor à cisplatina, evitando a apoptose e permitindo a contínua proliferação do tumor.

1.3. Mecanismos de resistência tumoral à cisplatina

1.3.1. Influxo/efluxo de cisplatina

A diminuição da concentração intracelular de cisplatina é um dos fatores que levam à resistência e pode ser observado em linhagens celulares resistentes à cisplatina (BARR et al., 2013; OISO et al., 2014). Essa diferença pode ser causada tanto pela menor absorção da droga pela célula como pela maior remoção da droga de dentro da célula. A cisplatina pode entrar na célula por transporte passivo ou por meio de transportadores, como os transportadores de homeostase de cobre CTR1, CTR2 (KILARI, 2016). Assim como ser removida do meio intracelular através da ação de transportadores como ATOX1, ATP7A e ATP7B. O aumento da expressão do

transportador ATP7B, por exemplo, já foi correlacionado com resistência à cisplatina em câncer de pulmão de células não pequenas (NAKAGAWA et al., 1994).

1.3.2. Detoxificação

A cisplatina no plasma sanguíneo se apresenta principalmente em sua forma inativa, por estar presente em um ambiente com alta concentração de cloretos (NEJDL et al., 2015). Contudo, dentro da célula essa concentração diminui, fazendo com que a molécula de cisplatina dissocie seus íons de cloro, que são substituídos por moléculas de água. Nessa forma, a cisplatina é reativa e, caso chegue ao núcleo, irá interagir com o DNA. Um dos mecanismos de resistência celular à cisplatina é a diminuição da sua citotoxicidade pela interação com moléculas contendo grupos tiol no citoplasma. A cisplatina tem alta afinidade e pode interagir com glutationa (DABROWIAK; GOODISMAN; SOUID, 2002) e metalotioneína (HAGRMAN, 2003), diminuindo sua concentração reativa e citotóxica intracelularmente.

1.3.3. Reparo a danos no DNA

A citotoxicidade da cisplatina se dá por meio da formação de adutos com o DNA, os quais desencadeiam uma série de vias de sinalização que culminam na morte celular. Contudo, o reparo ao dano causado pela cisplatina no DNA pode ser reparado, evitando a perpetuação do sinal e criando resistência ao efeito causado pela cisplatina. O reparo por excisão de nucleotídeos é o principal responsável pela remoção do dano causado pela cisplatina, pois repara as interações que causam mudanças na estrutura do DNA e consequente inibição da transcrição e replicação (MARTIN; HAMILTON; SCHILDER, 2008; XIONG; HUANG; YIN, 2017). O reparo de erro de pareamento também é um dos mecanismos que pode ser utilizado para o desenvolvimento de resistência, no qual o pareamento incorreto da base nucleotídica com a molécula de cisplatina é reconhecido e corrigido. O reparo de quebra de fita dupla atua em um estado de dano ao DNA mais avançado, o qual pode ser realizado pela recombinação homóloga ou não homóloga das fitas do DNA. Dessa forma, qualquer reconhecimento de dano ao DNA pode desencadear o recrutamento de uma gama de proteínas que podem reverter o dano causado pela cisplatina, caracterizando resistência à droga.

1.3.4. Sinalização da apoptose

O mecanismo final de resistência à cisplatina é a inibição da via de sinalização da apoptose em si, independente do dano causado ao DNA. A proteína supressora de tumor p53 tem papel importante na via apoptótica. A supressão dessa proteína causa diminuição da expressão de diversos genes pró-apoptóticos, resultando em um caráter resistente à cisplatina em câncer de pulmão de células não pequenas (FENG et al., 2017). A cisplatina desencadeia uma resposta por meio proteíno-quinases ativadas por mitógenos (MAPKs), como a proteína quinase c-Jun N-terminal ativada por estresse (SAPK/JNK) e p38 quinases (KÖBERLE et al., 2010). Essas vias podem ser ativadas por diversas outras proteínas, que podem ter como resultado final a inibição da apoptose e consequente resistência à cisplatina (BROZOVIC et al., 2004; BROZOVIC; OSMAK, 2007; QI et al., 2016).

1.4. Modelos celulares para o estudo da resistência à cisplatina

A resistência tumoral à cisplatina é um problema clínico que vem sendo amplamente estudado, tanto *in vivo* (ZHANG et al., 2017) quanto *in vitro* (QI et al., 2016). Diversas linhagens celulares resistentes à cisplatina já foram desenvolvidas com o intuito do melhor entendimento das vias pelas quais a resistência se estabelece (BARR et al., 2013; GUO et al., 2013; HARVEY et al., 2015).

Contudo, a maioria dos estudos utiliza longos tempos de exposição das células a altas doses de cisplatina para desenvolvimento da resistência celular. Linhagens celulares que passam por esse tratamento adquirem altos níveis de resistência à droga, na ordem de 30 vezes maiores do que aqueles apresentados pela linhagem parental (MCDERMOTT et al., 2014). Esses são os chamados modelos de laboratório de alto nível de resistência, os quais são comumente utilizados por serem mais estáveis e suportarem melhor o cultivo prolongado e diversos ciclos de congelamento/descongelamento, necessários para o desenvolvimento de um estudo científico. Apesar disso, os modelos celulares com altos níveis de resistência têm gerado resultados de aplicação clínica limitada (GILLET et al., 2011).

Linhagens celulares clinicamente relevantes, por outro lado, são aquelas que apresentam uma resistência mais moderada à cisplatina, mimetizando os níveis de resistência observados em células tumorais isoladas de pacientes antes e após o

tratamento com o quimioterápico (MCDERMOTT et al., 2014). Os níveis de resistência à cisplatina adquirida pelos pacientes após tratamento é na ordem de 2 a 5 vezes maior do que aquele do tumor sem resistência. Esse tipo de modelo pode ser desenvolvido a partir da utilização de menores concentrações da droga, como, por exemplo, a concentração plasmática encontrada em pacientes em tratamento (PUJOL et al., 1990), e pela utilização de protocolos que mimetizam o tratamento clínico, com ciclos de exposição ao quimioterápico seguido de períodos de recuperação em meio livre da droga (MCDERMOTT et al., 2014). As linhagens celulares resultantes normalmente apresentam resistência instável e baixos níveis de resistência, apresentando resultados mais tênues. Contudo, esses resultados tendem a ser mais aplicáveis à situação clínica.

1.5. Justificativas

O câncer de pulmão tem alta incidência mundial e é o segundo responsável por mortes por câncer no mundo, sendo a cisplatina o quimioterápico mais utilizado no tratamento. Contudo, a resistência à cisplatina se mantém como um obstáculo recorrente ao tratamento de pacientes com câncer de pulmão em estágio avançado. Apesar dos mecanismos moleculares de resistência a essa droga serem bem conhecidos, nenhuma alternativa efetiva para o problema foi desenvolvida. Linhagens celulares com altos níveis de resistência à cisplatina, comumente utilizadas para estudos nessa área, falham em ter seus resultados extrapolados para a pesquisa clínica. Desta forma, linhagens celulares clinicamente relevantes surgem como ferramentas de estudo alternativas e mais adequadas para entendimento dos mecanismos de resistência a quimioterápicos. O desenvolvimento de linhagens celulares resistentes à cisplatina utilizando baixas doses da droga e ciclos de exposição intervalados por cultivo sem cisplatina mimetizam melhor o tratamento clínico ministrado em pacientes. Sendo assim, este trabalho tem como objetivo desenvolver linhagens celulares de adenocarcinoma de pulmão clinicamente relevantes para o estudo da resistência à cisplatina. As linhagens celulares desenvolvidas foram caracterizadas em nível celular e proteômico e os mecanismos moleculares potencialmente envolvidos no desenvolvimento de resistência em cada uma delas foram avaliados e discutidos.

2. Objetivos

2.1. Objetivo geral

Desenvolvimento de linhagens celulares resistentes à cisplatina a partir da linhagem parental de adenocarcinoma de pulmão A549 e caracterização de seus mecanismos moleculares de resistência.

2.2. Objetivos específicos

2.2.1. Desenvolvimento de uma linhagem celular com resistência adquirida à cisplatina a partir da linhagem parental de adenocarcinoma de pulmão A549 utilizando exposição contínua à doses crescentes de cisplatina.

2.2.2. Desenvolvimento de uma linhagem celular com resistência adquirida à cisplatina mimetizando o tratamento clínico de pacientes com câncer de pulmão a partir da linhagem parental de adenocarcinoma de pulmão A549.

2.2.3. Avaliação e comparação da citotoxicidade da cisplatina, capacidade clonogênica, proliferação, capacidade de reparo ao DNA e distribuição do ciclo celular entre as linhagens celulares sensível e resistentes à cisplatina.

2.2.4. Avaliação e comparação dos perfis proteômicos das linhagens celulares sensível e resistentes à cisplatina.

3. Capítulo I - *Development and characterization of two A549 human lung cancer cell sublines with clinically relevant levels of cisplatin resistance*

O texto referente aos materiais e métodos e resultados está apresentado na forma de um manuscrito a ser submetido à revista científica *Experimental Cell Research* (https://www.journals.elsevier.com/experimental-cell-research). Os experimentos foram planejados por CLM, HBF, AZ e KMM. Os experimentos foram realizados por CLM, CSD, NAC, HBS e KMM. A análise dos dados foi realizada por CLM, CSD, HBS, HBS, AZ e KMM. A contribuição de materiais, reagentes e aparelhos foi realizada por FK, HBF, AZ e KMM. A redação do manuscrito foi realizada por CLM, HBF e KMM.

Development and characterization of two A549 human lung cancer cell sublines with clinically relevant levels of cisplatin resistance

Carolina Lumertz Martello[A], Cristine de Souza Dutra[A], Nathan Araujo Cadore[A], Helier Balbinotti da Silveira[A], Fábio Klamt[B], Henrique Bunselmeyer Ferreira[A], Arnaldo Zaha[C], Karina Mariante Monteiro[A]

[A]Laboratório de Genômica Estrutural e Funcional, Centro de Biotecnologia, Universidade Federal do Rio Grande do Sul, 91501-970, Bento Gonçalves 9500, 43421/206, +555133086070, Porto Alegre, Rio Grande do Sul, Brazil

[B]Laboratório 28, Departamento de Bioquímica, Instituto de Ciências Básicas da Saúde, Universidade Federal do Rio Grande do Sul, 90035-003, Ramiro Barcelos 2600, +555133085559, Porto Alegre, Rio Grande do Sul, Brazil

[C]Laboratório de Biologia Molecular de Cestódeos, Centro de Biotecnologia, Universidade Federal do Rio Grande do Sul, 91501-970, Bento Gonçalves 9500, 43421/204, +555133086070, Porto Alegre, Rio Grande do Sul, Brazil

The corresponding author is Karina Mariante Monteiro, email: karina@cbiot.ufrgs.br

ABSTRACT

Lung cancer, a major responsible by cancer death in the world, have platinum-based chemotherapy as first-line therapy for patients with advanced non-small cell lung cancer (NSCLC), being cisplatin the most frequently used drug. However, cisplatin resistance and consequent tumor recurrence remain an obstacle to treatment. In order to investigate the molecular pathways involved with cisplatin resistance in NSCLC, we developed two human lung adenocarcinoma A549 sublines with clinically relevant levels, A549/CDDP$_{CT}$ and A549/CDDP. Both sublines were analyzing by cellular characterization and protein expression modulation. A549/CDDP cells presented lower proliferation and increased cisplatin DNA damage repair when compared to A549 and A549/CDDP$_{CT}$. Proteomic and gene ontology analyses provided evidences of DNA repair proteins, endoplasmatic reticulum stress response, apoptotic process response, as others mechanisms potentially related to cisplatin resistance. A549/CDDP$_{CT}$ presented morphological changes already observed in cisplatin resistant cells, exclusive ribosomal profile as well as potential oxidative stress evasion. A549/CDDP presented fibroblast-like morphology and enriched proteins related to cytoskeletal organization, as a possible epithelial-mesenchymal transition (EMT). Therefore, A549/CDDP$_{CT}$ and A549/CDDP presented two unique sets of resistance mechanisms, standing as valuable clinically relevant cellular models to further investigations of drug resistance molecular mechanisms.

KEYWORDS: lung cancer, NSCLC, cancer resistance, cisplatin resistance

ABBREVIATIONS

A549/CDDP: acquired cisplatin-resistant A549 cell line

A549/CDDP$_{CT}$: acquired cisplatin-resistant A549 mimicking lung cancer clinical treatment cell line

A549: human A549 NSCLC adenocarcinoma cells

EMT: epithelial–mesenchymal transition

ER: endoplasmic reticulum

FASP: Filter Aided Sample Prep method

GI$_{50}$: cisplatin concentration to inhibit 50% of cellular growth

GO: gene ontology

GTP: guanosine-5'-triphosphate

MMR: DNA mismatch repair

NER: nucleotide excision repair

NHEJ: nonhomologous end joining repair

NSCLC: non-small cell lung cancer

PBS: phosphate buffered saline

PE: plating efficiency

pGL3: plasmid GL3

ROS: reactive oxygen species

SCLC: small cell lung cancer

SD: standard deviation

SF: surviving fraction

SRB: sulforhodamine B

INTRODUCTION

Lung cancer is the second more prevalent type of cancer in both men and women and the second cause of cancer death in the world (GLOBOCAN 2012: Estimated Cancer Incidence, Mortality and Prevalence Worldwide in 2012). Lung cancer can be histologically classified into two main types, non-small cell lung cancer (NSCLC) and small cell lung cancer (SCLC). NSCLC accounts for approximately 85% of lung cancer cases [1]. Survival rate of NSCLC remains low mainly because patients are in advanced stages of disease at diagnosis, when symptoms appear. Therefore, the 5-year relative survival of patients is only 18% [2].

Platinum-based chemotherapy is the standard first-line treatment for patients with advanced NSCLC, being cisplatin one of the most frequent used drugs [3]. Cisplatin primarily targets DNA, forming DNA adducts intra and inter-strand and resulting in double strand breaks which ultimately lead to cell death [4]. However, tumor resistance to cisplatin is a recurrent in clinical therapy and remains a major obstacle to the success of this drug in the lung cancer treatment [5].

Cellular cisplatin resistance is a multifactorial process that modulates the expression levels of a variety of genes and proteins to avoid cisplatin from causing cell death. Reduced intracellular cisplatin accumulation is one of the possible mechanisms of drug resistance and can involve increased intracellular drug efflux or decreased environmental drug uptake [3–6]. Drug cytotoxicity reduction by cytosolic inactivation through thiol-containing molecules conjugation can also lead to resistance. Moreover, cisplatin DNA damage repair by nonhomologous end joining (NHEJ), DNA mismatch repair (MMR) and mainly by nucleotide excision repair (NER) can overcome apoptosis. Furthermore, the cell death processes itself can be evaded by protein signaling pathways

as a last way to overcome cisplatin cytotoxicity. These mechanisms combined to characterize a cisplatin-resistant phenotype in a cellular model.

Multiples studies have investigated cisplatin resistance using laboratory cell lines with high-levels of drug resistance (>30 fold resistance than parental cell line) [7], which are generated by exposure of a parental cell line to high doses of the drug over long periods of time [8,9]. Although stable to longtime culture and freeze-thawing cycles, these high-level drug resistant sublines provide results that have been shown limited clinical utility [10]. Clinically relevant drug-resistant sublines, on the other hand, present lower levels of drug resistance, mimicking the levels observed in tumor cells isolated from patients before and after chemotherapy [7]. These cellular models can be developed by using low concentrations of the drug and protocols that mimic clinical treatment, with cycles of drug exposure followed by recovery periods in drug-free medium. Although the resulting sublines usually exhibit unstable resistance and produces subtle results, these results tend to be more reliable to clinical application.

In this study, we generated and characterized two cisplatin-resistant A549 lung adenocarcinoma sublines with clinically relevant levels of drug resistance. We have used different protocols to generate these cisplatin-resistant sublines, one mimicking the clinical treatment of patients with lung cancer (pulse treatment) and the other exposing the cells to increased concentrations of the drug (stepwise treatment). Cellular characterization of both sublines highlighted differences in cell morphology and behavior between cisplatin-sensitive and resistant cell lines. Proteomic analysis was able to identify differential expression of several proteins already described as involved in drug resistance in cancer and pointed to new potential targets to cisplatin resistance in lung cancer. Each resistant subline presented a unique set of proteins involved in

mechanisms of cisplatin resistance, making both sublines reliable and valuable tools to study cisplatin resistance in lung cancer.

MATERIALS AND METHODS

Cell culture and treatments

Human NSCLC A549 cells [11] were maintained in RPMI 1640 medium supplemented with 10% fetal bovine serum in the presence of penicillin (100 IU/mL) and streptomycin (100 μg/mL) at 37 °C in a humidified atmosphere of 5% CO_2. Cisplatin resistant subline A549/$CDDP_{CT}$ was developed by pulse treatment, which mimics lung cancer clinical treatment. A549/$CDDP_{CT}$ was obtained by exposing sub-confluent A549 cells to 5 μM of cisplatin for 72 h, followed by 18 days in drug-free medium, this 21-day cycle was repeated a total of 5 times. Resistant subline A549/CDDP was developed by stepwise treatment by continuously exposing A549 cells (5×10^5) to increasing concentration of cisplatin (0.1, 0.2, 0.3, 0.4 and 0.5 μM) for 72 h each. Cisplatin-resistance sublines were maintained in culture medium containing 0.5 μM of cisplatin until 3 days before the experiments to ensure maintenance of the resistant phenotype. Cisplatin-resistant sublines were independently generated three times, which were considered biological replicates in all experiments performed. Cell images were taken by Floid Cell Imaging Station (ThermoFisher Scientific) with 460 X magnification.

Cytotoxicity assay

Cisplatin cytotoxicity was determined with the sulforhodamine B (SRB) assay, as described by Vichai & Kirtikara (2006) [12], using 0.25, 0.5, 1, 2, 4, 8, 16, 32 and 64 μM of cisplatin. The GI_{50} value was calculated using a (log)dose–response curve with non-linear regression in GraphPad Prism 6.0 software. The assay was performed in triplicate.

Clonogenic assay

Cells were plated at a density of 500 cells/well in a 6-well plate and allowed to adhere overnight. Cells were treated with 0, 0.2, 0.3, 0.4, 0.5 or 1.0 μM of cisplatin for 72 h and cultured in drug-free medium for further 10 days. Colonies were washed once with phosphate-buffered saline (PBS), then fixed and stained with 6% glutaraldehyde and 0.5% crystal violet solution for at least 30 min, as described by Franken *et al.* (2006) [13]. The wells were washed with water and dried at room temperature. Colonies were counted using Clono-Counter software [14], with a threshold of 200, minimum of 10 and gray width of 45 as parameters. All images were subjected to visual inspection and manual correction. Plating efficiency (PE) was calculated as the number of colonies formed divided by the number of cells seeded. Surviving fraction (SF) was calculated as the number of colonies formed after treatment divided by the number of cells seeded multiplied by PE as described by Franken *et al.* (2006) [13]. All experiments were performed in triplicate.

Proliferation assay

A total of 5 x 10^3 cells/well of each cell line were seeded in 24-well plates in triplicate. The cells were collected by trypsinisation at 24, 48, 72, 96, 120 and 144 h after plating and counted using a flow cytometer Guava easyCyte. Population doubling times were calculated considering all time points using the Cell calculator++ mode of Doubling Time Online Calculator (http://www.doubling-time.com/compute.php).

Host cell reactivation assay

pGL3-Control vector (Promega) was treated with cisplatin at concentrations of 0.5, 1 and 2 μM in TE buffer (10 mM Tris; 1 mM EDTA; pH 8.0) at 37 ºC for 18 h. Damaged plasmid was recovered by precipitation with ethanol and resuspended in TE buffer. The

cell lines were co-transfected with 200 ng of cisplatin-damaged plasmid pGL3 and 40 ng of transfection control plasmid pRL-TK (Promega) using Lipofectamine LTX with Plus Reagent (ThermoFisher Scientific), according to manufacturer's instructions. Transfected cells were incubated for 24 h and then assayed for luciferase activities using the Dual-Glo Luciferase Assay System (Promega). Luminescence was measured with SpectraMax M5. Data were normalized by subtracting *Renilla* and firefly luminescence background and dividing firefly by *Renill*a luminescence for each measure [15]. Fold activity was calculated by normalized sample measure (pGL3 cisplatin-damaged) divided by control (pGL3 not damaged). Luciferase relative activity was calculated considering 100% luminescence from cells transfected with undamaged pGL3 plasmid.

Cell cycle analysis

Cells were cultured with 0, 0.25 or 0.5 μM of cisplatin for 72 h. After cisplatin exposure, samples were collected by trypsinization, washed once with PBS and fixed with ethanol 70% at 4 °C for at least 2 h. Fixed cells were washed once with PBS, stained with propidium iodide for 30 min at room temperature and washed again to stop staining. Cell cycle was analyzed by flow cytometry in a Guava easyCyte.

Protein extraction and sample preparation for mass spectrometry analysis

Protein extraction and sample preparation for mass spectrometry (MS) analysis were performed by Filter Aided Sample Preparation (FASP), as described by Wiśniewski (2016) [16]. Briefly, confluent flasks of cell culture from all cell lines were trypsinized and washed with PBS. Lysis buffer [2% SDS; 100 mM Tris-HCl pH 7.8; 0.05 M DTT (dithiothreitol)] was added to cell pellets, samples were sonicated, boiled and centrifuged. Proteins were quantified using Micro BCA Protein Assay Kit (Thermo Fisher Scientific) and 100 μg were mixed with UA solution [8 M urea; 0.1 M Tris-HCl

pH 8.5] at a Microcon-30 kDa Centrifugal Filter (Millipore) and centrifuged twice. IAA solution [0.05 iodoacetamide in UA solution] were added at the filter and incubated in dark for 20 min. Samples were centrifuged after incubation period, washed twice with UA solution and 0.05 M Tris-HCl pH 8.5. Peptides were obtained by trypsin digestion with 3 μg of trypsin for 300 μg of protein in 0.05 M Tris-HCl pH 8.5 at 37 °C for 18 h. Peptide samples were washed to remove residual trypsin with 0.05 M Tris-HCl pH 8.5 and collected with 0.05% TFA. Oasis HLB Extraction Cartridge (Waters) was used to promote the desalting of the samples.

Mass spectrometry analysis

Peptides were analyzed by LC-MS/MS using a using a nanoACQUITY UPLC system coupled to a Xevo G2-XS Q-Tof mass spectrometer (Waters) using a low-flow probe at the source. The peptides were separated by analytical chromatography (Acquity UPLC BEH C18, 1.7 μm, 2.1 × 50 mm, Waters), at a flow rate of 8 μl/min, using a 7–85% water/ACN 0.1% formic acid linear gradient over 90 min. The MS survey scan was set to 0.5 s and recorded from 50 to 2000 m/z. MS/MS scans were acquired from 50 to 2000 m/z, and scan time was set to 1 s. Data were collected in data-independent MS^E mode of acquisition.

Data processing and protein identification

Continuum LC-MS^E data were processed and searched using ProteinLynx Global Server version 3.0.3(PLGS 3.0.3, Waters Corporation). The searches were conducted against human proteome obtained from Uniprot (71,567 sequences, including canonical and isoform sequences) and tolerances were set to automatic (typically 10 ppm for precursor and 20 ppm for product ions), with trypsin as enzyme, maximum of one missed cleavage, fixed carbamidomethyl modification for cysteine residues, and

oxidation of methionine as variable modification. Scaffold software (Proteome Software Inc., version 4.8.3) was used to validate peptide and protein identifications. Peptides were accepted when established greater than 95.0% probability and protein when contained at least two identified peptides and established greater than 99% probability. The false discovery rate, FDR (Decoy), was 1% for proteins and 0.05% for peptides. Proteins differentially expressed between cells were identified by Student's t-test using Top 3 Precursor Intensity as quantitative value and *p*-values lower than 0.05 were considered significant. The Cytoscape plugin BiNGO [17] was used to protein functional annotation and ontology enrichment analysis. REVIGO was used to group gene ontologies (GO) with 0.7 of similarity using *Homo sapiens* database and SimRel semantic similarity measure [18].

Statistical analysis

Data were presented as mean ± standard deviation (SD). Comparison between two cell lines were subjected to paired Student t-test and comparisons between the three cell lines were subjected to ANOVA analysis and Tukey`s tests using GraphPad Prism 6 software. $p \leq 0.05$ was considered statistically significant.

RESULTS

Development of cisplatin-resistant sublines with clinically relevant resistance levels

Cisplatin-resistant sublines A549/$CDDP_{CT}$ and A549/CDDP were developed from parental cell line A549 using distinct protocols of drug exposure (pulse and stepwise, respectively). The resulting cisplatin-resistant cells presented a distinct morphology in comparison to parental A549 cell line, with A549/$CDDP_{CT}$ presenting a more enlarged morphology, while A549/CDDP presented a more elongated shape, with visible cell protrusions (Supplementary Figure 1). Cisplatin resistance was proven by comparison of average cytotoxicity between parental sensitive cell line and cisplatin-resistant sublines. The average cisplatin concentration to inhibit cellular growth by 50% (GI_{50}) was determinate by SRB assay. The average GI_{50} values obtained for A549, A549/$CDDP_{CT}$ and A549/CDDP were 3 μM, 14 μM and 7 μM, respectively (Figure 1). Therefore, A549/$CDDP_{CT}$ and A549/CDDP were validated as cisplatin-resistant sublines, presenting low, clinically relevant levels of drug resistance (GI_{50} values 4.7- and 2.3-foldhigher than that of cisplatin-sensitive A549 parental cell line, respectively). Cisplatin-resistant sublines presented unstable resistance, returning to parental cell resistance level after a month of drug-free medium culture. Therefore, A549/$CDDP_{CT}$ and A549/CDDP were culture in 0.05 μM of cisplatin.

Cisplatin-resistant sublines have increased clonogenic survival capacity

The clonogenic capacity of the cells was investigated as the number of cell colonies formed by each cell line and surviving fraction after treatment with cisplatin. Cisplatin-resistant sublines showed significant reduced clonogenicities when compared with A549 parental cell line, as determined by the number of colonies formed by each cell line in absence of cisplatin, with A549/CDDP forming the lowest number of colonies

(Figure 2). However, after cisplatin exposure, A549/CDDP$_{CT}$ and A549/CDDP showed a significant higher surviving fraction when compared to A549, for all cisplatin concentrations tested (Figure 2). Clonogenic survival data further confirmed the cisplatin-resistant phenotype of A549/CDDP and A549/CDDP$_{CT}$.

A549/CDDP presented reduced proliferation capacity

Cellular proliferation capacity of cisplatin-sensitive and resistant cells was evaluated and growth curves are shown in Figure 3. No differences were detected in the proliferation rate of the cells in 24, 48 and 72 h, but a significant decrease in cell proliferation of A549/CDDP was observed in 96, 120 and 144 h when compared with A549 and A549/CDDP$_{CT}$. Indeed, the doubling time of A549/CDDP subline (36.61 hours) was significant higher than those of A549 and A549/CDDP$_{CT}$ cells (27.43 and 25.68 hours, respectively) (Figure 3).

A549/CDDP showed increased cisplatin-damaged DNA repair capacity

We performed a host-cell reactivation (HCR) assay using a luciferase reporter gene to evaluate the ability of the cells to repair cisplatin-damaged plasmid DNA. Luciferase activity rate was expressed as the percentage of the reactivated luciferase activity of damaged relative to the activity of undamaged plasmid (100%). A549/CDDP showed a higher luciferase activity rate when compared with A549 and A549/CDDP$_{CT}$ in transfections with plasmid damaged with 0.5 and 1 μM of cisplatin (Figure 4). Cells transfected with plasmid damaged with 2 μM of cisplatin showed low DNA damage repair activity and no differences between cell lines.

Cell cycle analysis

Flow cytometry analysis of DNA content from cells exposed to cisplatin revealed that A549 presented a decreased in G1 phase arrest and an increased in G2 phase arrest when exposed to cisplatin, while cisplatin-resistant sublines showed no alteration of cell cycle in response to drug treatment (Table 1). A549/CDDP presented a lower G1 phase arrest when compared to A549 in all conditions. Moreover, cisplatin-resistant sublines showed two peaks in G1 phase after cisplatin exposure (Figure 5), as it seems that two G1 subpopulations were selected from A549/CDDP$_{CT}$ and A549/CDDP after cisplatin exposure.

Proteomic analysis and differentially expressed proteins

Distribution of identified proteins among A549, A549/CDDP$_{CT}$ and A549/CDDP is shown in Figure 6 and Supplementary Table 1. Samples were analyzed in triplicates and only proteins identified in at least two out of the three replicates were considered. In order to identify proteins and molecular mechanisms consistently involved in drug resistance, biological replicates from A549/CDDP$_{CT}$ and A549/CDDP were independently generated three times each. Most of the identified proteins presented significant quantitative differences between samples, based on MS precursor intensity values (Top 3 Precursor Intensity). Among the proteins shared between A549 and A549/CDDP$_{CT}$, 40 were found as differentially expressed, with all of them down-regulated in A549/CDDP$_{CT}$ (Supplementary Table 1). Seventeen proteins were found differentially abundant between A549 and A549/CDDP, with 15 and 2 of them being detected downregulated and upregulated, respectively, in A549/CDDP cells. We found 14 proteins differentially expressed between the two cisplatin-resistant sublines, all upregulated in A549/CDDP cells. Proteins found upregulated and exclusive in each cell

line were submitted to functional classification and enrichment analysis. GO terms identified were grouped considering medium similarity and are showed in Supplementary Table 2A, 2B and 2C.

Enrichment of functional categories

Functional categories overrepresented in cisplatin-resistant cells include ‘unfolded protein binding’, ‘response to unfolded protein’, ‘regulation of cellular response to stress’, ‘RNA export from nucleus’, ‘negative regulation of mRNA processing’, ‘endoplasmic reticulum’, ‘regulation of DNA damage response’, ‘signal transduction by p53 class mediator’, ‘double-strand break repair via nonhomologous end joining’ and ‘regulation of secondary metabolic process’ (Supplementary Table 2B and 2C). GO terms enriched exclusively in A549/CDDP$_{CT}$ cells include ‘ribonucleoprotein complex’, ‘pore complex’, ‘protein oligomerization’, ‘GTPase activity’, ‘response to oxidative stress’, ‘negative regulation of apoptotic process’, ‘vesicle’, ‘response to drug’, ‘regulation of DNA binding’ and ‘positive regulation of secretion’ (Supplementary Table 2B). On the other hand, categories found exclusively enriched in A549/CDDP include ‘actin polymerization or depolymerization’, ‘cell junction assembly’, ‘pseudopodium’, ‘actin filament-based movement’ and ‘regulation of cell migration’ (Supplementary Table 2C). Categories downrepresented in cisplatin-resistant sublines included ‘primary metabolic process’, ‘negative regulation of biological process’, ‘sequestering of calcium ion’, ‘chaperone-mediated protein complex assembly’ and ‘positive regulation of epithelial cell proliferation’ (Supplementary Table 2A).

DISCUSSION

First-line treatment of advanced-stage lung cancer is cisplatin chemotherapy, but drug resistance remains a major problem for cancer therapy. Cell lines with high levels of resistance are commonly used to study the molecular mechanisms involved in drug resistance [19,20]. However, the results obtained from these cellular models have limited clinical application [10]. In this way, clinically relevant cell lines appear as alternative tools to study resistance to chemotherapy, as these models produce more reliable results for clinical application. In this work, two cisplatin-resistant cell sublines with clinically relevant levels of drug resistance, namely A549/CDDP$_{CT}$ and A549/CDDP, were developed from human lung adenocarcinoma A549 cell using different protocols. Cisplatin-resistant sublines A549/CDDP$_{CT}$ and A549/CDDP presented GI_{50} values 4.7 and 2.3 fold higher than that of the sensitive parental cell line A549. These levels of drug resistance are similar to those observed in tumor cells isolated from patients before and after chemotherapy, therefore our cellular models were classified as clinically relevant [7].

Compared to parental cell line, cisplatin-resistant subline A549/CDDP$_{CT}$ presented a morphology more expanded, while A549/CDDP presented a more elongated fibroblast-like shape, with cell protrusions. The enlarged morphology observed in A549/CDDP$_{CT}$ cells has already been described for other cisplatin-resistant cells [21] and 'actin cytoskeleton reorganization' was a functional category enriched in A549/CDDP$_{CT}$. A549/CDDP presented actin cytoskeleton-associated proteins differentially expressed when compared to A549, as upregulated vimentin (VIM) [22], exclusive myosin light polypeptide 6 (MYL6) [23] and catenin alpha-1 (CTNNA1) [24]. Moreover, A549/CDDP showed 'actin polymerization or depolymerization', 'cell junction assembly', 'pseudopodium', 'actin filament-based movement' and 'negative

regulation of cellular component movement' as enriched GO terms. Therefore, these morphological changes could be an initial evidence of epithelial mesenchymal transition [25], but specific investigation would be necessary to confirm it.

Cellular characterization showed that our cisplatin-resistant sublines presented a general lower clonogenic capacity than A549, but had an increased surviving fraction when exposed to cisplatin, as expected from cisplatin-resistant phenotypes. However, the A549/CDDP subline presented a lower proliferation rate, resulting in an increased doubling time when compared to A549 and A549/CDDP$_{CT}$. As cellular multiplication is necessary to cisplatin reach DNA, slow proliferation is a way to protect the cell from cisplatin DNA damage and can be related to elevated ROS level [26]. Moreover, A549/CDDP$_{CT}$ presented 'response to oxidative stress' as an exclusive enriched functional category, so it could overcome oxidative stress and continue normal proliferation. The differences observed in proliferation rate of cisplatin-resistant cells A549/CDDP and A549/CDDP$_{CT}$ are probably resultant from the experimental protocol used to develop each cell subline. The recovery time in drug-free medium may have differentially influenced the proliferation rate of A549/CDDP $_{CT}$ in relation to A549/CDDP cells, which were continuously exposed to the drug during resistance development.

In addition to different cellular characteristics, the protocol used for the development of our clinically relevant cisplatin-resistant cells also seems to have led to the activation of different molecular mechanisms of drug resistance. In cell cycle experiments, we observed that A549 decreased G1 and increased G2 phase arrest as a consequence of DNA damaged caused by cisplatin [27]. Also, A549/CDDP had a lower G1 phase arrest when compared to parental cells A549 in all conditions, which can be associated to its lower proliferation. DNA damage repair in G1 phase is made by NHEJ

[28] involving XRCC5 and XRCC6 heterodimer [29], both proteins presented only in A549/CDDP. Likewise, ‘double-strand break repair via nonhomologous end joining’ was a GO term enriched in cisplatin-resistant sublines. Therefore, the increased A549/CDDP cisplatin DNA damage repair can be by NHEJ in G1 phase, being more effective and spending less time in this cell cycle checkpoint when compared to A549. A549/$CDDP_{CT}$ did not show any cell cycle distribution difference and had ‘negative regulation of cell cycle arrest’ as enriched functional category. Moreover, A549/$CDDP_{CT}$ and A549/CDDP selection of two G1 subpopulations after cisplatin exposure is not surprising once tumors are composed of a variety of different subpopulations, as cancer cells differentiate so quickly [30]. Isolation and characterization of these subpopulations would lead to a better understand of cisplatin-resistant sublines resistance mechanisms.

Elongation factor 1-alpha 1 (EEF1A1) was identified only in cisplatin-resistant sublines and has already been described as involved in cisplatin resistance. EEF1A1 upregulation is associated with chemoresistance in gastric cancer [31], as EEF1A1 acts inhibiting p53 and p73 proteins, therefore evading cisplatin-induced apoptosis [32]. Also, EEF1A1 can possibly promote the acceleration of synthesis of free thiol-containing proteins in response to stress [33], inactivating cisplatin by conjugation with cytosolic thiol-containing molecules [3,5]. Likewise, GO terms associated with EEF1A1 were ‘translational elongation’ and ‘gene expression’. Exclusive in A549/$CDDP_{CT}$ was identified ‘GTPase activity’, which can be involved in reduced accumulation of cisplatin [34].

Enriched functional categories lead to an overall view of cellular mechanisms induced by cisplatin treatment. Endoplasmic reticulum (ER) stress is associated to cisplatin response in A549 cells, which trigger unfolded protein response to respond to

environmental factors [35]. Moreover, ER-stress inhibits cell viability, enhancing cell apoptosis after cisplatin exposure. Cisplatin-resistant sublines presented ‘endoplasmic reticulum’, ‘unfolded protein binding’, ‘response to unfolded protein’, ‘regulation of cellular response to stress’ and ‘regulation of apoptotic process’ as enriched functional categories. Likewise, ‘regulation of secondary metabolic process’ is associated with regulation of cisplatin-induced apoptosis [36]. So, A549/CDDP$_{CT}$ and A549/CDDP could be using these mechanisms as a way to avoid cisplatin-induced apoptosis caused from cisplatin treatment.

Histones H1.3 and H4 were found downregulated in cisplatin-resistant sublines when compared to parental cell line A549. Histone H1.3 was described as apoptogenic when PKC kinase is cleaved or its signaling is inhibited in cisplatin-induced DNA damage, as histone phosphorylation by PKC supress this function [37]. Therefore, cisplatin-resistant sublines could be cleaving histone H1.3 to reduce its apoptotic activity. In addition, overexpression of histones competes with DNA repair factors and reduction of free histones pools can reduce DNA damage sensitivity [38]. Hence, downregulation of histones (H1.3 and H4) and enhanced cisplatin-damage DNA repair can possible be related as mechanisms involved in A549/CDDP cisplatin resistance.

A549/CDDP$_{CT}$ cells presented an interesting ribosomal protein profile different from A549 and A549/CDDP, as RPLP2 e RPL4 were downregulated, RPS7 e HNRNPA1 were absent and RPS28, RPS8, RPL12, RPL7A, RPL8 e RPL9 were exclusive to this subline. Ribosomal proteins can have functions besides transduction, being even involved with cancer [39]. Silencing RPS7 in ovarian cancer increased proliferation and cell cycle progression, as well as decreased apoptosis *in vitro* and *in vivo* [40]. Moreover, RPS8, RPL7A e RPL12 genes were upregulated in cisplatin-resistant esophageal cancer cell lines when compared to sensitive cell line [41]. Both

cisplatin-resistant sublines presented many ribosomal related enriched GO terms, as ‘ribosomal large subunit biogenesis’, ‘ribosomal small subunit biogenesis’, ‘ribosomal large subunit export from nucleus’ and ‘ribosome assembly’. Therefore, the differential ribosomal proteins pattern presented by A549/CDDP$_{CT}$ could be a consequence from its cisplatin resistance.

Some proteins related to cisplatin-resistance were identified as upregulated in A549 when compared to A549/CDDP$_{CT}$ and A549/CDDP. However, studies which report these proteins make use of high level cisplatin-resistant cell lines, hindering a direct correlation. YWHAE, for example, is described as an upregulated protein in cells treated with a 100-fold cisplatin concentration than the used in this work [42]. Likewise, *HSPD1* increased transcription was related to resistance in A2780 cells that remained cisplatin-resistant after 2 years in absence of drug [43]. Cisplatin-treatment protocol can also influence in proteomic results, as A549/CDDP$_{CT}$ and A549/CDDP were treated with low doses of cisplatin for shorter periods. Therefore, different protocols of cisplatin-resistant sublines development could be the reason for such discordant results.

Overall, our results showed that A549/CDDP$_{CT}$ and A549/CDDP present different molecular mechanisms of drug cytotoxicity evasion, as cisplatin resistance is a multifactorial process [5]. Cisplatin-resistant sublines present regulation of cellular response to stress, negative regulation of mRNA processing and regulation of DNA damage response as resistance mechanisms. A549/CDDP$_{CT}$ cells present ribosomal biogenesis, assembly and localization, ‘GTPase activity’, ‘response to oxidative stress’, ‘negative regulation of apoptotic process’, ‘regulation of DNA binding’ and ‘positive regulation of secretion’ as exclusive functional categories and possible cisplatin-resistant mechanisms. On the other hand, A549/CDDP cells present lower proliferation rate and enhanced cisplatin DNA damage repair and enriched GO terms pointing to

EMT phenotype. Moreover, both cisplatin-resistant sublines present their own proteome set correlated to drug resistance, which presented some differences from resistance mechanisms commonly observed for cellular models with high levels of resistance. Therefore, A549/CDDP$_{CT}$ and A549/CDDP were two cisplatin-resistant sublines with their unique set of cisplatin resistance mechanisms and represent important alternative cellular models to further investigations of drug resistance molecular mechanisms.

ACKNOWLEDGMENTS

This work was supported by Fundação de Amparo à Pesquisa do Estado do Rio Grande do Sul (FAPERGS). CLM and CSD were recipients of Conselho Nacional de Desenvolvimento Científico e Tecnológico (CNPq) M.Sc. fellowships. NAC was recipient of BIC-UFRGS undergraduate fellowship.

REFERENCES

[1] S.M. Haghgoo, A. Allameh, E. Mortaz, J. Garssen, G. Folkerts, P.J. Barnes, I.M. Adcock, Pharmacogenomics and targeted therapy of cancer: Focusing on non-small cell lung cancer, Eur. J. Pharmacol. 754 (2015) 82–91. doi:10.1016/j.ejphar.2015.02.029.

[2] R.L. Siegel, K.D. Miller, A. Jemal, Cancer statistics, 2016, CA. Cancer J. Clin. 66 (2016) 7–30. doi:10.3322/caac.21332.

[3] B. Köberle, M.T. Tomicic, S. Usanova, B. Kaina, Cisplatin resistance: Preclinical findings and clinical implications, Biochim. Biophys. Acta - Rev. Cancer. 1806 (2010) 172–182. doi:10.1016/j.bbcan.2010.07.004.

[4] S. Dasari, P.B. Tchounwou, Cisplatin in cancer therapy: Molecular mechanisms of action, Eur. J. Pharmacol. 740 (2014) 364–378. doi:10.1016/j.ejphar.2014.07.025.

[5] Z.H. Siddik, Cisplatin: mode of cytotoxic action and molecular basis of resistance, Oncogene. 22 (2003) 7265–7279. doi:10.1038/sj.onc.1206933.

[6] D.A. Fennell, Y. Summers, J. Cadranel, T. Benepal, D.C. Christoph, R. Lal, M. Das, F. Maxwell, C. Visseren-Grul, D. Ferry, Cisplatin in the modern era: The backbone of first-line chemotherapy for non-small cell lung cancer, Cancer Treat. Rev. 44 (2016) 42–50. doi:10.1016/j.ctrv.2016.01.003.

[7] M. McDermott, A.J. Eustace, S. Busschots, L. Breen, J. Crown, M. Clynes, N. O???Donovan, B. Stordal, In vitro Development of Chemotherapy and Targeted Therapy Drug-Resistant Cancer Cell Lines: A Practical Guide with Case Studies, Front. Oncol. 4 (2014). doi:10.3389/fonc.2014.00040.

[8] V.B. Cetintas, A.S. Kucukaslan, B. Kosova, A. Tetik, N. Selvi, G. Cok, C. Gunduz, Z. Eroglu, Cisplatin resistance induced by decreased apoptotic activity in non-small-cell lung cancer cell lines, Cell Biol. Int. 36 (2012) 261–265. doi:10.1042/CBI20110329.

[9] W. Xu, S. Wang, Q. Chen, Y. Zhang, P. Ni, X. Wu, J. Zhang, F. Qiang, A. Li, O.D. Røe, S. Xu, M. Wang, R. Zhang, J. Zhou, TXNL1-XRCC1 pathway regulates cisplatin-induced cell death and contributes to resistance in human gastric cancer, Cell Death Dis. 5 (2014) e1055. doi:10.1038/cddis.2014.27.

[10] J.-P. Gillet, S. Varma, M.M. Gottesman, The Clinical Relevance of Cancer Cell Lines, JNCI J. Natl. Cancer Inst. 105 (2013) 452–458. doi:10.1093/jnci/djt007.

[11] M. Lieber, B. Smith ', A. Szakal, W. Nelson-Rees, G. Todaro, A Continuous Tumor-Cell Line From A Human Lung Carcinoma With Properties Of Type II Alveolar Epithelial Cells, Int. J. Cancer. 17 (1976) 62–70.

[12] V. Vichai, K. Kirtikara, Sulforhodamine B colorimetric assay for cytotoxicity screening, Nat. Protoc. 1 (2006) 1112–1116. doi:10.1038/nprot.2006.179.

[13] N.A.P. Franken, H.M. Rodermond, J. Stap, J. Haveman, C. van Bree, Clonogenic assay of cells in vitro, Nat. Protoc. 1 (2006) 2315–2319. doi:10.1038/nprot.2006.339.

[14] M. Niyazi, I. Niyazi, C. Belka, Counting colonies of clonogenic assays by using densitometric software, Radiat. Oncol. 2 (2007) 4. doi:10.1186/1748-717X-2-4.

[15] T. Schagat, A. Paguio, K. Kopish, Normalizing Genetic Reporter Assays : Approaches and Considerations for Increasing Consistency and Statistical Significance, Cell Notes. (2007) 9–12.

[16] J.R. Wiśniewski, Quantitative Evaluation of Filter Aided Sample Preparation (FASP) and Multienzyme Digestion FASP Protocols, Anal. Chem. 88 (2016) 5438–5443. doi:10.1021/acs.analchem.6b00859.

[17] S. Maere, K. Heymans, M. Kuiper, BiNGO: a Cytoscape plugin to assess overrepresentation of Gene Ontology categories in Biological Networks, Bioinformatics. 21 (2005) 3448–3449. doi:10.1093/bioinformatics/bti551.

[18] F. Supek, M. Bošnjak, N. Škunca, T. Šmuc, REVIGO Summarizes and Visualizes Long Lists of Gene Ontology Terms, PLoS One. 6 (2011) e21800. doi:10.1371/journal.pone.0021800.

[19] H. Zhang, B. Hu, Z. Wang, F. Zhang, H. Wei, L. Li, miR-181c contributes to cisplatin resistance in non-small cell lung cancer cells by targeting Wnt inhibition factor 1, Cancer Chemother. Pharmacol. (2017). doi:10.1007/s00280-017-3435-1.

[20] K. Qi, Y. Li, X. Li, X. Lei, B. Wang, L. Zhang, X. Chu, Id4 promotes cisplatin resistance in lung cancer through the p38 MAPK pathway., Anticancer. Drugs. 27 (2016) 970–8. doi:10.1097/CAD.0000000000000414.

[21] M.-H. Jamal, W.-C. Ch'ng, K. Yusoff, N. Shafee, Reduced Newcastle disease virus-induced oncolysis in a subpopulation of cisplatin-resistant MCF7 cells is associated with survivin stabilization, Cancer Cell Int. 12 (2012) 35. doi:10.1186/1475-2867-12-35.

[22] C.-Y. Liu, H.-H. Lin, M.-J. Tang, Y.-K. Wang, Vimentin contributes to epithelial-mesenchymal transition cancer cell mechanics by mediating cytoskeletal organization and focal adhesion maturation, Oncotarget. 6 (2015) 15966–15983. doi:10.18632/oncotarget.3862.

[23] L. Xie, B.K. Law, M.E. Aakre, M. Edgerton, Y. Shyr, N.A. Bhowmick, H.L. Moses, Transforming growth factor beta-regulated gene expression in a mouse mammary gland epithelial cell line, Breast Cancer Res. 5 (2003) R187. doi:10.1186/bcr640.

[24] S. Lamouille, J. Xu, R. Derynck, Molecular mechanisms of epithelial–mesenchymal transition, Nat. Rev. Mol. Cell Biol. 15 (2014) 178–196. doi:10.1038/nrm3758.

[25] E. Prieto-García, C.V. Díaz-García, I. García-Ruiz, M.T. Agulló-Ortuño, Epithelial-to-mesenchymal transition in tumor progression, Med. Oncol. 34 (2017) 122. doi:10.1007/s12032-017-0980-8.

[26] G. Duan, Q. Tang, H. Yan, L. Xie, Y. Wang, X.E. Zheng, Y. Zhuge, S. Shen, B. Zhang, X. Zhang, J. Wang, W. Wang, X. Zou, A Strategy to Delay the Development of Cisplatin Resistance by Maintaining a Certain Amount of Cisplatin-Sensitive Cells, Sci. Rep. 7 (2017) 432. doi:10.1038/s41598-017-00422-2.

[27] N. Sarin, F. Engel, G. V. Kalayda, M. Mannewitz, J. Cinatl, F. Rothweiler, M. Michaelis, H. Saafan, C.A. Ritter, U. Jaehde, R. Frötschl, Cisplatin resistance in non-small cell lung cancer cells is associated with an abrogation of cisplatin-induced G2/M cell cycle arrest, PLoS One. 12 (2017) e0181081. doi:10.1371/journal.pone.0181081.

[28] M.H., Yun, K., Hiom, CtIP-BRCA1 modulates the choice of DNA double-strand-break repair pathway throughout the cell cycle. Nature. 21 (2009) 460-463. doi: 10.1038/nature07955.

[29] D.-T. Bau, C.-W. Tsai, C.-N. Wu, Role of the XRCC5/XRCC6 dimer in carcinogenesis and pharmacogenomics, Pharmacogenomics. 12 (2011) 515–534. doi:10.2217/pgs.10.209.

[30] A. Jögi, M. Vaapil, M. Johansson, S. Påhlman, Cancer cell differentiation heterogeneity and aggressive behavior in solid tumors, Ups. J. Med. Sci. 117 (2012) 217–224. doi:10.3109/03009734.2012.659294.

[31] H.-D. Hu, F. Ye, D.-Z. Zhang, P. Hu, H. Ren, S.-L. Li, iTRAQ Quantitative Analysis of Multidrug Resistance Mechanisms in Human Gastric Cancer Cells, J. Biomed. Biotechnol. 2010 (2010) 1–11. doi:10.1155/2010/571343.

[32] A. Blanch, F. Robinson, I.R. Watson, L.S. Cheng, M.S. Irwin, Eukaryotic Translation Elongation Factor 1-Alpha 1 Inhibits p53 and p73 Dependent Apoptosis and Chemotherapy Sensitivity, PLoS One. 8 (2013) e66436. doi:10.1371/journal.pone.0066436.

[33] G. Chacko, Q. Ling, K.A. Hajjar, Induction of Acute Translational Response Genes by Homocysteine, J. Biol. Chem. 273 (1998) 19840–19846. doi:10.1074/jbc.273.31.19840.

[34] D.-W. Shen, L.M. Pouliot, J.-P. Gillet, W. Ma, A.C. Johnson, M.D. Hall, M.M. Gottesman, The Transcription Factor GCF2 Is an Upstream Repressor of the Small GTPAse RhoA, Regulating Membrane Protein Trafficking, Sensitivity to Doxorubicin, and Resistance to Cisplatin, Mol. Pharm. 9 (2012) 1822–1833. doi:10.1021/mp300153z.

[35] S. SHI, P. TAN, B. YAN, R. GAO, J. ZHAO, J. WANG, J. GUO, N. LI, Z. MA, ER stress and autophagy are involved in the apoptosis induced by cisplatin in human lung cancer cells, Oncol. Rep. 35 (2016) 2606–2614. doi:10.3892/or.2016.4680.

[36] P. Loar, H. Wahl, M. Kshirsagar, G. Gossner, K. Griffith, J.R. Liu, Inhibition of glycolysis enhances cisplatin-induced apoptosis in ovarian cancer cells, Am. J. Obstet. Gynecol. 202 (2010) 371.e1-371.e8. doi:10.1016/j.ajog.2009.10.883.

[37] M. Garg, N. Ramdas, M. Vijayalakshmi, G. V Shivashankar, A. Sarin, The C-terminal domain (CTD) in linker histones antagonizes anti-apoptotic proteins to modulate apoptotic outcomes at the mitochondrion, Cell Death Dis. 5 (2014) e1058. doi:10.1038/cddis.2014.20.

[38] D. Liang, S.L. Burkhart, R.K. Singh, M.-H.M. Kabbaj, A. Gunjan, Histone dosage regulates DNA damage sensitivity in a checkpoint-independent manner by the homologous recombination pathway, Nucleic Acids Res. 40 (2012) 9604–9620. doi:10.1093/nar/gks722.

[39] W. Wang, S. Nag, X. Zhang, M.-H. Wang, H. Wang, J. Zhou, R. Zhang, Ribosomal Proteins and Human Diseases: Pathogenesis, Molecular Mechanisms, and Therapeutic Implications, Med. Res. Rev. 35 (2015) 225–285. doi:10.1002/med.21327.

[40] Z. Wang, J. Hou, L. Lu, Z. Qi, J. Sun, W. Gao, J. Meng, Y. Wang, H. Sun, H. Gu, Y. Xin, X. Guo, G. Yang, Small Ribosomal Protein Subunit S7 Suppresses Ovarian Tumorigenesis through Regulation of the PI3K/AKT and MAPK Pathways, PLoS One. 8 (2013) e79117. doi:10.1371/journal.pone.0079117.

[41] H. Toshimitsu, K. Hashimoto, A. Tangoku, N. Iizuka, K. Yamamoto, S. Kawauchi, A. Oga, T. Furuya, M. Oka, K. Sasaki, Molecular signature linked to acquired resistance to cisplatin in esophageal cancer cells, Cancer Lett. 211 (2004) 69–78. doi:10.1016/j.canlet.2004.01.038.

[42] A. Castagna, P. Antonioli, H. Astner, M. Hamdan, S.C. Righetti, P. Perego, F. Zunino, P.G. Righetti, A proteomic approach to cisplatin resistance in the cervix squamous cell carcinoma cell line A431, Proteomics. 4 (2004) 3246–3267. doi:10.1002/pmic.200400835.

[43] M. Abu-hadid, J.D. Wilkes, Z. Elakawi, L. Pendyala, R.P. Perez, Relationship between heat shock protein 60 (HSP60) mRNA expression and resistance to platinum analogues in human ovarian and bladder carcinoma cell lines, Cancer Lett. 119 (1997) 63–70. doi:10.1016/S0304-3835(97)00255-3.

FIGURES

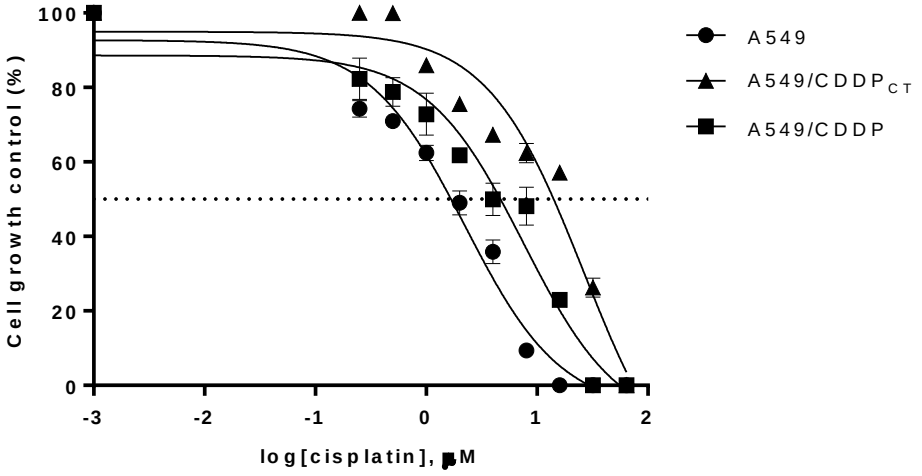

Figure 1: Cisplatin exposure led to acquisition of resistance in A549/CDDP$_{CT}$ and A549/CDDP sublines. Dose-response curves of A549 parental cell line and cisplatin-resistant sublines A549/CDDP$_{CT}$ and A549/CDDP. GI_{50} values were calculated as a dose-response with non-linear regression in GraphPad Prism. Representative data were shown for each cell line. Graphic show mean ± SD and dotted line indicates the 50% of cellular growth inhibition. Each assay was performed in triplicate.

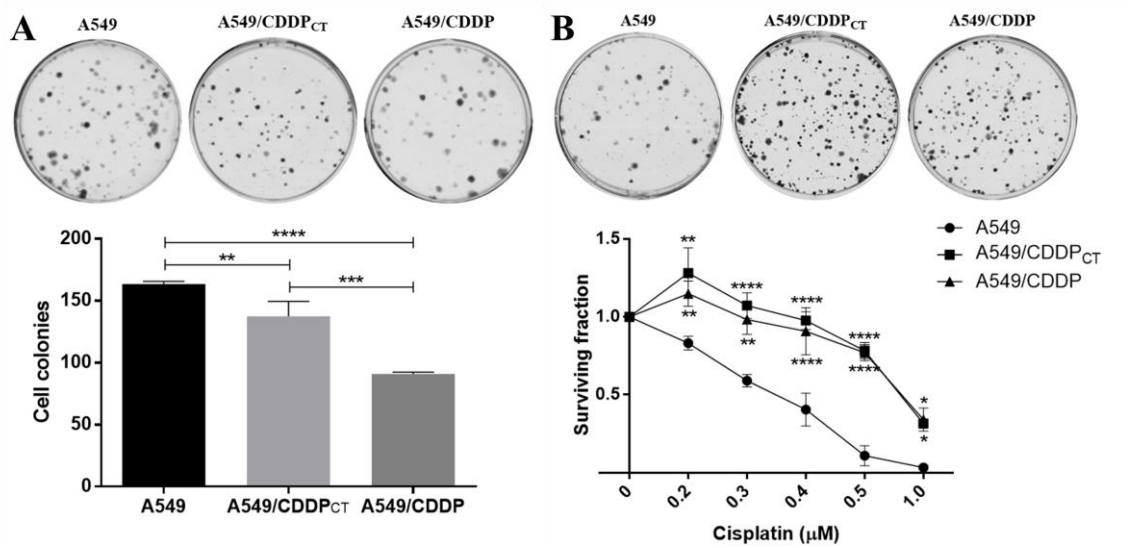

Figure 2: A549, A549/CDDP$_{CT}$ and A549/CDDP presented different cell colony formation capacity and cell surviving fraction. Clonogenic assay was performed exposing cells to increased cisplatin concentration from 0 to 0.5 μM for 72 hours following culture in drug-free medium for 10 days. Representative crystal violet stained A549, A549/CDDP$_{CT}$ and A549/CDDP colonies (*top*) without cisplatin exposure (**A**) and pre-exposed to 0.3 μM of cisplatin (**B**). **A)** The colonies were counted from three independent experiments using Clono-Counter software and plotted as mean ± SD (*bottom*). **B)** Surviving fraction was calculated as the number of colonies after cisplatin treatment divided by the number of cells seeded multiplies by Platting Efficiency and plotted as mean ± SD (*bottom*). A549/CDDP$_{CT}$ and A549/CDDP showed a higher surviving fraction for all cisplatin-concentrations when compared to A549. Statistical analysis was made using ANOVA with Tukey's test considering significant $p \leq 0.01$ (**), $p \leq 0.001$ (***) and $p \leq 0.0001$ (****). Each assay was performed in triplicate.

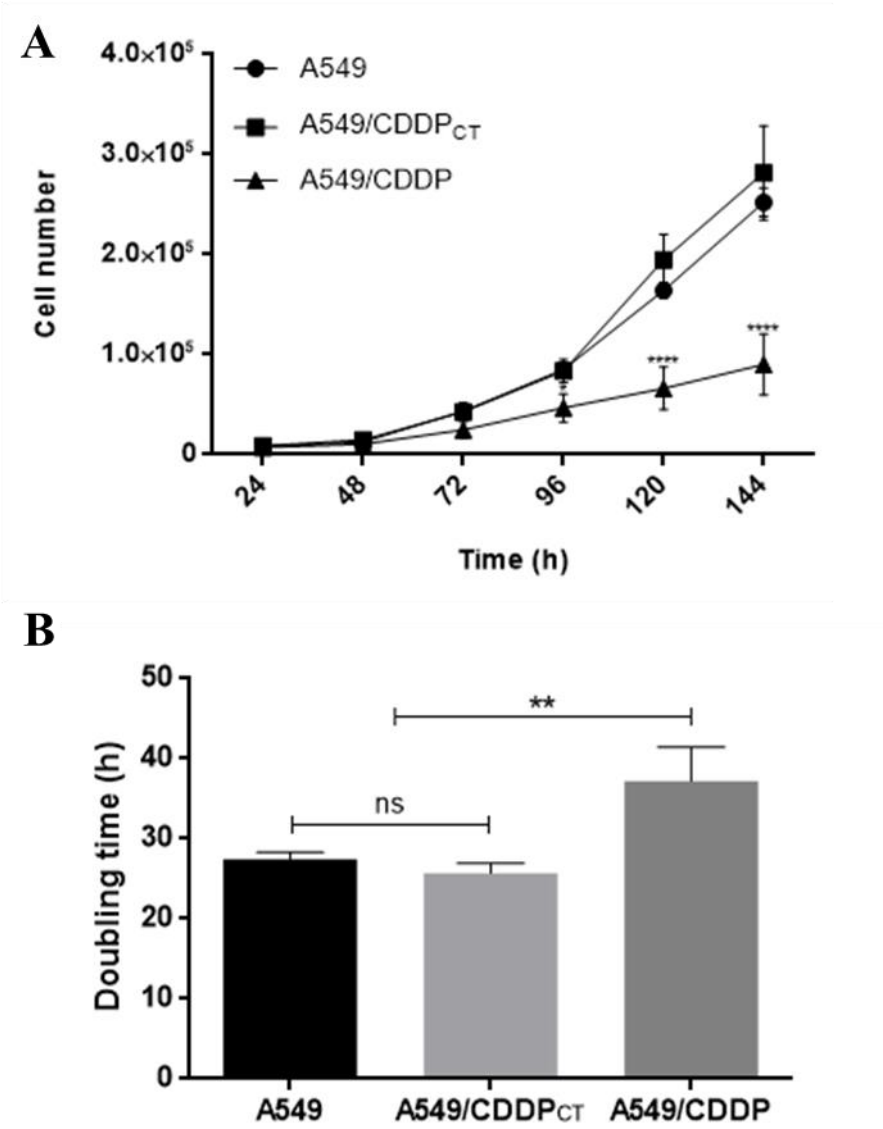

Figure 3: A549/CDDP presented lower proliferation rate and higher doubling time. Growth curves from A549, A549/CDDP$_{CT}$ and A549/CDDP were determined by cell counting in 24, 48, 72, 96, 120 and 144 h. **A)** A549 and A549/CDDP$_{CT}$ showed a higher proliferation than A549/CDDP after 96 h. **B)** Doubling time was calculated from A549, A549/CDDPCT and A549/CDDP considering cell number in all times using Doubling Time Online Calculator (http://www.doubling-time.com). Graphic show mean ± SD. Statistical analysis was made using ANOVA with Tukey's test considering significant $p \leq 0.05$ (*), $p \leq 0.01$ (**), $p \leq 0.0001$ (****) and (ns) no significant. Each assay was performed in triplicate.

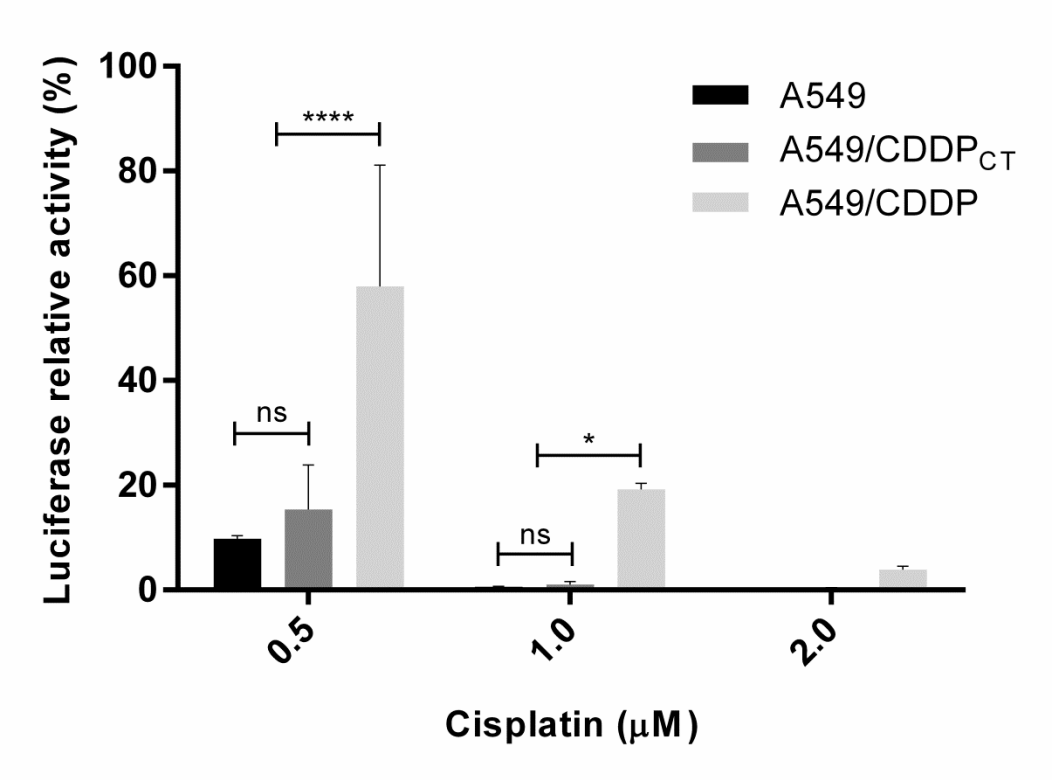

Figure 4: A549/CDDP cells were able to repair of cisplatin-damaged DNA. Luciferase relative activity of A549, A549/CDDP$_{CT}$ and A549/CDDP cells transfected with cisplatin-damaged pGL3 vector. Luciferase activity rate of cells transfected with undamaged pGL3 were assumed as 100%. Graphic show mean ± SD. Statistical analysis was made using ANOVA with Tukey's test considering significant $p \leq 0.05$ (*) and $p \leq 0.0001$ (****) and (ns) no significant. Each assay was performed in triplicate.

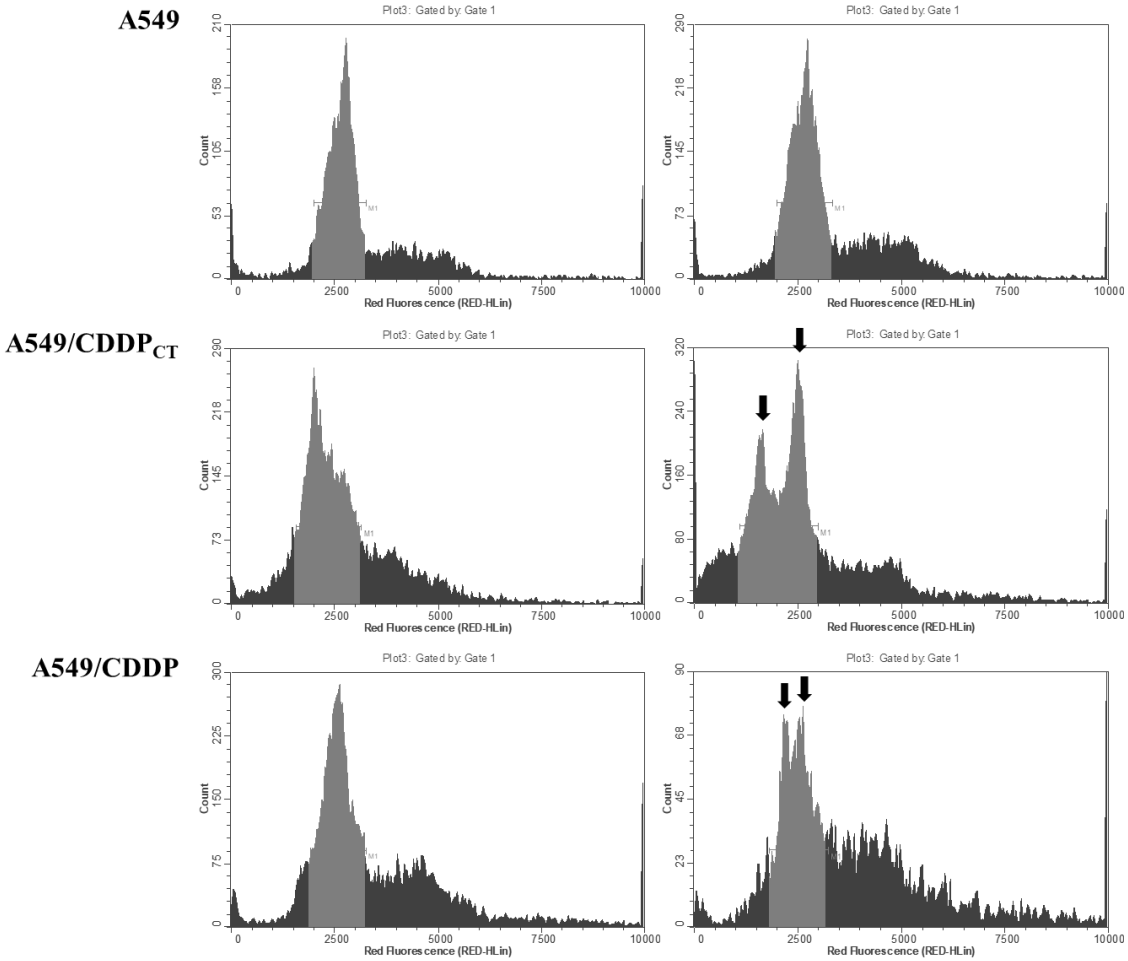

Figure 5: A549/CDDP$_{CT}$ and A549/CDDP cells differentiate in two G1 subpopulations after cisplatin exposure. Histogram representation of A549, A549/CDDPCT and A549/CDDP before (*left*) and after (*right*) treatment with 0.5 µM of cisplatin. A549/CDDP$_{CT}$ and A549/CDDP presented two subpopulations (black arrows) in cell cycle G1 phase (light grey), which are more evident in A549/CDDP$_{CT}$.

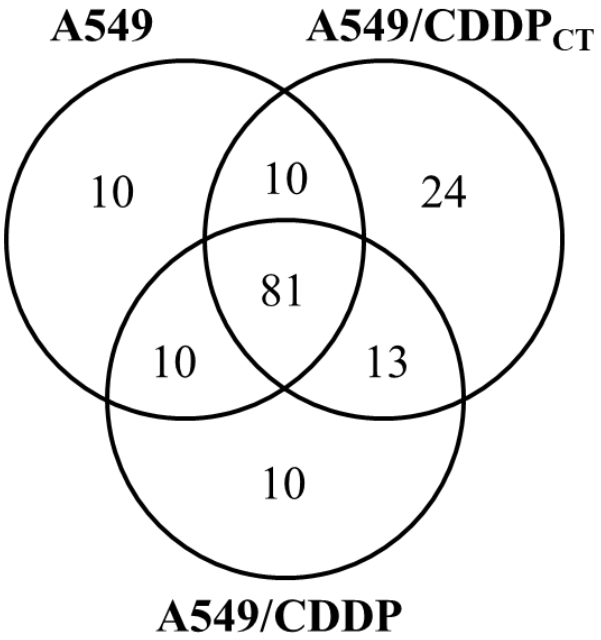

Figure 6: Overview of the proteins identified from A549, A549/CDDP$_{CT}$ and A549/CDDP cells. Venn diagrams of proteins identified by LC-MS/MS. Each assay was performed in triplicate and only proteins identified in at least two samples from triplicate and over 95% Scaffold probability were considered valid.

TABLES

Table 1: Cell cycle analysis from A549, A549/CDDP$_{CT}$ and A549/CDDP after cisplatin exposure. Statistical significance is represented between conditions as **a**, **b**, **c** e **d** ($p \leq 0.01$) and **e** ($p \leq 0.05$).

		Cisplatin (µM)		
		0	**0.25**	**0.5**
A549	**G1**	59.21 ± 2.10**ac**	55.88 ± 0.89**ad**	57.23 ± 1.24**e**
	S	8.39 ± 0.18	9.82 ± 0.21	9.05 ± 0.52
	G2	15.86 ± 1.26**b**	17.86 ± 0.13	18.40 ± 1.29**b**
A549/CDDP$_{CT}$	**G1**	52.42 ± 5.89	54.01 ± 2.62	51.96 ± 4.61
	S	11.58 ± 0.60	12.66 ± 0.41	11.06 ± 5.34
	G2	19.94 ± 2.45	15.53 ± 2.26	15.75 ± 1.32
A549/CDDP	**G1**	45.27 ± 8.61**c**	48.55 ± 4.63**d**	44.88 ± 8.96**e**
	S	13.05 ± 2.72	11.41 ± 1.07	13.00 ± 1.11
	G2	21.90 ± 2.30	21.01 ± 2.19	20.93 ± 3.68

SUPPLEMENTARY MATERIAL

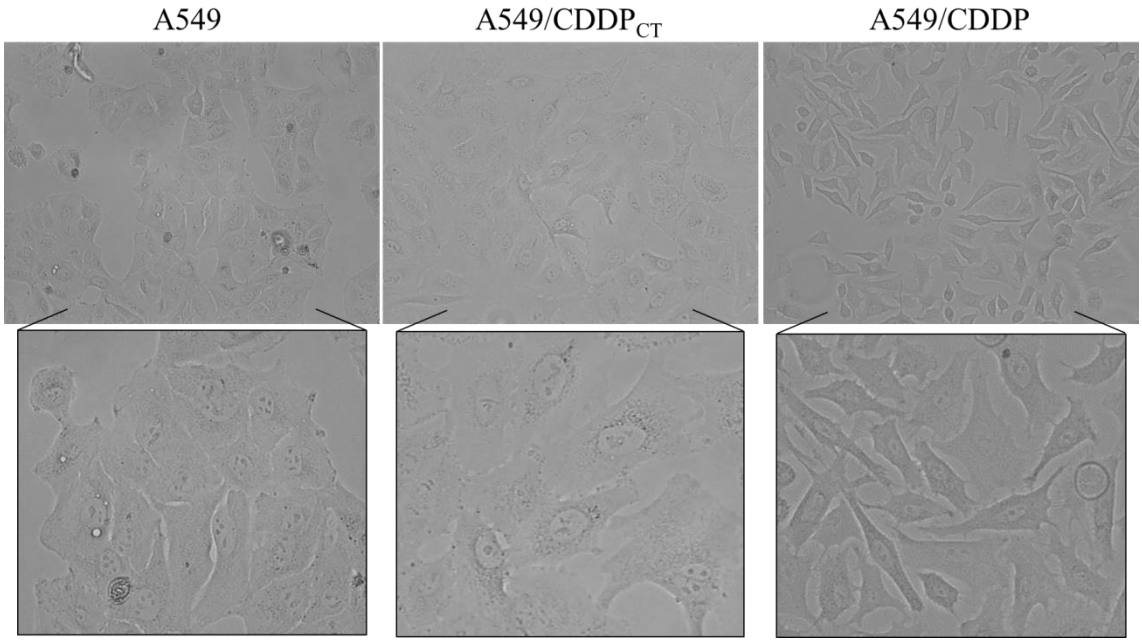

Supplementary Figure 1: Morphological differences between A549, A549/CDDP$_{CT}$ and A549/CDDP cells. Microscopies of the cells with 460X magnification (*up*) and manually enlarge highlight (*down*). Morphological changes undergone by A549 sublines after development of cisplatin resistance.

Supplementary Table 1: Protein identified by LC-MS/MS from A549, A549/$CDDP_{CT}$ and A549/CDDP. Proteins differentially expressed between cell line pairs (gray lines) are indicated with *p*-values and expression profiles (up ↑ or low ↓).

Identified Proteins	**Accession Number**	**Gene name**	**A549**	**A549 /CDDP$_{CT}$**	**A549 /CDDP**	A549 vs A549/ $CDDP_{CT}$	A549 vs A549/ CDDP	A549/ $CDDP_{CT}$ vs A549/ CDDP
10 kDa heat shock protein, mitochondrial	CH10_HUMAN	HSPE1	x	x	x	↑A549 ↓A549/ $CDDP_{CT}$ p = 0.036		
14-3-3 protein epsilon	1433E_HUMAN	YWHAE	x	x	x	↑A549 ↓A549/ $CDDP_{CT}$ p = 0.026		
14-3-3 protein gamma	1433G_HUMAN	YWHAG	x	x	x			
14-3-3 protein theta	1433T_HUMAN	YWHAQ	x	x	x			
14-3-3 protein zeta/delta	1433Z_HUMAN	YWHAZ	x	x	x	↑A549 ↓A549/ $CDDP_{CT}$ p = 0.032		
40S ribosomal protein S3a (Fragment)	D6RG13_HUMAN	RPS3A	x	x	x			
4F2 cell-surface antigen heavy chain	F5GZS6_HUMAN	SLC3A2	x	x	x			
60 kDa heat shock protein, mitochondrial	CH60_HUMAN	HSPD1	x	x	x	↑A549 ↓A549/ $CDDP_{CT}$ p = 0.037	↑A549 ↓A549/ CDPP p = 0.031	
60S acidic ribosomal protein P1	RLA1_HUMAN	RPLP1	x	x	x			
60S acidic ribosomal protein P2	RLA2_HUMAN	RPLP2	x	x	x	↑A549 ↓A549/ $CDDP_{CT}$ p = 0.020		
60S ribosomal protein L4	RL4_HUMAN	RPL4	x	x	x	↑A549 ↓A549/ $CDDP_{CT}$ p = 0.045		
78 kDa glucose-regulated protein	GRP78_HUMAN	HSPA5	x	x	x	↑A549 ↓A549/ $CDDP_{CT}$ p = 0.0081		↑A549/ CDDP

								↓A549/ $CDDP_{CT}$ p = 0.043
Actin, cytoplasmic 2	ACTG_HUMAN	ACTG1	x	x	x	↑A549 ↓A549/ $CDDP_{CT}$ p = 0.021		
Aldehyde dehydrogenase, dimeric NADP-preferring	AL3A1_HUMAN	ALDH3A1	x	x	x			
Aldo-keto reductase family 1 member B10	AK1BA_HUMAN	AKR1B10	x	x	x	↑A549 ↓A549/ $CDDP_{CT}$ p = 0.023	↑A549 ↓A549/ CDDP p = 0.0044	
Aldo-keto reductase family 1 member C1	AK1C1_HUMAN	AKR1C1	x	x	x		↑A549 ↓A549/ CDDP p = 0.025	
Aldo-keto reductase family 1 member C2	AK1C2_HUMAN	AKR1C2	x	x	x	↑A549 ↓A549/ $CDDP_{CT}$ p = 0.014		
Aldo-keto reductase family 1 member C3	AK1C3_HUMAN	AKR1C3	x	x	x	↑A549 ↓A549/ $CDDP_{CT}$ p = 0.026	↑A549 ↓A549/ CDDP p = 0.010	
Aldose reductase	ALDR_HUMAN	AKR1B1	x	x	x			
Alpha-actinin-4	ACTN4_HUMAN	ACTN4	x	x	x	↑A549 ↓A549/ $CDDP_{CT}$ p = 0.041		↑A549/ CDDP ↓A549/ $CDDP_{CT}$ p = 0.015
Alpha-enolase	ENOA_HUMAN	ENO1	x	x	x	↑A549 ↓A549/ $CDDP_{CT}$ p = 0.043		
Annexin A1	ANXA1_HUMAN	ANXA1	x	x	x			
Annexin A4	ANXA4_HUMAN	ANXA4	x	x	x	↑A549 ↓A549/ $CDDP_{CT}$ p = 0.0078	↑A549 ↓A549/ CDDP p = 0.0041	
Annexin A5	ANXA5_HUMAN	ANXA5	x	x	x	↑A549 ↓A549/ $CDDP_{CT}$ p = 0.0093		↑A549/ CDDP ↓A549/ $CDDP_{CT}$ p = 0.0008
ATP synthase subunit beta, mitochondria	ATPB_HUMAN	ATP5B	x	x	x			

l								
Brain acid soluble protein 1	BASP1_HUMAN	BASP1	x	x	x			
Calreticulin	CALR_HUMAN	CALR	x	x	x			↑A549/ CDDP ↓A549/ $CDDP_{CT}$ p = 0.016
Cofilin-1	E9PK25_HUMAN	CFL1	x	x	x			↑A549/ CDDP ↓A549/ $CDDP_{CT}$ p = 0.0081
Elongation factor 1-alpha 2	EF1A2_HUMAN	EEF1A2	x	x	x			
Elongation factor 2	EF2_HUMAN	EEF2	x	x	x	↑A549 ↓A540/ $CDDP_{CT}$ p = 0.020		
Endoplasmin	ENPL_HUMAN	HSP90B1	x	x	x	↑A549 ↓A540/ $CDDP_{CT}$ p = 0.015		↑A549/ CDDP ↓A540/ $CDDP_{CT}$ p = 0.049
Filamin-A	FLNA_HUMAN	FLNA	x	x	x			
Glutathione S-transferase P	GSTP1_HUMAN	GSTP1	x	x	x	↑A549 ↓A540/ $CDDP_{CT}$ p = 0.011	↑A549 ↓A540/ CDDP p = 0.021	
Glyceraldehyde-3-phosphate dehydrogenase	G3P_HUMAN	GAPDH	x	x	x	↑A549 ↓A540/ $CDDP_{CT}$ p = 0.029		
Heat shock 70 kDa protein 1B	HS71B_HUMAN	HSPA1B	x	x	x	↑A549 ↓A540/ $CDDP_{CT}$ p = 0.0042	↑A549 ↓A540/ CDDP p = 0.024	↑A549/ CDDP ↓A540/ $CDDP_{CT}$ p = 0.046
Heat shock cognate 71 kDa protein	HSP7C_HUMAN	HSPA8	x	x	x	↑A549 ↓A540/ $CDDP_{CT}$ p = 0.013	↑A549 ↓A540/ CDDP p = 0.048	
Heat shock protein beta-1	HSPB1_HUMAN	HSPB1	x	x	x	↑A549 ↓A540/ $CDDP_{CT}$ p = 0.0046		↑A549/ CDDP ↓A540/ $CDDP_{CT}$ p = 0.0013
Heat shock protein HSP 90-beta	HS90B_HUMAN	HSP90AB1	x	x	x	↑A549 ↓A540/ $CDDP_{CT}$ p = 0.021		

Histone H1.3	H13_HUMAN	HIST1H1D	x	x	x	↑A549 ↓A540/ $CDDP_{CT}$ p = 0.021	↑A549 ↓A540/ CDDP p = 0.019	
Histone H2B	U3KQK0_HUMAN	HIST1H2BN	x	x	x			
Histone H3.2	H32_HUMAN	HIST2H3A	x	x	x			
Histone H4	H4_HUMAN	HIST1H4A	x	x	x	↑A549 ↓A540/ $CDDP_{CT}$ p = 0.025	↑A549 ↓A540/ CDDP p = 0.026	
Isoform 1 of Vinculin	P18206-2 VINC_HUMAN	VCL	x	x	x		↑A549/ CDDP ↓A549 p = 0.014	↑A549/ CDDP ↓A540/ $CDDP_{CT}$ p = 0.0080
Isoform 2 of Annexin A2	P07355-2 ANXA2_HUMAN	ANXA2	x	x	x			↑A549/ CDDP ↓A540/ $CDDP_{CT}$ p = 0.0059
Isoform 2 of Fructose-bisphosphate aldolase A	P04075-2 ALDOA_HUMAN	ALDOA	x	x	x			
Isoform 2 of Heterogeneous nuclear ribonucleoprotein K	P61978-2 HNRPK_HUMAN	HNRNPK	x	x	x	↑A549 ↓A540/ $CDDP_{CT}$ p = 0.019		
Isoform 2 of Triosephosphate isomerase	P60174-TPIS_HUMAN	TPI1	x	x	x			
Isoform 3 of Beta-enolase	P13929-ENOB_HUMAN	ENO3	x	x	x			
Isoform 3 of Glucose-6-phosphate 1-dehydrogenase	P11413-G6PD_HUMAN	G6PD	x	x	x			
Isoform 3 of L-lactate dehydrogenase A chain	P00338-LDHA_HUMAN	LDHA	x	x	x			
Isoform 5 of Protein disulfide-isomerase A6	Q15084-5 PDIA6_HUMAN	PDIA6	x	x	x	↑A549 ↓A540/ $CDDP_{CT}$ p = 0.026		
Keratin, type I cytoskeletal 18	K1C18_HUMAN	KRT18	x	x	x		↑A549 ↓A549/ CDDP p = 0.018	
Keratin, type	K2C1_HUM	KRT1	x	x	x			

II cytoskeletal 1	AN							
Keratin, type II cytoskeletal 7	K2C7_HUMAN	KRT7	x	x	x		↑A549 ↓A549/ CDDP p = 0.036	
Kynureninase	KYNU_HUMAN	KYNU	x	x	x	↑A549 ↓A549/ $CDDP_{CT}$ p = 0.046		
L-lactate dehydrogenase B chain	LDHB_HUMAN	LDHB	x	x	x		↑A549 ↓A549/ CDDP p = 0.044	
Malate dehydrogenase, mitochondrial	MDHM_HUMAN	MDH2	x	x	x			
Myosin-9	MYH9_HUMAN	MYH9	x	x	x			↑A549/ CDDP ↓A549/ $CDDP_{CT}$ p = 0.0079
Nicotinamide N-methyltransferase	NNMT_HUMAN	NNMT	x	x	x			
Nucleoside diphosphate kinase	Q32Q12_HUMAN	NME1-NME2	x	x	x	↑A549 ↓A549/ $CDDP_{CT}$ p = 0.025		
Peptidyl-prolyl cis-trans isomerase A	PPIA_HUMAN	PPIA	x	x	x	↑A549 ↓A549/ $CDDP_{CT}$ p = 0.036		
Peroxiredoxin-1	PRDX1_HUMAN	PRDX1	x	x	x		↑A549 ↓A549/ CDDP p = 0.045	
Phosphoglycerate kinase 1	PGK1_HUMAN	PGK1	x	x	x			
Polypyrimidine tract-binding protein 1	PTBP1_HUMAN	PTBP1	x	x	x	↑A549 ↓A549/ $CDDP_{CT}$ p = 0.027		
Profilin-1	PROF1_HUMAN	PFN1	x	x	x	↑A549 ↓A549/ $CDDP_{CT}$ p = 0.038		↑A549/ CDDP ↓A549/ $CDDP_{CT}$ p = 0.038
Protein disulfide-isomerase A3	PDIA3_HUMAN	PDIA3	x	x	x			

Protein disulfide-isomerase	PDIA1_HUMAN	P4HB	x	x	x	↑A549 ↓A549/ $CDDP_{CT}$ p = 0.029		
Protein S100-A11	S10AB_HUMAN	S100A11	x	x	x			
Protein-glutamine gamma-glutamyltransferase 2	TGM2_HUMAN	TGM2	x	x	x			
Pyruvate kinase PKM	KPYM_HUMAN	PKM	x	x	x			
Retinal dehydrogenase 1	AL1A1_HUMAN	ALDH1A1	x	x	x			
Stress-70 protein, mitochondrial	GRP75_HUMAN	HSPA9	x	x	x			
Talin-1	TLN1_HUMAN	TLN1	x	x	x	↑A549 ↓A549/ $CDDP_{CT}$ p = 0.016		
Transgelin-2 (Fragment)	X6RJP6_HUMAN	TAGLN2	x	x	x			↑A549/ CDDP ↓A549/ $CDDP_{CT}$ p = 0.019
Transitional endoplasmic reticulum ATPase	TERA_HUMAN	VCP	x	x	x	↑A549 ↓A549/ $CDDP_{CT}$ p = 0.025		
Tubulin alpha-1B chain	TBA1B_HUMAN	TUBA1B	x	x	x	↑A549 ↓A549/ $CDDP_{CT}$ p = 0.029		
Tubulin beta chain	TBB5_HUMAN	TUBB	x	x	x			
Tubulin beta-4B chain	TBB4B_HUMAN	TUBB4B	x	x	x			
Ubiquitin carboxyl-terminal hydrolase isozyme L1	UCHL1_HUMAN	UCHL1	x	x	x			
UDP-glucose 6-dehydrogenase	UGDH_HUMAN	UGDH	x	x	x	↑A549 ↓A549/ $CDDP_{CT}$ p = 0.030		
Vimentin	VIME_HUMAN	VIM	x	x	x	↑A549 ↓A549/ $CDDP_{CT}$ p = 0.033	↑A549/ CDDP ↓A549 p = 0.0064	↑A549/ CDDP ↓A549/ $CDDP_{CT}$ p = 0.00086

40S ribosomal protein S13	RS13_HUMAN	RPS13	x	x				
ADP/ATP translocase 2	ADT2_HUMAN	SLC25A5	x	x		↑A549 ↓A549/ $CDDP_{CT}$ p = 0.0077		
Clathrin heavy chain	A0A087WVQ6_HUMAN	CLTC	x	x		↑A549 ↓A549/ $CDDP_{CT}$ p = 0.0030		
Heterogeneous nuclear ribonucleoprotein U	HNRPU_HUMAN	HNRNPU	x	x				
Isoform 2 of Calnexin	P27824-2 CALX_HUMAN	CANX	x	x				
Nicotinamide phosphoribosyltransferase	NAMPT_HUMAN	NAMPT	x	x				
Peroxiredoxin-4	PRDX4_HUMAN	PRDX4	x	x				
Peroxiredoxin-6	PRDX6_HUMAN	PRDX6	x	x				
Plastin-3	PLST_HUMAN	PLS3	x	x				
T-complex protein 1 subunit zeta	TCPZ_HUMAN	CCT6A	x	x				
40S ribosomal protein S7	RS7_HUMAN	RPS7	x		x			
Epoxide hydrolase 1	HYEP_HUMAN	EPHX1	x		x			
Heterogeneous nuclear ribonucleoprotein A1	F8W6I7_HUMAN	HNRNPA1	x		x			
Isoform 2 of Transketolase	P29401-2 TKT_HUMAN	TKT	x		x		↑A549 ↓A549/ CDDP p = 0.046	
Matrin-3	MATR3_HUMAN	MATR3	x		x			
Moesin	MOES_HUMAN	MSN	x		x			
NAD(P)H dehydrogenase [quinone] 1	B4DLR8_HUMAN	NQO1	x		x			
Prosaposin	C9JIZ6_HUMAN	PSAP	x		x			
Rab GDP dissociation inhibitor beta	GDIB_HUMAN	GDI2	x		x			

X-ray repair cross-complementing protein 5	XRCC5_HUMAN	XRCC5	x		x			
40S ribosomal protein SA	C9J9K3_HUMAN	RPSA		x	x			
Elongation factor 1-alpha 1	EF1A1_HUMAN	EEF1A1		x	x			
Eukaryotic translation initiation factor 5A-1	I3L504_HUMAN	EIF5A		x	x			
Isoform 2 of Heat shock protein HSP 90-alpha	P07900-2 HS90A_HUMAN	HSP90AA1		x	x			
Isoform 2 of Keratin, type II cytoskeletal 8	P05787-2 K2C8_HUMAN	KRT8		x	x			
Isoform 2 of Nucleophosmin	P06748-2 NPM_HUMAN	NPM1		x	x			
Isoform 9 of Filamin-B	O75369-9 FLNB_HUMAN	FLNB		x	x			
Peptidyl-prolyl cis-trans isomerase B	PPIB_HUMAN	PPIB		x	x			
Phosphoglycerate mutase 1	PGAM1_HUMAN	PGAM1		x	x			
Plectin	PLEC_HUMAN	PLEC		x	x			
Reticulon-4	RTN4_HUMAN	RTN4		x	x			
Serpin H1	SERPH_HUMAN	SERPINH1		x	x			
X-ray repair cross-complementing protein 6	B1AHC9_HUMAN	XRCC6		x	x			
40S ribosomal protein S4, X isoform	RS4X_HUMAN	RPS4X	x					
60S acidic ribosomal protein P0	F8VWS0_HUMAN	RPLP0	x					
60S ribosomal protein L7	RL7_HUMAN	RPL7	x					

Anterior gradient protein 2 homolog	AGR2_HUMAN	AGR2	x					
Cathepsin D	CATD_HUMAN	CTSD	x					
Galectin-1	LEG1_HUMAN	LGALS1	x					
Heat shock protein HSP 90-alpha	HS90A_HUMAN	HSP90AA1	x					
Isoform 2 of Thioredoxin-dependent peroxide reductase, mitochondrial	P30048-2 PRDX3_HUMAN	PRDX3	x					
Thioredoxin reductase 1, cytoplasmic	TRXR1_HUMAN	TXNRD1	x					
Tubulin beta-6 chain	TBB6_HUMAN	TUBB6	x					
40S ribosomal protein S28	RS28_HUMAN	RPS28		x				
40S ribosomal protein S8	RS8_HUMAN	RPS8		x				
60S ribosomal protein L12	RL12_HUMAN	RPL12		x				
60S ribosomal protein L7a	RL7A_HUMAN	RPL7A		x				
60S ribosomal protein L8 (Fragment)	E9PKZ0_HUMAN	RPL8		x				
60S ribosomal protein L9 (Fragment)	D6RAN4_HUMAN	RPL9		x				
Flavin reductase (NADPH)	BLVRB_HUMAN	BLVRB		x				
Glucosidase 2 subunit beta	K7ELL7_HUMAN	PRKCSH		x				
GTP-binding nuclear protein Ran (Fragment)	J3KQE5_HUMAN	RAN		x				
Heterogeneous nuclear ribonucleopr	G3V2Q1_HUMAN	HNRNPC		x				

oteins C1/C2								
Isoform 2 of ATP-dependent 6-phosphofructokinase, platelet type	Q01813-2 PFKAP_HUMAN	PFKP		x				
Isoform 2 of Elongation factor 1-gamma	P26641-2 EF1G_HUMAN	EEF1G		x				
Isoform 2 of T-complex protein 1 subunit delta	P50991-2 TCPD_HUMAN	CCT4		x				
Isoform 2 of Tropomyosin alpha-4 chain	P67936-2 TPM4_HUMAN	TPM4		x				
Isoform Cytoplasmic+peroxisomal of Peroxiredoxin-5, mitochondrial	P30044-2 PRDX5_HUMAN	PRDX5		x				
Isoform Short of 14-3-3 protein beta/alpha	P31946-2 1433B_HUMAN	YWHAB		x				
Macrophage migration inhibitory factor	MIF_HUMAN	MIF		x				
Nucleolin	NUCL_HUMAN	NCL		x				
Protein deglycase DJ-1	PARK7_HUMAN	PARK7		x				
Transaldolase	TALDO_HUMAN	TALDO1		x				
Trifunctional enzyme subunit alpha, mitochondrial	ECHA_HUMAN	HADHA		x				
Tubulin beta-2A chain	TBB2A_HUMAN	TUBB2A		x				
Tubulin beta-3 chain	TBB3_HUMAN	TUBB3		x				
Voltage-dependent anion-selective channel	VDAC1_HUMAN	VDAC1		x				

protein 1								
ATP-citrate synthase	ACLY_HUMAN	ACLY			x			
Calpain-2 catalytic subunit	CAN2_HUMAN	CAPN2			x			
Catenin alpha-1	CTNA1_HUMAN	CTNNA1			x			
Destrin	F6RFD5_HUMAN	DSTN			x			
Eukaryotic initiation factor 4A-I	IF4A1_HUMAN	EIF4A1			x			
Isoform 2 of 6-phosphogluconate dehydrogenase, decarboxylating	P52209-2 6PGD_HUMAN	PGD			x			
Isoform 4 of Alpha-actinin-1	P12814-4 ACTN1_HUMAN	ACTN1			x			
Keratin, type II cuticular Hb1	A0A087X106_HUMAN	KRT81			x			
Myosin light polypeptide 6	J3KND3_HUMAN	MYL6			x			
Surfeit 4	Q5T8U5_HUMAN	SURF4			x			

Supplementary Table 2A: Significant gene ontology terms from A549. Ontologies statistical significant ($p < 0.05$) identified by Cytoscape plugin BiNGO and grouped by REVIGO.

p value	Gene ontology	Proteins
A549		
9,75E-03	4-hydroxyproline metabolic process	UGDH
9,99E-04	actin cytoskeleton organization	MYH9|ACTN4|PFN1|TLN1|HSP90B1|ACTN4|HSP90B1
2,61E-02	actin filament organization	ACTN4|HSP90B1
1,32E-03	actin filament-based process	MYH9|ACTN4|PFN1|TLN1|HSP90B1
3,26E-03	actin rod assembly	HSPD1
6,51E-03	activation of signaling protein activity involved in unfolded protein response	HIST1H4A
1,30E-02	aggresome assembly	ENO1
2,10E-03	alcohol catabolic process	LDHB|ENO1|GAPDH
2,58E-02	anatomical structure arrangement	HSPD1
3,26E-03	anthranilate metabolic process	KYNU
3,26E-03	B cell cytokine production	PRDX3
1,94E-02	benzene and derivative metabolic process	MYH9
6,51E-03	benzoate metabolic process	HSPA5
2,90E-02	bile acid and bile salt transport	TLN1
3,17E-04	biological regulation	YWHAE|VCP|HSP90AB1|GSTP1|HSPB1|ENO1|HSPD1|HSP90B1|RPS4X|PRDX3|LGALS1|PRDX1|AGR2|HSP90AA1|HSPA5|ANXA4|AKR1C1|TXNRD1|ANXA5|NME2|KRT7|ACTN4|HSPE1|YWHAZ|PDIA6|NME1|HIST1H4A|HNRNPK|KRT18|MYH9|P4HB|PFN1|TLN1|TKT|PPIA|HSPA1B
3,16E-06	biological_process	YWHAE|RPL4|HSP90AB1|CLTC|RPLP0|HSPB1|ENO1|ACTG1|RPL7|RPS4X|PTBP1|TUBA1B|TUBB6|LGALS1|KYNU|HIST1H1D|RPLP2|CTSD|HSP90AA1|ANXA4|ANXA5|NME2|KRT7|ACTN4|YWHAZ|PDIA6|NME1|UGDH|MYH9|PFN1|TLN1|SLC25A5|TKT|GAPDH|PPIA|VCP|GSTP1|HSPD1|HSP90B1|PRDX3|LDHB|PRDX1|AGR2|HSPA8|HSPA5|AKR1C1|TXNRD1|AKR1C3|AKR1C2|HSPE1|EEF2|HIST1H4A|AKR1B10|HNRNPK|KRT18|P4HB|VIM|HSPA1B
2,89E-02	biosynthetic process	RPL4|RPS4X|UGDH|KYNU|RPLP0|NME2|RPLP2|KRT7|EEF2|RPL7|NME1
7,97E-05	catabolic process	PRDX3|LDHB|VCP|HSPA5|KYNU|PRDX1|MYH9|ENO1|CTSD|GAPDH|HSPA1B|HSP90B1

1,83E-03	cell death	YWHAE|VCP|LGALS1|HSPB1|PFN1|HSPE1|CTSD|HSPD1
2,37E-06	cell redox homeostasis	PRDX3|PRDX1|TXNRD1|P4HB|PDIA6
1,90E-02	cellular biosynthetic process	RPL4|RPS4X|UGDH|KYNU|RPLP0|NME2|RPLP2|KRT7|EEF2|RPL7|NME1
5,77E-06	cellular component assembly	HSP90AA1|VCP|AKR1C1|ANXA5|ACTN4|HSPD1|HSP90B1|TUBA1B|TUBB6|HIST1H4A|HIST1H1D|TLN1|CTSD|TUBA1B|TUBB6|HSP90AA1|VCP|HIST1H4A|AKR1C1|ANXA5|HIST1H1D|HSPD1
7,50E-07	cellular component biogenesis	HSP90AA1|VCP|AKR1C1|RPLP0|ANXA5|ACTN4|RPL7|HSPD1|HSP90B1|TUBA1B|TUBB6|HIST1H4A|HIST1H1D|TLN1|CTSD
4,35E-03	cellular component movement	YWHAE|HSPB1|MYH9|VIM|TLN1|ACTG1
3,02E-05	cellular component organization	HSPA8|HSP90AA1|VCP|AKR1C1|CLTC|ANXA5|KRT7|ACTN4|YWHAZ|NME1|HSPD1|HSP90B1|PRDX3|TUBA1B|TUBB6|HIST1H4A|HIST1H1D|MYH9|PFN1|TLN1|CTSD
4,00E-03	cellular homeostasis	PRDX3|PRDX1|TXNRD1|P4HB|PDIA6|HSP90B1
2,61E-03	cellular ketone metabolic process	UGDH|LDHB|KYNU|AKR1C1|AKR1C3|AKR1C2|P4HB
4,12E-03	cellular localization	YWHAE|HSPA8|HSP90AA1|VCP|KRT18|CLTC|MYH9|TLN1|YWHAZ
5,58E-04	cellular macromolecular complex assembly	TUBA1B|TUBB6|HSP90AA1|HIST1H4A|HIST1H1D|HSPD1
1,43E-02	cellular macromolecule catabolic process	VCP|HSPA5|MYH9|HSPA1B|HSP90B1
1,37E-02	cellular macromolecule localization	YWHAE|VCP|KRT18|CLTC|YWHAZ
1,26E-04	cellular macromolecule metabolic process	RPL4|HSPA8|HSP90AA1|VCP|HSP90AB1|HSPA5|CLTC|RPLP0|KRT7|HSPE1|EEF2|PDIA6|RPL7|HSPD1|HSP90B1|RPS4X|PTBP1|HNRNPK|RPLP2|MYH9|P4HB|TKT|PPIA|HSPA1B
6,12E-10	cellular metabolic process	RPL4|VCP|HSP90AB1|CLTC|RPLP0|ENO1|RPL7|HSPD1|HSP90B1|RPS4X|PRDX3|PTBP1|LDHB|KYNU|PRDX1|RPLP2|CTSD|HSPA8|HSP90AA1|HSPA5|AKR1C1|TXNRD1|NME2|AKR1C3|KRT7|AKR1C2|HSPE1|EEF2|PDIA6|NME1|UGDH|AKR1B10|HNRNPK|MYH9|P4HB|TKT|GAPDH|PPIA|HSPA1B
1,47E-02	cellular nitrogen compound metabolic process	VCP|NME2|KRT7|RPL7|NME1|HSPD1|PTBP1|UGDH|LDHB|HNRNPK|KYNU|PPIA|HSPA1B

2,00E-11	cellular process	YWHAE|RPL4|HSP90AB1|CLTC|RPLP0|HSPB1|ENO1|ACTG1|RPL7|RPS4X|PTBP1|TUBA1B|TUBB6|LGALS1|KYNU|HIST1H1D|RPLP2|CTSD|HSP90AA1|NME2|KRT7|ACTN4|YWHAZ|PDIA6|NME1|UGDH|MYH9|PFN1|TLN1|SLC25A5|TKT|GAPDH|PPIA|VCP|HSPD1|HSP90B1|PRDX3|LDHB|PRDX1|HSPA8|HSPA5|AKR1C1|TXNRD1|AKR1C3|AKR1C2|HSPE1|EEF2|HIST1H4A|AKR1B10|HNRNPK|KRT18|P4HB|VIM|HSPA1B
1,48E-03	cellular protein complex assembly	TUBA1B|TUBB6|HSP90AA1|HSPD1|TUBA1B|TUBB6|TUBA1B|TUBB6|HSP90AA1|VCP|AKR1C1|ANXA5|HSPD1
7,91E-06	cellular protein metabolic process	RPL4|HSPA8|HSP90AA1|VCP|HSP90AB1|HSPA5|RPLP0|HSPE1|EEF2|PDIA6|RPL7|HSPD1|HSP90B1|RPS4X|RPLP2|MYH9|P4HB|TKT|PPIA|HSPA1B
9,75E-03	cellular response to ATP	HSPD1
1,11E-02	cellular response to biotic stimulus	NME2|NME1
4,29E-05	cellular response to chemical stimulus	PRDX3|VCP|LGALS1|HSPA5|KYNU|PRDX1|AKR1C1|HSP90B1
1,30E-02	cellular response to glucose stimulus	HSP90AA1|KYNU|TKT|HSPD1
2,99E-03	cellular response to hydrogen peroxide	HSP90AA1|HSP90AB1|HIST1H4A|HIST1H1D|RPL7|AKR1C1|TLN1|HSP90B1|PRDX1|TLN1|P4HB|PRDX3|PRDX1
1,30E-02	cellular response to monosaccharide stimulus	HSPD1
2,55E-02	cellular response to nutrient levels	ACTN4|HSPA1B
9,75E-03	cellular response to organic cyclic substance	HSP90B1
7,64E-03	cellular response to organic substance	VCP|LGALS1|HSPA5|HSP90B1
3,48E-03	cellular response to protein stimulus	VCP|HSP90AB1|HSPA8|HSP90AA1|VCP|HSPA5|HSPB1|HSPE1|HSPA1B|HSPD1
6,81E-03	cellular response to reactive oxygen species	PRDX3|PRDX1
8,66E-03	cellular response to starvation	HSPA5|CTSD|AKR1C1|ACTN4|HSPA1B
4,40E-03	cellular response to stimulus	PRDX3|VCP|LGALS1|HSPA5|KYNU|PRDX1|AKR1C1|CTSD|HSP90B1
2,11E-03	cellular response to unfolded protein	VCP|HSPA5
5,17E-03	cellular response to xenobiotic stimulus	KYNU|AKR1C1
2,58E-02	cerebellar Purkinje cell layer development	AKR1C1

6,51E-03	cerebellum structural organization	LGALS1|KYNU
2,17E-04	chaperone-mediated protein complex assembly	PRDX3|PRDX1
3,27E-02	chromatin assembly	HIST1H4A|HIST1H1D
9,75E-03	cytokine production involved in immune response	PRDX1
2,26E-02	cytoskeletal anchoring at plasma membrane	TLN1
6,08E-04	cytoskeleton organization	TUBA1B|KRT7|MYH9|ACTN4|PFN1|TLN1|HSP90B1
1,91E-03	death	YWHAE|VCP|LGALS1|HSPB1|PFN1|HSPE1|CTSD|HSPD1
3,26E-03	digestion	AKR1B10|AKR1C1|AKR1C2
3,21E-02	ER overload response	MYH9
1,92E-02	ER-associated ubiquitin-dependent protein catabolic process	VCP|HSPA5|MYH9|HSP90B1|YWHAE|VCP|HSPA5|VCP|HSP90AB1|VCP|HSPA5|HSP90B1
6,13E-03	ER-nucleus signaling pathway	NME2|NME1
1,80E-02	establishment of localization	YWHAE|HSPA8|HSP90AA1|VCP|AKR1C1|TXNRD1|CLTC|ACTN4|YWHAZ|NME1|HSP90B1|KRT18|AGR2|MYH9|SLC25A5
6,72E-03	establishment of localization in cell	YWHAE|HSPA8|HSP90AA1|VCP|KRT18|CLTC|MYH9|YWHAZ
6,51E-03	establishment of lymphocyte polarity	LGALS1
6,51E-03	establishment of meiotic spindle localization	ACTN4|HSPD1
3,27E-03	establishment of protein localization	YWHAE|VCP|KRT18|CLTC|MYH9|ACTN4|YWHAZ|HSP90B1
3,53E-02	establishment of spindle localization	HSPD1
6,51E-03	establishment of T cell polarity	MYH9
6,51E-03	ferric iron transport	SLC25A5
2,81E-02	gastrulation	UGDH|TXNRD1
2,02E-02	gene expression	RPL4|RPS4X|PTBP1|HNRNPK|RPLP0|RPLP2|EEF2|RPL7|HSPD1
1,88E-02	generation of precursor metabolites and energy	LDHB|TXNRD1|ENO1|GAPDH
1,62E-02	glucuronate metabolic process	TXNRD1

1,30E-03	glycolytic process	LDHB|ENO1|GAPDH|MYH9|UGDH|LDHB|ENO1|GAPDH|NME2|NME1|PRDX3|HSPA5|LDHB|KYNU|NME2|NME1|VCP|HSPA5|VCP|HSP90B1|KYNU|NME2|NME1|ANXA5|HSPD1|NME2|AKR1C1|AKR1C3|AKR1C2|LDHB|KYNU|TXNRD1
3,26E-03	Golgi to plasma membrane CFTR protein transport	HSP90B1|HSPA5|HSP90AB1
1,30E-02	Golgi to plasma membrane protein transport	HSP90AB1
9,01E-04	Golgi vesicle transport	HSPA8|VCP|KRT18|CLTC
4,62E-04	GTP biosynthetic process	NME2|NME1
6,75E-04	GTP metabolic process	NME2|NME1
2,41E-02	heterocycle metabolic process	KYNU|NME2|P4HB|NME1
6,51E-03	hindbrain structural organization	KYNU
3,26E-03	histamine secretion by mast cell	YWHAZ|KYNU|MYH9|HSPA5
1,26E-02	homeostatic process	PRDX3|PRDX1|AKR1C1|TXNRD1|P4HB|PDIA6|HSP90B1
1,38E-03	hydrogen peroxide catabolic process	NME2|NME1
3,23E-03	hydrogen peroxide metabolic process	PRDX3|PRDX1
8,60E-03	immune effector process	PRDX1|YWHAZ|HSPD1
1,30E-02	inclusion body assembly	YWHAE
9,17E-08	interspecies interaction between organisms	YWHAE|HSPA8|HNRNPK|KRT18|RPLP0|KRT7|VIM|SLC25A5|PPIA|HSPD1
2,58E-02	intestinal cholesterol absorption	KYNU
1,34E-03	intracellular transport	YWHAE|HSPA8|HSP90AA1|VCP|KRT18|CLTC|MYH9|YWHAZ
3,53E-02	isotype switching	HSPD1
3,26E-03	isotype switching to IgG isotypes	KRT18|HSPD1|MYH9
9,75E-03	lactate metabolic process	UGDH
3,53E-02	leukocyte mediated cytotoxicity	ACTN4|P4HB
2,51E-03	leukocyte mediated immunity	PRDX1|YWHAZ|HSPD1|PRDX1|HSPD1
3,21E-02	lipid digestion	PRDX1
2,63E-02	localization	YWHAE|HSPA8|HSP90AA1|VCP|AKR1C1|TXNRD1|CLTC|ACTN4|YWHAZ|NME1|HSP90B1|KRT18|AGR2|MYH9|TLN1|SLC25A5
1,80E-02	lymphocyte mediated immunity	PRDX1|HSPD1

3,15E-04	macromolecular complex assembly	TUBA1B|TUBB6|HSP90AA1|VCP|HIST1H4A|AKR1C1|ANXA5|HIST1H1D|HSPD1
5,19E-04	macromolecular complex subunit organization	TUBA1B|TUBB6|HSP90AA1|VCP|HIST1H4A|AKR1C1|ANXA5|HIST1H1D|HSPD1
2,04E-02	macromolecule biosynthetic process	RPL4|RPS4X|UGDH|RPLP0|RPLP2|KRT7|EEF2|RPL7
2,91E-03	macromolecule localization	YWHAE|VCP|KRT18|AKR1C1|CLTC|MYH9|ACTN4|TLN1|YWHAZ|HSP90B1
1,42E-04	macromolecule metabolic process	RPL4|VCP|HSP90AB1|CLTC|RPLP0|RPL7|HSPD1|HSP90B1|RPS4X|PTBP1|RPLP2|CTSD|HSPA8|HSP90AA1|HSPA5|KRT7|HSPE1|EEF2|PDIA6|UGDH|HNRNPK|MYH9|P4HB|TKT|PPIA|HSPA1B
3,21E-02	maintenance of location	PRDX3|PRDX1
2,26E-02	mast cell activation	YWHAZ
1,62E-02	mast cell degranulation	YWHAZ
1,94E-02	mast cell mediated immunity	YWHAZ
6,51E-03	meiotic metaphase I	KYNU
1,30E-02	meiotic spindle organization	P4HB
3,53E-08	metabolic process	RPL4|VCP|HSP90AB1|GSTP1|CLTC|RPLP0|ENO1|RPL7|HSPD1|HSP90B1|RPS4X|PRDX3|PTBP1|LDHB|KYNU|PRDX1|RPLP2|CTSD|HSPA8|HSP90AA1|HSPA5|AKR1C1|TXNRD1|NME2|AKR1C3|KRT7|AKR1C2|HSPE1|EEF2|PDIA6|NME1|UGDH|AKR1B10|HNRNPK|MYH9|P4HB|TKT|GAPDH|PPIA|HSPA1B
1,94E-02	metaphase	KYNU
1,30E-02	mitochondrial outer membrane translocase complex assembly	ACTN4
2,49E-02	mitochondrial transport	HSP90AA1|YWHAZ
8,97E-03	mitochondrion organization	PRDX3|HSP90AA1|YWHAZ
5,66E-05	monocarboxylic acid metabolic process	UGDH|LDHB|KYNU|AKR1C1|AKR1C3|AKR1C2|P4HB
1,62E-02	monocyte differentiation	HSPD1
3,26E-03	mucus secretion	AKR1C3
3,22E-02	multicellular organismal process	YWHAE|HSP90AB1|HSPA5|GSTP1|AKR1C1|TXNRD1|ANXA5|AKR1C2|YWHAZ|NME1|HSPD1|RPS4X|PRDX3|UGDH|LGALS1|AKR1B10|PRDX1|AGR2|MYH9|PFN1|TLN1
1,09E-06	multi-organism process	YWHAE|HSPA8|RPLP0|HSPB1|KRT7|ENO1|HSPD1|PRDX3|HNRNPK|KRT18|VIM|SLC25A5|PPIA
1,62E-02	MyD88-dependent toll-like receptor signaling pathway	HSPA1B
3,53E-02	myoblast fusion	NME1
2,58E-02	NAD biosynthetic process	HSPA5

2,58E-02	natural killer cell mediated cytotoxicity	P4HB
2,58E-02	natural killer cell mediated immunity	PPIA
1,22E-05	negative regulation of biological process	YWHAE|HSP90AB1|HSPA5|ANXA4|GSTP1|ANXA5|NME2|HSPB1|ENO1|ACTN4|YWHAZ|NME1|HSPD1|HSP90B1|PRDX3|HIST1H4A|LGALS1|KRT18|HSPA1B
3,21E-06	negative regulation of cellular process	YWHAE|HSP90AB1|HSPA5|ANXA4|GSTP1|ANXA5|NME2|HSPB1|ENO1|ACTN4|YWHAZ|NME1|HSPD1|HSP90B1|PRDX3|HIST1H4A|LGALS1|KRT18|HSPA1B
1,30E-02	negative regulation of dephosphorylation	ACTN4
9,75E-03	negative regulation of inclusion body assembly	UGDH|VCP|ENO1
1,83E-04	negative regulation of myeloid cell differentiation	HIST1H4A|NME2|NME1|MYH9|YWHAZ|NME2|NME1
2,31E-03	negative regulation of myeloid leukocyte differentiation	NME2|NME1
2,88E-09	negative regulation of programmed cell death	PRDX3|KRT18|HSPA5|ANXA4|GSTP1|ANXA5|NME2|HSPB1|YWHAZ|HSPA1B|HSPD1|HSP90B1|YWHAE|VCP|HSPA5|ANXA4|GSTP1|ANXA5|NME2|HSPB1|ACTN4|HSPE1|YWHAZ|NME1|HSPD1|HSP90B1|PRDX3|LGALS1|KRT18|PRDX1|HSPA1B
9,58E-03	nitrogen compound metabolic process	VCP|NME2|KRT7|RPL7|NME1|HSPD1|PTBP1|UGDH|LDHB|HNRNPK|KYNU|P4HB|PPIA|HSPA1B
2,22E-02	nucleobase, nucleoside, nucleotide and nucleic acid biosynthetic process	KYNU|NME2|NME1
4,27E-03	nucleobase, nucleoside, nucleotide and nucleic acid metabolic process	VCP|NME2|KRT7|RPL7|NME1|HSPD1|PTBP1|UGDH|LDHB|HNRNPK|KYNU|PPIA|HSPA1B
1,94E-02	nucleosome positioning	LDHB|PRDX3|TXNRD1|HIST1H4A|HIST1H1D
1,07E-04	organelle organization	HSP90AA1|CLTC|KRT7|ACTN4|YWHAZ|HSP90B1|PRDX3|TUBA1B|HIST1H4A|HIST1H1D|MYH9|PFN1|TLN1|CTSD
2,44E-03	organic acid metabolic process	UGDH|LDHB|KYNU|AKR1C1|AKR1C3|AKR1C2|P4HB
1,30E-02	outer mitochondrial membrane organization	LGALS1
4,07E-05	oxidation reduction	PRDX3|UGDH|LDHB|AKR1B10|PRDX1|AKR1C1|TXNRD1|AKR1C3|AKR1C2|GAPDH
2,28E-03	oxoacid metabolic process	UGDH|LDHB|KYNU|AKR1C1|AKR1C3|AKR1C2|P4HB

1,91E-02	oxygen and reactive oxygen species metabolic process	PRDX3|PRDX1
9,75E-03	peptidyl-proline hydroxylation	KYNU|HSP90B1
9,75E-03	peptidyl-proline hydroxylation to 4-hydroxy-L-proline	HSP90B1
1,30E-02	peptidyl-proline modification	HSPA5
3,27E-02	placenta development	PRDX3|HSP90AB1
6,51E-03	platelet formation	HSP90AB1
1,00E-02	positive regulation of biological process	YWHAE|HSP90AA1|VCP|HSP90AB1|HSPA5|NME2|ACTN4|NME1|HSPD1|RPS4X|PRDX3|LGALS1|PRDX1|TKT
1,67E-02	positive regulation of cell proliferation	RPS4X|PRDX3|NME2|TKT|NME1
4,29E-03	positive regulation of cellular process	YWHAE|HSP90AA1|VCP|HSP90AB1|HSPA5|NME2|ACTN4|NME1|HSPD1|RPS4X|PRDX3|LGALS1|PRDX1|TKT
1,62E-02	positive regulation of epidermal cell differentiation	YWHAZ|PRDX1|ENO1|LDHB
9,05E-03	positive regulation of epithelial cell proliferation	NME2|NME1
3,26E-03	positive regulation of erythrocyte aggregation	LGALS1|HSPD1
3,95E-03	positive regulation of hydrolase activity	VCP|HSPA5|HSPE1|HSPD1
1,30E-02	positive regulation of interferon-alpha production	SLC25A5|PFN1
2,58E-02	positive regulation of interleukin-10 production	HSPD1
3,21E-02	positive regulation of interleukin-12 production	ANXA5
3,53E-02	positive regulation of ion transmembrane transporter activity	MYH9
1,62E-02	positive regulation of keratinocyte differentiation	LDHB
1,30E-02	positive regulation of macrophage activation	LGALS1|NME2
4,54E-03	positive regulation of molecular function	PRDX3|VCP|HSPA5|ACTN4|HSPE1|NME1|HSPD1
2,99E-03	positive regulation of nitric oxide biosynthetic process	PRDX3|PRDX1|PRDX3|HSPA5

9,75E-03	positive regulation of nuclease activity	P4HB|HIST1H4A
6,51E-03	positive regulation of pinocytosis	MYH9|HSPD1
2,90E-02	positive regulation of response to biotic stimulus	ACTN4
6,51E-03	positive regulation of sodium:hydrogen antiporter activity	HSPA5|LGALS1
3,53E-02	positive regulation of T cell mediated immunity	HSPD1
8,49E-04	post-Golgi vesicle-mediated transport	HSPA8|KRT18|CLTC
7,87E-03	posttranscriptional regulation of gene expression	RPS4X|HSPB1|KRT7|HSPD1
1,25E-06	primary metabolic process	RPL4|VCP|HSP90AB1|RPLP0|ENO1|RPL7|HSPD1|HSP90B1|RPS4X|PTBP1|LDHB|KYNU|RPLP2|CTSD|HSPA8|HSP90AA1|HSPA5|AKR1C1|NME2|AKR1C3|KRT7|AKR1C2|HSPE1|EEF2|PDIA6|NME1|UGDH|AKR1B10|HNRNPK|MYH9|P4HB|TKT|GAPDH|PPIA|HSPA1B
1,94E-02	production of molecular mediator involved in inflammatory response	LGALS1
2,11E-03	prostaglandin metabolic process	AKR1C3|AKR1C2
2,11E-03	prostanoid metabolic process	AKR1C3|AKR1C2
2,46E-02	protein catabolic process	VCP|HSPA5|MYH9|HSP90B1|VCP|HSPA5|MYH9|HSPA1B|HSP90B1|PRDX3|VCP|HSPA5|KYNU|PRDX1|MYH9|CTSD|HSPA1B|HSP90B1
1,25E-03	protein complex assembly	TUBA1B|TUBB6|HSP90AA1|VCP|AKR1C1|ANXA5|HSPD1
1,25E-03	protein complex biogenesis	TUBA1B|TUBB6|HSP90AA1|VCP|AKR1C1|ANXA5|HSPD1
3,83E-09	protein folding	HSPA8|HSP90AA1|HSP90AB1|HSPE1|PDIA6|PPIA|HSPA1B|HSPD1|HSP90B1
4,74E-03	protein homooligomerization	VCP|AKR1C1|ANXA5
4,00E-05	protein metabolic process	RPL4|HSPA8|HSP90AA1|VCP|HSP90AB1|HSPA5|RPLP0|HSPE1|EEF2|PDIA6|RPL7|HSPD1|HSP90B1|RPS4X|RPLP2|MYH9|P4HB|TKT|CTSD|PPIA|HSPA1B
2,41E-02	protein oligomerization	VCP|AKR1C1|ANXA5
2,72E-06	protein refolding	HSP90AA1|HSPA1B|HSPD1
3,00E-03	protein transport	YWHAE|VCP|KRT18|CLTC|MYH9|ACTN4|YWHAZ|HSP90B1|YWHAE|VCP|KRT18|CLTC|YWHAZ|YWHAE|VCP|KRT18|CLTC|MYH9|ACTN4|TLN1|YWHAZ|HSP90B1

1,86E-02	proteolysis involved in cellular protein catabolic process	VCP|HSPA5|MYH9|HSP90B1
9,27E-04	pyrimidine nucleoside triphosphate metabolic process	NME2|NME1
1,55E-03	pyrimidine ribonucleoside metabolic process	NME2|NME1
5,64E-04	pyrimidine ribonucleoside triphosphate biosynthetic process	NME2|NME1
5,64E-04	pyrimidine ribonucleoside triphosphate metabolic process	NME2|NME1
1,38E-03	pyrimidine ribonucleotide metabolic process	PRDX3|PRDX1|NME2|NME1
9,75E-03	quinolinate biosynthetic process	HSPA5|HSPD1
1,46E-03	regulation of biological process	YWHAE|VCP|HSP90AB1|GSTP1|HSPB1|ENO1|HSPD1|HSP90B1|RPS4X|PRDX3|LGALS1|PRDX1|HSP90AA1|HSPA5|ANXA4|TXNRD1|ANXA5|NME2|KRT7|ACTN4|HSPE1|YWHAZ|PDIA6|NME1|HIST1H4A|HNRNPK|KRT18|MYH9|P4HB|PFN1|TKT|PPIA|HSPA1B
9,10E-05	regulation of biological quality	AKR1C1|TXNRD1|ANXA5|ENO1|YWHAZ|PDIA6|HSPD1|HSP90B1|PRDX3|PRDX1|AGR2|MYH9|P4HB|TLN1|HSPA1B
1,51E-11	regulation of cell death	YWHAE|VCP|HSPA5|ANXA4|GSTP1|ANXA5|NME2|HSPB1|ACTN4|HSPE1|YWHAZ|NME1|HSPD1|HSP90B1|PRDX3|LGALS1|KRT18|PRDX1|HSPA1B|YWHAE|VCP|LGALS1|PFN1|HSPE1|HSPD1
3,19E-02	regulation of cell growth	ENO1|TKT|HSPA1B
1,28E-03	regulation of cellular process	YWHAE|VCP|HSP90AB1|GSTP1|HSPB1|ENO1|HSPD1|HSP90B1|RPS4X|PRDX3|LGALS1|PRDX1|HSP90AA1|HSPA5|ANXA4|TXNRD1|ANXA5|NME2|KRT7|ACTN4|HSPE1|YWHAZ|PDIA6|NME1|HIST1H4A|HNRNPK|KRT18|MYH9|P4HB|PFN1|TKT|HSPA1B
2,19E-03	regulation of cellular protein metabolic process	YWHAE|RPS4X|VCP|HSP90AB1|HSPA5|HSPB1|KRT7
4,87E-03	regulation of dephosphorylation	YWHAE|HSP90B1|ACTN4|KRT18
2,93E-04	regulation of endopeptidase activity	VCP|HSPA5|HSPE1|HSPD1|VCP|HSPE1|HSPD1
3,14E-02	regulation of epithelial cell proliferation	NME2|NME1

3,26E-03	regulation of erythrocyte aggregation	HSPD1
1,30E-02	regulation of homotypic cell-cell adhesion	HSPD1
7,44E-03	regulation of hydrolase activity	VCP|HSPA5|HSPE1|HSPD1|HSP90B1
2,90E-02	regulation of interferon-alpha production	PFN1
1,30E-02	regulation of interferon-gamma-mediated signaling pathway	KRT18
3,53E-02	regulation of macrophage activation	NME2
3,53E-02	regulation of mitochondrial membrane potential	PRDX1
2,12E-02	regulation of molecular function	PRDX3|VCP|HSPA5|ACTN4|HSPE1|NME1|HSPD1|HSP90B1
1,30E-02	regulation of nuclease activity	VCP
1,30E-02	regulation of pinocytosis	HSPD1
3,26E-03	regulation of protein folding in endoplasmic reticulum	LGALS1
4,43E-03	regulation of protein metabolic process	YWHAE|RPS4X|VCP|HSP90AB1|HSPA5|HSPB1|KRT7
1,96E-02	regulation of proteolysis	AKR1C1|AKR1C2
2,26E-02	regulation of proton transport	PTBP1
3,26E-03	regulation of T cell mediated immune response to tumor cell	YWHAZ|PRDX1|HSPD1|HSP90B1|AGR2
1,29E-02	regulation of translation	RPS4X|HSPB1|KRT7
6,51E-03	regulation of type I interferon-mediated signaling pathway	MYH9|KRT18
4,78E-02	regulation of viral genome replication	YWHAE
1,75E-07	response to biotic stimulus	PRDX3|HSPA8|HSP90AA1|VCP|HSP90AB1|HSPA5|HSPB1|ENO1|HSPE1|HSPA1B|HSPD1
1,59E-08	response to chemical stimulus	HSPA8|HSP90AA1|VCP|HSP90AB1|HSPA5|AKR1C1|ANXA5|HSPB1|ACTN4|HSPE1|YWHAZ|NME1|HSPD1|HSP90B1|PRDX3|LGALS1|KYNU|PRDX1|PFN1|HSPA1B
5,48E-03	response to endoplasmic reticulum stress	VCP|HSPA5
2,58E-02	response to insecticide	MYH9
1,06E-08	response to organic substance	HSPA8|HSP90AA1|VCP|HSP90AB1|HSPA5|ANXA5|HSPB1|HSPE1|NME1|HSPD1|HSP90B1|PRDX3|LGALS1|KYNU|PFN1|HSPA1B

1,30E-02	response to organophosphorus	ENO1
1,60E-03	response to stimulus	HSPA8|HSP90AA1|VCP|HSP90AB1|HSPA5|AKR1C1|ANXA5|HSPB1|ENO1|ACTN4|HSPE1|YWHAZ|NME1|HSPD1|HSP90B1|PRDX3|LGALS1|KYNU|PRDX1|PFN1|CTSD|HSPA1B
1,78E-06	response to stress	HSPA8|HSP90AA1|VCP|HSP90AB1|HSPA5|ANXA5|HSPB1|ACTN4|HSPE1|YWHAZ|HSPD1|HSP90B1|PRDX3|LGALS1|KYNU|PRDX1|PFN1|CTSD|HSPA1B
6,97E-13	response to unfolded protein	HSPA8|HSP90AA1|VCP|HSP90AB1|HSPA5|HSPB1|HSPE1|HSPA1B|HSPD1|VCP|HSPA5
3,26E-03	response to vitamin B6	KYNU
6,47E-03	response to xenobiotic stimulus	KYNU|AKR1C1
3,53E-02	ribosomal large subunit biogenesis	MYH9
9,75E-03	sequestering of calcium ion	P4HB|HSPD1
2,58E-02	sequestering of metal ion	HSPD1
1,09E-02	small molecule catabolic process	LDHB|KYNU|ENO1|GAPDH
4,27E-03	small molecule metabolic process	UGDH|LDHB|KYNU|AKR1C1|NME2|AKR1C3|AKR1C2|ENO1|P4HB|GAPDH|NME1
3,53E-02	spindle localization	HSPD1
3,04E-02	steroid metabolic process	AKR1B10|AKR1C1|AKR1C2
6,51E-03	transferrin transport	KYNU|SLC25A5
7,24E-07	translational elongation	RPL4|RPS4X|RPLP0|RPLP2|EEF2|RPL7|RPS4X|HSPB1|KRT7
1,61E-02	transport	YWHAE|HSPA8|HSP90AA1|VCP|AKR1C1|TXNRD1|CLTC|ACTN4|YWHAZ|NME1|HSP90B1|KRT18|AGR2|MYH9|SLC25A5
6,51E-03	tryptophan catabolic process to acetyl-CoA	HSPA5|KYNU|HSP90AB1|HIST1H4A|TNL1|YWHAZ
9,75E-03	UDP-glucose metabolic process	LGALS1
9,75E-03	UDP-glucuronate biosynthetic process	TKT|AKR1C3|LGALS1
1,29E-02	unsaturated fatty acid metabolic process	AKR1C3|AKR1C2
6,51E-03	uropod organization	HSP90AA1
1,22E-02	vesicle-mediated transport	HSPA8|VCP|KRT18|CLTC|YWHAZ|NME1
5,17E-03	xenobiotic metabolic process	VCP|HSPB1|KYNU|AKR1C1

Supplementary Table 2B: Significant gene ontology terms from A549/CDDP$_{CT}$. Ontologies statistical significant ($p < 0.05$) identified by Cytoscape plugin BiNGO and grouped by REVIGO.

p value	Gene ontology	Proteins
A549/CDDP$_{CT}$		
4,28E-02	actin cytoskeleton reorganization	MIF
4,48E-02	activation of pro-apoptotic gene products	YWHAB
2,27E-04	aging	EIF5A|NPM1|MIF|RTN4
5,66E-04	alcohol catabolic process	PGAM1|TALDO1|PFKP
1,24E-02	anatomical structure regression	MIF
3,98E-02	angiogenesis	NCL|RTN4
2,87E-02	behavioral defense response	VDAC1
2,67E-02	behavioral fear response	VDAC1
3,10E-04	biological_process	PRKCSH|YWHAB|RPL12|PARK7|RPL8|RPL9|RTN4|RPL7A|PRDX5|TUBB3|SERPINH1|FLNB|CCT4|EIF5A|HSP90AA1|NPM1|XRCC6|TPM4|RPS8|PGAM1|KRT8|TALDO1|RPSA|MIF|EEF1G|EEF1A1|HADHA|RPS28|TUBB2A|NCL|BLVRB|VDAC1|HNRNPC|PPIB|RAN|PFKP|PLEC
1,82E-04	biosynthetic process	EIF5A|EEF1G|EEF1A1|RPL7A|RPS28|RPS8|RPL12|SERPINH1|RPSA|MIF|RPL8|RPL9
1,42E-03	carbohydrate catabolic process	PGAM1|TALDO1|PFKP
1,67E-02	catabolic process	HADHA|PGAM1|NCL|TALDO1|BLVRB|PFKP
1,41E-02	cell death	YWHAB|NCL|VDAC1|PARK7|RTN4
2,87E-02	cell volume homeostasis	NPM1
4,52E-04	cellular biosynthetic process	EIF5A|EEF1G|EEF1A1|RPL7A|RPS28|RPS8|RPL12|RPSA|MIF|RPL8|RPL9
4,77E-04	cellular component assembly	HSP90AA1|NPM1|TUBB2A|YWHAB|TUBB3|MIF|PFKP|PLEC
3,51E-05	cellular component biogenesis	RPL7A|HSP90AA1|NPM1|RPS28|TUBB2A|YWHAB|TUBB3|MIF|PFKP|PLEC
3,71E-04	cellular component organization	HSP90AA1|NPM1|XRCC6|YWHAB|KRT8|MIF|TUBB2A|TUBB3|NCL|SERPINH1|FLNB|RAN|PFKP|PLEC
1,55E-02	cellular homeostasis	PRDX5|NPM1|NCL|PARK7
1,46E-02	cellular localization	EIF5A|HSP90AA1|NPM1|YWHAB|FLNB|RAN
4,07E-03	cellular macromolecular complex assembly	HSP90AA1|NPM1|TUBB2A|TUBB3
3,45E-05	cellular macromolecule biosynthetic process	EIF5A|EEF1G|EEF1A1|RPL7A|RPS28|RPS8|RPL12|RPSA|RPL8|RPL9
1,24E-02	cellular macromolecule localization	EIF5A|NPM1|YWHAB|RAN|HSP90AA1

9,34E-04	cellular macromolecule metabolic process	EIF5A|HSP90AA1|XRCC6|RPS8|RPL12|RPSA|RPL8|RPL9|EEF1G|EEF1A1|RPL7A|RPS28|HNRNPC|PPIB|RAN|CCT4
1,54E-05	cellular metabolic process	EIF5A|HSP90AA1|XRCC6|RPS8|RPL12|PGAM1|TALDO1|RPSA|PARK7|MIF|RPL8|RPL9|EEF1G|EEF1A1|RPL7A|HADHA|RPS28|BLVRB|HNRNPC|PPIB|RAN|PFKP|CCT4
1,66E-09	cellular process	YWHAB|RPL12|PARK7|RPL8|RPL9|RTN4|RPL7A|PRDX5|TUBB3|SERPINH1|FLNB|CCT4|EIF5A|HSP90AA1|NPM1|XRCC6|TPM4|RPS8|PGAM1|KRT8|TALDO1|RPSA|MIF|EEF1G|EEF1A1|HADHA|RPS28|TUBB2A|NCL|BLVRB|VDAC1|HNRNPC|PPIB|RAN|PFKP|PLEC
3,77E-03	cellular protein complex assembly	HSP90AA1|TUBB2A|TUBB3|NPM1|YWHAB|MIF|PFKP
1,21E-02	cellular protein localization	EIF5A|NPM1|YWHAB|RAN
2,46E-04	cellular protein metabolic process	EIF5A|HSP90AA1|RPS8|RPL12|RPSA|RPL8|RPL9|EEF1G|EEF1A1|RPL7A|RPS28|PPIB|CCT4
1,45E-02	chaperone-mediated protein complex assembly	HSP90AA1
1,04E-02	collagen biosynthetic process	SERPINH1
4,28E-02	cranial nerve development	RTN4
2,22E-03	cytoskeleton organization	NPM1|KRT8|FLNB|MIF|RAN
1,45E-02	death	YWHAB|NCL|VDAC1|PARK7|RTN4
3,48E-02	DNA integration	XRCC6
1,86E-02	DNA ligation	XRCC6
2,06E-02	double-strand break repair via nonhomologous end joining	XRCC6
1,76E-02	endoplasmic reticulum	EIF5A|PRKCSH|NCL|SERPINH1|PPIB|RTN4
3,23E-02	establishment of localization in cell	EIF5A|HSP90AA1|NPM1|YWHAB|RAN
4,16E-03	establishment of ribosome localization	NPM1
3,48E-02	fear response	VDAC1
1,04E-02	fructose 1,6-bisphosphate metabolic process	PFKP
8,79E-05	fructose 6-phosphate metabolic process	TALDO1|PFKP
5,62E-04	fructose metabolic process	TALDO1|PFKP
5,41E-06	gene expression	EIF5A|EEF1G|EEF1A1|RPL7A|RPS28|RPS8|RPL12|SERPINH1|RPSA|HNRNPC|RPL8|RPL9
4,16E-03	glyceraldehyde-3-phosphate metabolic process	TALDO1
6,23E-03	gonadal mesoderm development	MIF

9,03E-04	GTPase activity	EEF1A1|TUBB2A|TUBB3|RAN
8,30E-03	heme catabolic process	BLVRB
2,27E-02	hemidesmosome assembly	PLEC
3,02E-04	hexose catabolic process	PGAM1|TALDO1|PFKP
2,12E-02	homeostatic process	PRDX5|NPM1|XRCC6|NCL|PARK7
1,04E-02	hypusine metabolic process	EIF5A
4,28E-02	initiation of viral infection	XRCC6
4,28E-02	initiation of viral infection	XRCC6
4,59E-03	interspecies interaction between organisms	NPM1|KRT8|VDAC1|RAN
8,30E-03	lysosomal lumen acidification	NCL
4,23E-04	macromolecular complex assembly	HSP90AA1|NPM1|TUBB2A|YWHAB|TUBB3|MIF|PFKP
6,37E-04	macromolecular complex subunit organization	HSP90AA1|NPM1|TUBB2A|YWHAB|TUBB3|MIF|PFKP
6,16E-06	macromolecule biosynthetic process	EIF5A|EEF1G|EEF1A1|RPL7A|RPS28|RPS8|RPL12|SERPINH1|RPSA|RPL8|RPL9
4,37E-04	macromolecule metabolic process	EIF5A|HSP90AA1|XRCC6|RPS8|RPL12|RPSA|RPL8|RPL9|EEF1G|EEF1A1|RPL7A|RPS28|NCL|SERPINH1|HNRNPC|PPIB|RAN|CCT4
1,38E-02	maintenance of location	YWHAB|FLNB
9,05E-03	maintenance of protein location	YWHAB|FLNB
6,69E-03	maintenance of protein location in cell	YWHAB|FLNB
2,27E-02	membrane hyperpolarization	PARK7
5,25E-06	metabolic process	RPL12|PARK7|RPL8|RPL9|RPL7A|PRDX5|SERPINH1|CCT4|EIF5A|HSP90AA1|XRCC6|RPS8|PGAM1|TALDO1|RPSA|MIF|EEF1G|EEF1A1|HADHA|RPS28|NCL|BLVRB|HNRNPC|PPIB|RAN|PFKP
3,65E-02	microtubule cytoskeleton organization	NPM1|RAN
2,19E-02	microtubule-based movement	TUBB2A|TUBB3|NPM1|RAN
1,67E-03	microtubule-based process	NPM1|TUBB2A|TUBB3|RAN
8,30E-03	mitochondrial outer membrane translocase complex assembly	HSP90AA1
3,28E-02	mitotic spindle organization	RAN
3,08E-02	monoamine transport	PARK7
1,01E-02	monosaccharide metabolic process	PGAM1|TALDO1|PFKP
8,30E-03	Mullerian duct regression	MIF

2,08E-03	multi-layer follicle stage	MIF
2,24E-02	multi-organism process	EEF1G|NPM1|KRT8|VDAC1|RAN
3,48E-02	NADP metabolic process	TALDO1
2,06E-02	NADPH regeneration	TALDO1
8,30E-03	negative regulation of anti-apoptosis	RTN4
8,42E-03	negative regulation of apoptotic process	EIF5A|PRDX5|NPM1|MIF|YWHAB|RTN4
1,24E-02	negative regulation of cell cycle arrest	MIF
6,23E-03	negative regulation of centrosome duplication	NPM1
8,30E-03	negative regulation of dephosphorylation	YWHAB
2,47E-02	negative regulation of developmental growth	RTN4
8,30E-03	negative regulation of mRNA processing	NPM1
8,30E-03	negative regulation of neuron projection regeneration	RTN4
2,82E-02	negative regulation of response to stimulus	MIF|RTN4
1,24E-02	negative regulation of RNA splicing	NPM1
1,65E-03	nerve-nerve synaptic transmission	VDAC1|PARK7
4,08E-02	neuron maturation	NCL
2,87E-02	non-recombinational repair	XRCC6
2,36E-04	nuclear export	EIF5A|NPM1|RAN
3,43E-03	nuclear transport	EIF5A|NPM1|RAN
1,79E-03	nucleobase, nucleoside, nucleotide and nucleic acid transport	EIF5A|NPM1|RAN
6,23E-03	olfactory nerve development	RTN4
8,30E-03	oogenesis stage	MIF
1,71E-03	organelle organization	HSP90AA1|NPM1|XRCC6|TUBB2A|NCL|KRT8|FLNB|MIF|RAN
4,28E-02	organic alcohol transport	PARK7
8,30E-03	outer mitochondrial membrane organization	HSP90AA1
2,47E-02	pentose metabolic process	TALDO1
1,86E-02	pentose-phosphate shunt	TALDO1
3,68E-02	peptidyl-lysine modification	EIF5A

1,04E-02	peptidyl-lysine modification to hypusine	EIF5A
8,30E-03	pigment catabolic process	BLVRB
6,10E-04	pore complex	EIF5A|VDAC1|RAN
2,87E-02	positive regulation of amine transport	RTN4
2,16E-02	positive regulation of binding	NPM1|MIF|PARK7
1,70E-02	positive regulation of biosynthetic process	EIF5A|HSP90AA1|NPM1|XRCC6|RAN
1,86E-02	positive regulation of catecholamine secretion	RTN4
1,60E-02	positive regulation of cellular biosynthetic process	EIF5A|HSP90AA1|NPM1|XRCC6|RAN
1,39E-02	positive regulation of cellular metabolic process	EIF5A|HSP90AA1|NPM1|XRCC6|MIF|RAN
4,16E-03	positive regulation of centrosome duplication	NPM1
3,51E-02	positive regulation of developmental process	EIF5A|XRCC6|RTN4
2,67E-02	positive regulation of glial cell differentiation	RTN4
1,76E-02	positive regulation of metabolic process	EIF5A|HSP90AA1|NPM1|XRCC6|MIF|RAN
3,28E-02	positive regulation of muscle cell differentiation	EIF5A
9,30E-03	positive regulation of neurogenesis	XRCC6|RTN4|TUBB2A|TUBB3|NCL|EIF5A
5,83E-03	positive regulation of NF-kappaB transcription factor activity	NPM1|MIF
2,87E-02	positive regulation of peptidyl-serine phosphorylation	MIF
1,65E-02	positive regulation of protein complex disassembly	EIF5A
3,16E-02	positive regulation of secretion	MIF|RTN4
1,26E-02	positive regulation of transcription regulator activity	NPM1|MIF
6,23E-03	positive regulation of translational elongation	EIF5A
6,23E-03	positive regulation of translational termination	EIF5A

2,08E-03	preantral ovarian follicle growth	MIF
4,31E-05	primary metabolic process	EIF5A|HSP90AA1|XRCC6|RPS8|RPL12|PGAM1|TALDO1|RPSA|MIF|RPL8|RPL9|EEF1G|EEF1A1|RPL7A|HADHA|RPS28|NCL|SERPINH1|HNRNPC|PPIB|RAN|PFKP|CCT4
2,67E-02	prostaglandin biosynthetic process	MIF
4,28E-02	prostaglandin metabolic process	MIF
7,19E-05	protein complex assembly	HSP90AA1|NPM1|TUBB2A|YWHAB|TUBB3|MIF|PFKP
7,19E-05	protein complex biogenesis	HSP90AA1|NPM1|TUBB2A|YWHAB|TUBB3|MIF|PFKP
5,25E-03	protein folding	HSP90AA1|PPIB|CCT4
1,97E-02	protein homooligomerization	MIF|PFKP
1,86E-02	protein homotrimerization	MIF
4,07E-02	protein localization	EIF5A|NPM1|YWHAB|FLNB|RAN
1,15E-04	protein metabolic process	EIF5A|HSP90AA1|RPS8|RPL12|RPSA|RPL8|RPL9|EEF1G|EEF1A1|RPL7A|RPS28|NCL|SERPINH1|PPIB|CCT4
6,33E-04	protein oligomerization	NPM1|YWHAB|MIF|PFKP
1,86E-02	protein refolding	HSP90AA1
8,33E-03	protein targeting	EIF5A|YWHAB|RAN|NPM1|HSP90AA1
3,28E-02	protein trimerization	MIF
1,65E-02	regulation of androgen receptor signaling pathway	PARK7
8,22E-03	regulation of binding	NPM1|PARK7|MIF
1,24E-02	regulation of biological quality	PRDX5|NPM1|XRCC6|YWHAB|NCL|FLNB|PARK7|RTN4
3,08E-02	regulation of cell cycle arrest	MIF
3,33E-02	regulation of cell cycle process	NPM1|MIF
8,40E-03	regulation of cell death	EIF5A|PRDX5|NPM1|YWHAB|MIF|RTN4
2,08E-03	regulation of cellular amide metabolic process	PGAM1
2,48E-02	regulation of cellular component organization	EIF5A|NPM1|MIF|RTN4
3,48E-02	regulation of cellular pH	NCL
2,53E-03	regulation of cellular response to stress	NPM1|MIF|RTN4
2,87E-02	regulation of cofactor metabolic process	PGAM1
4,22E-02	regulation of DNA binding	NPM1|MIF

2,29E-04	regulation of DNA damage response, signal transduction by p53 class mediator	NPM1|MIF
4,02E-02	regulation of establishment of protein localization	YWHAB|MIF
6,23E-03	regulation of integrin biosynthetic process	MIF
2,27E-02	regulation of macrophage activation	MIF
4,28E-02	regulation of mRNA processing	NPM1
1,45E-02	regulation of neuron projection regeneration	RTN4
4,08E-02	regulation of peptidyl-serine phosphorylation	MIF
1,24E-02	regulation of protein kinase A signaling cascade	MIF
4,97E-02	regulation of protein localization	YWHAB|MIF
3,65E-02	regulation of protein transport	YWHAB|MIF
2,83E-02	regulation of response to stress	NPM1|MIF|RTN4
2,08E-03	regulation of secondary metabolic process	PGAM1|TALDO1
2,87E-02	regulation of sensory perception	RTN4
2,87E-02	regulation of sensory perception of pain	RTN4
3,25E-02	regulation of transcription regulator activity	NPM1|MIF
1,45E-02	regulation of translational elongation	EIF5A
1,45E-02	regulation of translational termination	EIF5A
2,67E-02	respiratory burst	PGAM1
4,88E-02	response to activity	RTN4
2,91E-02	response to chemical stimulus	HADHA|PRDX5|HSP90AA1|TPM4|SERPINH1|PARK7|MIF
1,60E-02	response to drug	HADHA|PARK7|MIF
6,54E-03	response to oxidative stress	PRDX5|TPM4|PARK7
2,46E-02	response to protein stimulus	HSP90AA1|SERPINH1

1,38E-02	response to reactive oxygen species	PRDX5|PARK7
8,94E-03	response to stress	PRDX5|HSP90AA1|NPM1|XRCC6|TPM4|SERPINH1|VDAC1|PARK7|MIF
8,31E-03	response to unfolded protein	HSP90AA1|SERPINH1
7,67E-03	ribonucleoprotein complex biogenesis	RPL7A|NPM1|RPS28
2,08E-03	ribosomal large subunit export from nucleus	NPM1
3,77E-04	ribosomal small subunit biogenesis	NPM1|RPS28|RPL7A
2,47E-02	ribosome assembly	NPM1
2,53E-03	ribosome biogenesis	RPL7A|NPM1|RPS28
4,16E-03	ribosome localization	NPM1
9,00E-05	RNA export from nucleus	EIF5A|NPM1|RAN
1,31E-03	RNA localization	EIF5A|NPM1|RAN
4,16E-03	rRNA transport	NPM1
3,88E-02	sex determination	MIF
2,16E-03	small molecule catabolic process	HADHA|PGAM1|TALDO1|PFKP
4,48E-02	somatic cell DNA recombination	XRCC6
4,88E-02	somatic diversification of immune receptors	XRCC6
4,48E-02	somatic diversification of immune receptors via germline recombination within a single locus	XRCC6
2,78E-10	translation	EIF5A|EEF1G|EEF1A1|RPL7A|RPS28|RPS8|RPL12|RPSA|RPL8|RPL9
3,20E-13	translational elongation	EEF1G|EEF1A1|RPL7A|RPS28|RPS8|RPL12|RPSA|RPL8|RPL9|EIF5A
6,23E-03	translational frameshifting	EIF5A
3,51E-06	unfolded protein binding	HSP90AA1|NPM1|SERPINH1|PPIB|CCT4
2,06E-02	V(D)J recombination	XRCC6
1,55E-02	vesicle	HSP90AA1|YWHAB|PPIB|RAN|CCT4

Supplementary Table 2C: Significant gene ontology terms from A549/CDDP. Ontologies statistical significant ($p < 0.05$) identified by Cytoscape plugin BiNGO and grouped by REVIGO.

p value	Gene ontology	Proteins
A549/CDDP		
4,27E-02	actin cytoskeleton organization	DSTN|FLNB
5,61E-03	actin filament severing	DSTN
3,05E-02	actin filament-based movement	MYL6
5,02E-03	actin filament-based process	MYL6|DSTN|FLNB
2,78E-02	actin polymerization or depolymerization	DSTN|FLNB
1,26E-02	actin-mediated cell contraction	MYL6
1,07E-03	aging	EIF5A|NPM1|RTN4
5,33E-03	alcohol catabolic process	PGAM1|PGD
2,47E-02	anatomical structure development	EIF4A1|XRCC6|MYL6|CAPN2|FLNB|PGD|RTN4|VCL
9,80E-03	ATP catabolic process	ACLY
1,65E-02	biological adhesion	ACTN1|CTNNA1|RPSA|VCL
3,04E-02	biological_process	EIF5A|EIF4A1|HSP90AA1|NPM1|XRCC6|ACTN1|PGAM1|SURF4|KRT8|DSTN|RPSA|PGD|RTN4|EEF1A1|ACLY|MYL6|CAPN2|CTNNA1|SERPINH1|FLNB|VIM|PPIB|VCL|PLEC
3,47E-02	biosynthetic process	EIF5A|EEF1A1|ACLY|SERPINH1|RPSA|PGD
9,83E-03	carbohydrate catabolic process	PGAM1|PGD|ACLY
3,58E-02	carbohydrate metabolic process	ACLY|PGAM1|PGD
1,64E-02	cell adhesion	ACTN1|CTNNA1|RPSA|VCL
4,81E-02	cell aging	NPM1
9,15E-07	cell junction assembly	ACTN1|CTNNA1|VCL|PLEC
2,93E-06	cell junction organization	ACTN1|CTNNA1|VCL|PLEC
1,95E-02	cell volume homeostasis	NPM1
1,73E-03	cell-cell junction organization	CTNNA1|VCL
6,30E-03	cell-matrix adhesion	ACTN1|VCL
8,46E-03	cell-substrate adhesion	ACTN1|VCL
1,37E-03	cellular component assembly	HSP90AA1|NPM1|ACTN1|CTNNA1|VCL|PLEC
2,60E-03	cellular component biogenesis	HSP90AA1|NPM1|ACTN1|CTNNA1|VCL|PLEC
3,42E-04	cellular component organization	HSP90AA1|NPM1|XRCC6|ACTN1|CTNNA1|SERPINH1|KRT8|DSTN|FLNB|VCL|PLEC

1,94E-03	cellular localization	EIF5A|HSP90AA1|NPM1|MYL6|FLNB|VCL
1,32E-02	cellular macromolecular complex subunit organization	HSP90AA1|NPM1|DSTN
2,25E-02	cellular macromolecule localization	EIF5A|NPM1|VCL
2,10E-04	cellular process	EIF5A|HSP90AA1|NPM1|XRCC6|ACTN1|PGAM1|KRT8|DSTN|RPSA|PGD|RTN4|EEF1A1|ACLY|MYL6|CAPN2|CTNNA1|SERPINH1|FLNB|VIM|PPIB|VCL|PLEC
2,21E-02	cellular protein localization	EIF5A|NPM1|VCL
7,01E-03	cellular response to indole-3-methanol	CTNNA1
9,80E-03	chaperone-mediated protein complex assembly	HSP90AA1
9,80E-03	citrate metabolic process	ACLY
1,40E-02	coenzyme A metabolic process	ACLY
1,96E-02	coenzyme metabolic process	ACLY|PGD
3,30E-02	cofactor metabolic process	ACLY|PGD
7,01E-03	collagen biosynthetic process	SERPINH1
3,73E-02	collagen fibril organization	SERPINH1
4,13E-02	collagen metabolic process	SERPINH1
2,91E-02	cranial nerve development	RTN4
9,80E-03	cytoskeletal anchoring at plasma membrane	FLNB
3,30E-03	cytoskeleton organization	NPM1|KRT8|DSTN|FLNB
8,89E-03	developmental process	EIF5A|EIF4A1|NPM1|XRCC6|MYL6|CAPN2|FLNB|PGD|RTN4|VCL
2,36E-02	DNA integration	XRCC6
1,26E-02	DNA ligation	XRCC6
1,40E-02	double-strand break repair via nonhomologous end joining	XRCC6
1,24E-02	endoplasmic reticulum	EIF5A|SURF4|SERPINH1|PPIB|RTN4
1,12E-02	epithelial cell-cell adhesion	VCL
3,11E-02	establishment of localization in cell	EIF5A|HSP90AA1|NPM1|MYL6
2,81E-03	establishment of ribosome localization	NPM1
2,88E-02	gene expression	EIF5A|EEF1A1|CAPN2|SERPINH1|RPSA
2,50E-03	glucose catabolic process	PGAM1|PGD
3,51E-03	hexose catabolic process	PGAM1|PGD
7,01E-03	hypusine metabolic process	EIF5A
2,91E-02	initiation of viral infection	XRCC6

2,91E-02	initiation of viral infection	XRCC6
2,91E-02	intermediate filament-based process	VIM
1,05E-02	interspecies interaction between organisms	NPM1|KRT8|VIM
1,31E-02	intracellular transport	EIF5A|HSP90AA1|NPM1|MYL6
2,09E-02	lamellipodium assembly	VCL
4,21E-03	L-serine biosynthetic process	PGD
1,12E-02	L-serine metabolic process	PGD
4,54E-02	microtubule organizing center organization	NPM1
4,00E-02	mitochondrial membrane organization	HSP90AA1
5,61E-03	mitochondrial outer membrane translocase complex assembly	HSP90AA1
3,67E-02	monosaccharide metabolic process	PGAM1|PGD
4,52E-02	multicellular organismal development	EIF4A1|XRCC6|MYL6|CAPN2|FLNB|PGD|RTN4|VCL
1,96E-02	muscle contraction	MYL6|VCL
1,26E-02	muscle filament sliding	MYL6
3,76E-02	muscle organ development	MYL6|FLNB
5,90E-03	muscle structure development	MYL6|CAPN2|FLNB
2,31E-02	muscle system process	MYL6|VCL
1,54E-02	myoblast fusion	CAPN2
2,50E-02	myotube differentiation	CAPN2
2,36E-02	NADP metabolic process	PGD
1,40E-02	NADPH regeneration	PGD
5,61E-03	negative regulation of anti-apoptosis	RTN4
4,56E-03	negative regulation of cellular component movement	ACTN1|VCL|RTN4
2,54E-02	negative regulation of cellular component organization	NPM1|RTN4
4,21E-03	negative regulation of centrosome duplication	NPM1
1,67E-02	negative regulation of developmental growth	RTN4
5,61E-03	negative regulation of mRNA processing	NPM1

5,61E-03	negative regulation of neuron projection regeneration	RTN4
8,40E-03	negative regulation of RNA splicing	NPM1
3,86E-02	nerve development	RTN4
1,95E-02	non-recombinational repair	XRCC6
2,99E-03	nuclear export	EIF5A|NPM1
1,77E-02	nuclear transport	EIF5A|NPM1
1,15E-02	nucleobase, nucleoside, nucleotide and nucleic acid transport	EIF5A|NPM1
1,67E-02	nucleoside bisphosphate metabolic process	ACLY
4,21E-03	olfactory nerve development	RTN4
4,94E-02	organ regeneration	EIF4A1
1,07E-02	organelle organization	HSP90AA1|NPM1|XRCC6|KRT8|DSTN|FLNB
5,61E-03	outer mitochondrial membrane organization	HSP90AA1
4,21E-03	pentose biosynthetic process	PGD
1,67E-02	pentose metabolic process	PGD
1,26E-02	pentose-phosphate shunt	PGD
2,50E-02	peptidyl-lysine modification	EIF5A
7,01E-03	peptidyl-lysine modification to hypusine	EIF5A
1,80E-02	positive regulation of biosynthetic process	EIF5A|HSP90AA1|NPM1|XRCC6
5,30E-03	positive regulation of cell differentiation	EIF5A|XRCC6|RTN4
1,71E-02	positive regulation of cellular biosynthetic process	EIF5A|HSP90AA1|NPM1|XRCC6
3,85E-02	positive regulation of cellular component organization	EIF5A|NPM1
4,40E-02	positive regulation of cellular metabolic process	EIF5A|HSP90AA1|NPM1|XRCC6
2,81E-03	positive regulation of centrosome duplication	NPM1
1,23E-02	positive regulation of developmental process	EIF5A|XRCC6|RTN4
5,61E-03	positive regulation of dopamine secretion	RTN4
1,81E-02	positive regulation of glial cell differentiation	RTN4

1,95E-02	positive regulation of gliogenesis	RTN4
2,23E-02	positive regulation of muscle cell differentiation	EIF5A|MYL6|FLNB
3,46E-02	positive regulation of nitric oxide biosynthetic process	HSP90AA1
1,12E-02	positive regulation of protein complex disassembly	EIF5A
4,40E-02	positive regulation of translation	EIF5A
4,21E-03	positive regulation of translational elongation	EIF5A
4,21E-03	positive regulation of translational termination	EIF5A
1,12E-02	protein autoprocessing	CAPN2
2,36E-02	protein folding	HSP90AA1|PPIB
3,79E-02	protein localization	EIF5A|NPM1|FLNB|VCL
1,95E-02	protein localization at cell surface	VCL
1,13E-02	protein maturation	CAPN2|SERPINH1
1,26E-02	protein refolding	HSP90AA1
1,26E-02	pseudopodium	ACTN1
4,27E-02	purine nucleoside metabolic process	ACLY
4,27E-02	purine ribonucleoside metabolic process	ACLY
1,26E-02	purine ribonucleoside triphosphate catabolic process	ACLY
1,81E-02	purine ribonucleotide catabolic process	ACLY
3,05E-02	regulation of apoptotic process	EIF5A|NPM1|ACTN1|RTN4
3,73E-02	regulation of catecholamine secretion	RTN4
3,13E-02	regulation of cell death	EIF5A|NPM1|ACTN1|RTN4
4,77E-02	regulation of cell development	XRCC6|RTN4
4,14E-02	regulation of cell differentiation	EIF5A|XRCC6|RTN4
3,67E-02	regulation of cell migration	RTN4|VCL
3,76E-02	regulation of cell size	NPM1|RTN4

1,41E-03	regulation of cellular amide metabolic process	PGAM1|EIF5A|EEF1A1|RPSA
4,43E-03	regulation of cellular component movement	ACTN1|RTN4|VCL
3,86E-02	regulation of cellular component organization	EIF5A|NPM1|RTN4
1,45E-02	regulation of cellular response to stress	NPM1|RTN4
1,95E-02	regulation of cofactor metabolic process	PGAM1|ACLY|PGD
1,54E-02	regulation of DNA damage response, signal transduction by p53 class mediator	NPM1
4,54E-02	regulation of generation of precursor metabolites and energy	PGAM1
4,47E-02	regulation of locomotion	RTN4|VCL
2,91E-02	regulation of mRNA processing	NPM1
4,01E-02	regulation of nervous system development	XRCC6|RTN4
4,27E-02	regulation of nitric oxide biosynthetic process	HSP90AA1
3,86E-02	regulation of RNA splicing	NPM1
1,41E-03	regulation of secondary metabolic process	PGAM1|PGD
1,95E-02	regulation of sensory perception	RTN4
1,95E-02	regulation of sensory perception of pain	RTN4
9,80E-03	regulation of translational elongation	EIF5A
9,80E-03	regulation of translational termination	EIF5A
1,81E-02	respiratory burst	PGAM1
3,32E-02	response to activity	RTN4
7,01E-03	response to indole-3-methanol	CTNNA1
1,17E-02	response to protein stimulus	HSP90AA1|SERPINH1
3,85E-03	response to unfolded protein	HSP90AA1|SERPINH1
1,26E-02	ribonucleoside triphosphate catabolic process	ACLY

2,09E-02	ribonucleotide catabolic process	ACLY
1,54E-02	ribosomal large subunit biogenesis	NPM1
1,41E-03	ribosomal large subunit export from nucleus	NPM1
1,95E-02	ribosomal small subunit biogenesis	NPM1
1,67E-02	ribosome assembly	NPM1
2,81E-03	ribosome localization	NPM1
1,58E-03	RNA export from nucleus	EIF5A|NPM1
9,30E-03	RNA localization	EIF5A|NPM1
2,81E-03	rRNA transport	NPM1
3,59E-02	serine family amino acid metabolic process	PGD
5,90E-03	small molecule catabolic process	ACLY|PGAM1|PGD
3,05E-02	somatic cell DNA recombination	XRCC6
3,32E-02	somatic diversification of immune receptors	XRCC6
3,05E-02	somatic diversification of immune receptors via germline recombination within a single locus	XRCC6
1,95E-02	syncytium formation	CAPN2
4,46E-02	system development	EIF4A1|XRCC6|MYL6|FLNB|PGD|RTN4|VCL
4,13E-02	telomere maintenance	XRCC6
4,27E-02	telomere organization	XRCC6
8,14E-03	translational elongation	EEF1A1|RPSA
4,21E-03	translational frameshifting	EIF5A
1,76E-05	unfolded protein binding	HSP90AA1|NPM1|SERPINH1|PPIB
1,40E-02	V(D)J recombination	XRCC6

4. DISCUSSÃO

O câncer de pulmão é o principal responsável por mortes relacionadas ao câncer no mundo. Apesar do tratamento ser realizado com cisplatina, o tumor adquire resistência ao quimioterápico durante o tratamento. Portanto, estudos para aumentar o conhecimento acerca dos mecanismos envolvidos na resistência tumoral à cisplatina e o desenvolvimento de ferramentas celulares e moleculares que auxiliam nesses estudos são essenciais para a reversão desse problema clínico. Dessa forma, linhagens celulares resistentes à cisplatina de fácil desenvolvimento e que produzam resultados confiáveis, como as desenvolvidas nesse trabalho, são ferramentas extremamente valiosas.

Apesar de A549 e A549/CDDP$_{CT}$ apresentarem fenótipos celulares parecidos, as linhagens diferem significativamente em relação ao perfil proteico. A diminuição da expressão de VIM, por exemplo, está diretamente relacionada com a resistência à cisplatina em células de câncer de ovário (HUO et al., 2014) e o silenciamento desta proteína estimulou a resistência à cisplatina por diminuir o acúmulo intracelular da droga. Além disso, VIM foi identificada positivamente regulada em células NG108-15 com senescência induzida por cisplatina (LI et al., 2014a). Portanto, a diminuição da expressão de VIM em células de A549/CDDP$_{CT}$ pode ser um mecanismo de proteção para diminuir o acúmulo intracelular de cisplatina e evadir a senescência celular causada pela droga. Por outro lado, a maior expressão de VIM na sublinhagem A549/CDDP pode ser responsável pela morfologia diferencial que as células apresentam e pode estar envolvida com transição epitelial-mesenquimal (LIU et al., 2015a).

Diversas proteínas já relacionadas com resistência à cisplatina foram identificadas nas células A549/CDDP$_{CT}$, como o fator MIF, a proteína DJ-1 (PARK7), a proteína de ligação à GTP nuclear Ran (RAN) e a tubulina TUBB3, podendo estar envolvidas nos mecanismos de resistência apresentados por essa sublinhagem. MIF

promove proliferação e migração em células de osteosarcoma pela ativação da via RAS/MAPK, além do silenciamento desse fator aumentar a sensibilidade à cisplatina (WANG et al., 2017a). Especificamente em NSCLC, o silenciamento de MIF induz a diminuição de proliferação e migração celular (GOTO et al., 2017). Da mesma forma, MIF foi relacionada à reorganização do citoesqueleto de actina, regulação negativa de morte celular e resposta ao dano no DNA entre as ontologias enriquecidas para A549/CDDP$_{CT}$.

A proteína DJ-1, por sua vez, foi associada à resistência à cisplatina em células A549, reparando a proliferação perdida após exposição à cisplatina (ZENG et al., 2011). Aumento da expressão de DJ-1 também foi associado à diminuição da apoptose induzida pela cisplatina em células de carcinoma renal (TRIVEDI et al., 2016). Da mesma forma, a proteína RAN, quando associada à RCC1, é descrita como responsável pela evasão de apoptose e inibição da pausa no ciclo celular induzidos pela cisplatina (CEKAN et al., 2016). TUBB3 também foi associada com resistência à cisplatina em NSCLC (LENG et al., 2012; SEVE, 2005) e seu silenciamento levou à diminuição de crescimento de tumor de NSCLC em camundongos (MCCARROLL et al., 2010). Além disso, a diminuição da expressão de TUBB3 foi relacionada a uma melhor resposta à quimioterapia com compostos de platina em pacientes de NSCLC (AZUMA et al., 2009; LI et al., 2014c). Associado a isso estão as ontologias enriquecidas em A549/CDDP$_{CT}$, que incluem reorganização do citoesqueleto de actina, regulação negativa da apoptose e da morte celular, regulação negativa do dano ao DNA, complexo de poros, resposta a droga e resposta a estresse oxidativo.

Igualmente, A549/CDDP$_{CT}$ apresentou a proteína nucleosídeo difosfato quinase (NME1-NME2) diferencialmente expressa. A diminuição da expressão da proteína NME foi associado à resistência à cisplatina em células de carcinoma de cabeça e

pescoço (WANG et al., 2014), enquanto que sua superexpressão reverteu a resistência, além de ser sugerido como um marcador de células de carcinoma escamoso esofágico (IIZUKA et al., 1999). Além disso, a diminuição da expressão de NME pode prevenir o dano causado pela cisplatina no DNA genômico e mitocondrial (LIZUKA et al., 2000). A549/CDDP$_{CT}$ apresentou categorias funcionais como complexo da proteína ligase 4 DNA-quinase dependente de DNA e a regulação negativa da resposta ao dano no DNA, sinal de transdução pelo mediador p53 que se relacionam com as possíveis funções dessas proteínas. Ontologias enriquecidas que incluem NME foram regulação de apoptose, regulação de morte celular programada e resposta a estímulo químico, entre outras.

A proteína aldo-keto redutase membro C1 da família 1 (AKR1C1), identificada menos expressa em A549/CDDP, é descrita como negativamente expressa em células de NSCLC tratadas com baixas doses de cisplatina (LEUNG et al., 2016), como realizado nesse trabalho. Da mesma forma, o aumento da expressão de AKR1C1 promove proliferação e migração celular em câncer de pulmão de células pequenas (TIAN et al., 2016). Além disso, calpaina 2 (CAPN2), exclusivamente identificada em A549/CDDP, foi observada mais expressa em tumores de ovário resistentes à cisplatina (STORR et al., 2012) e seu silenciamento causou sensibilidade à cisplatina em câncer de mama (GRIEVE et al., 2016). A proliferação reduzida apresentada pela A549/CDDP, assim como ontologias enriquecidas na linhagem, como polimerização e depolimerização de actina e regulação da migração celular suportam a ideia dessas proteínas estarem envolvidas nos mecanismos de resistência à cisplatina da sublinhagem.

Algumas proteínas foram identificadas diferencialmente expressas entre A549/CDDP e A549/CDDP$_{CT}$ e, apesar de não poderem ser diretamente relacionadas à resistência à cisplatina, valem ser destacas. A expressão do gene da alfa-actinina 4

(ACTN4) foi associado com resistência à compostos de platina em neuroblastoma (PISKAREVA et al., 2015) e especificamente com resistência à cisplatina em câncer de ovário (LIU et al., 2015b). A inibição da endoplasmina HSP90B causa sensibilidade à cisplatina e apoptose em câncer de pulmão (WANG et al., 2017b; WENG et al., 2012). O silenciamento da miosina MYH9 desencadeia capacidade invasiva em tumor de células escamosas (SCHRAMEK et al., 2014). A profilina PFN1 é descrita como menos expressa em linhagemcelular EC109 resistente à cisplatina (WEN et al., 2009). A proteína anexina A5 (ANXA5) é descrita como mais expressa em linhagem celular de carcinoma nasofaríngeo resistente à cisplatina quando comparada à linhagem parental (TANG et al., 2012). A proteína de choque térmico beta-1 (HSPB1) foi descrita como responsável pela resistência à cisplatina, tendo o silenciamento desta proteína inibido a resistência em câncer de pulmão (KIM et al., 2007) e câncer de ovário (LU et al., 2016). Além disso, células cancerosas laríngeas resistentes à cisplatina que apresentam maior expressão de HSPB1 obtiveram um menor crescimento celular (LEE et al., 2006).

A proteína de 78 kDa regulada por glicose (HSPA5) foi encontrada menos expressa em A549/CDDP$_{CT}$ em relação a A549 e A549/CDDP e serve como um bom exemplo da dualidade de algumas proteínas em relação à resistência à cisplatina. A HSPA5, quando regulada positivamente, aumenta a sensibilidade das células à cisplatina pela ativação da via JNK e NF-κB, levando a apoptose (AHMAD; HAHN; CHATTERJEE, 2014). Da mesma forma, a exposição das células à cisplatina reprime a expressão de HSPA5 pela inibição de ATF6α-p50, sendo inclusive sugerido que sua maior expressão poderia auxiliar no tratamento da cisplatina contra o câncer (KUO et al., 2016). Contudo, a superexpressão da proteína foi descrita como tendo papel protetor da senescência celular induzida pela cisplatina, sendo essa característica revertida quando a proteína é inibida (LI et al., 2014b). Assim como sua inibição causa aumento

da sensibilidade à quimioterápicos em câncer coloretal (MHAIDAT et al., 2016). Portanto, a expressão diferencial dessa proteína entre A549/CDDP$_{CT}$ e A549/CDDP pode auxiliar o fenótipo de resistência à cisplatina de ambas sublinhagens, contudo mais estudos seriam necessários para comprovar isso.

Apesar de diversas proteínas identificadas serem bem relacionadas com resistência à cisplatina, algumas não possuem papel definido pela literatura e se apresentam como potenciais alvos para melhor estudo. O fator de alongamento 2 (EEF2), por exemplo, é bem descrito como mais expresso em diversos tipos de tumores (CHEN et al., 2011; OJI et al., 2014; SUN et al., 2013), mas nenhuma relação com resistência à cisplatina foi descrita ainda. Da mesma maneira, nenhum trabalho envolvendo a proteína de choque térmico HSPE1 em câncer de pulmão resistente à cisplatina foi realizado. Portanto, maiores estudos nessas duas proteínas nas sublinhagens resistentes à cisplatina podem levar a um melhor entendimento do papel dessas proteínas nos mecanismos de resistência e descoberta de possível biomarcadores da resistência em câncer de pulmão.

A identificação de tantas proteínas já anteriormente relacionadas à resistência à cisplatina confirma o caráter resistente das sublinhagens A549/CDDP$_{CT}$ e A549/CDDP. Os mecanismos de resistência identificados na A549/CDDP$_{CT}$, baseados nas ontologias enriquecidas, podem estar relacionados ao perfil ribossomal, resposta ao estresse oxidativo e regulação negativa de morte celular. Os mecanismos apresentados pela A549/CDDP, por outro lado, seriam definidos pelo maior reparo ao dano no DNA causado pela cisplatina e presença de ontologias enriquecidas associadas à transição epitelial-mesenquimal. Portanto, ambas as sublinhagens se mostram como ferramentas adequadas para estudos que visam o estudo dos mecanismos de resistência à cisplatina em câncer de pulmão.

5. PERSPECTIVAS

5.1. Realização de nova análise proteômica com o intuito de aumentar o número de proteínas identificadas.

5.2. Seleção de proteínas-alvo descritas no trabalho para estudos de silenciamento e superexpressão gênica nas linhagens celulares sensível e resistentes à cisplatina para avaliação de seu potencial papel na resistência à cisplatina.

6. REFERÊNCIAS

AHMAD, M.; HAHN, I. F.; CHATTERJEE, S. GRP78 up-regulation leads to hypersensitization to cisplatin in A549 lung cancer cells. **Anticancer research**, v. 34, n. 7, p. 3493–500, 2014.

AMERICAN CANCER SOCIETY. **About Small Cell Lung Cancer**. Disponível em: <https://www.cancer.org/content/dam/CRC/PDF/Public/8708.00.pdf>. Acesso em: 18 dez. 2017a.

AMERICAN CANCER SOCIETY. **Treating Non-Small Cell Lung Cancer**. Disponível em: <https://www.cancer.org/cancer/non-small-cell-lung-cancer/treating.html>. Acesso em: 18 dez. 2017b.

AZUMA, K. et al. Expression of ERCC1 and class III β-tubulin in non-small cell lung cancer patients treated with carboplatin and paclitaxel. **Lung Cancer**, v. 64, n. 3, p. 326–333, 2009.

BARR, M. P. et al. Generation and Characterisation of Cisplatin-Resistant Non-Small Cell Lung Cancer Cell Lines Displaying a Stem-Like Signature. **PLoS ONE**, v. 8, n. 1, p. e54193, 2013.

BROZOVIC, A. et al. Long-term activation of SAPK/JNK, p38 kinase and fas-L expression by cisplatin is attenuated in human carcinoma cells that acquired drug resistance. **International Journal of Cancer**, v. 112, n. 6, p. 974–985, 2004.

BROZOVIC, A.; OSMAK, M. Activation of mitogen-activated protein kinases by cisplatin and their role in cisplatin-resistance. **Cancer Letters**, v. 251, n. 1, p. 1–16, 2007.

CEKAN, P. et al. RCC1-dependent activation of Ran accelerates cell cycle and DNA repair, inhibiting DNA damage-induced cell senescence. **Molecular Biology of the Cell**, v. 27, n. 8, p. 1346–1357, 2016.

CHEN, C.-Y. et al. Sumoylation of eukaryotic elongation factor 2 is vital for protein stability and anti-apoptotic activity in lung adenocarcinoma cells. **Cancer Science**, v. 102, n. 8, p. 1582–1589, 2011.

Cisplatin-Based Adjuvant Chemotherapy in Patients with Completely Resected Non–Small-Cell Lung Cancer. **New England Journal of Medicine**, v. 350, n. 4, p. 351–360, 2004.

DABROWIAK, J. C.; GOODISMAN, J.; SOUID, A.-K. Kinetic study of the reaction of cisplatin with thiols. **Drug metabolism and disposition: the biological fate of chemicals**, v. 30, n. 12, p. 1378–84, 2002.

DASARI, S.; TCHOUNWOU, P. B. Cisplatin in cancer therapy: Molecular mechanisms of action. **European Journal of Pharmacology**, v. 740, p. 364–378, 2014.

DESANTIS, C. E. et al. Cancer treatment and survivorship statistics, 2014. **CA: A Cancer Journal for Clinicians**, v. 64, n. 4, p. 252–271, 2014.

FENG, X. et al. Annexin A2 contributes to cisplatin resistance by activation of JNK-

p53 pathway in non-small cell lung cancer cells. **Journal of Experimental & Clinical Cancer Research**, v. 36, n. 1, p. 123, 2017.

GILLET, J.-P. et al. Redefining the relevance of established cancer cell lines to the study of mechanisms of clinical anti-cancer drug resistance. **Proceedings of the National Academy of Sciences**, v. 108, n. 46, p. 18708–18713, 2011.

GLOBOCAN. **GLOBOCAN: Estimated Cancer Incidence, Mortality and Prevalence Worldwide in 2012**. Disponível em: <http://globocan.iarc.fr>. Acesso em: 18 dez. 2017.

GOTO, A. et al. The low expression of miR-451 predicts a worse prognosis in non-small cell lung cancer cases. **PLOS ONE**, v. 12, n. 7, p. e0181270, 2017.

GRIEVE, S. et al. Calpain Genetic Disruption and HSP90 Inhibition Combine To Attenuate Mammary Tumorigenesis. **Molecular and Cellular Biology**, v. 36, n. 15, p. 2078–2088, 2016.

GUO, R. et al. Promoter methylation profiles between human lung adenocarcinoma multidrug resistant A549/cisplatin (A549/DDP) cells and its progenitor A549 cells. **Biological & pharmaceutical bulletin**, v. 36, n. 8, p. 1310–6, 2013.

HAGRMAN, D. KINETIC STUDY ON THE REACTION OF CISPLATIN WITH METALLOTHIONEIN. **Drug Metabolism and Disposition**, v. 31, n. 7, p. 916–923, 2003.

HARVEY, H. et al. Modulation of chemotherapeutic drug resistance in neuroblastoma SK-N-AS cells by the neural apoptosis inhibitory protein and miR-520f. **International Journal of Cancer**, v. 136, n. 7, p. 1579–1588, 2015.

HUO, Y. et al. Downregulation of vimentin expression increased drug resistance in ovarian cancer cells. **Oncotarget**, 2014.

IIZUKA, N. et al. The nm23-H1 gene as a predictor of sensitivity to chemotherapeutic agents in oesophageal squamous cell carcinoma. **British Journal of Cancer**, v. 81, n. 3, p. 469–475, 1999.

INSTITUTO NACIONAL DO CÂNCER. **PULMÃO**. Disponível em: <http://www2.inca.gov.br/wps/wcm/connect/tiposdecancer/site/home/pulmao/definicao>. Acesso em: 18 dez. 2017.

KILARI, D. Role of copper transporters in platinum resistance. **World Journal of Clinical Oncology**, v. 7, n. 1, p. 106, 2016.

KIM, E.-H. et al. Inhibition of Heat Shock Protein 27-Mediated Resistance to DNA Damaging Agents by a Novel PKC -V5 Heptapeptide. **Cancer Research**, v. 67, n. 13, p. 6333–6341, 2007.

KÖBERLE, B. et al. Cisplatin resistance: Preclinical findings and clinical implications. **Biochimica et Biophysica Acta (BBA) - Reviews on Cancer**, v. 1806, n. 2, p. 172–182, 2010.

KUO, J. et al. Cisplatin-induced regulation of signal transduction pathways and transcription factors in p53-mutated subclone variants of hepatoma cells: Potential

application for therapeutic targeting. **Oncology Letters**, 2016.

LEE, J.-H. et al. Overexpression of human 27 kDa heat shock protein in laryngeal cancer cells confers chemoresistance associated with cell growth delay. **Journal of Cancer Research and Clinical Oncology**, v. 133, n. 1, p. 37–46, 2006.

LENG, X.-F. et al. Combined analysis of mRNA expression of ERCC1, BAG-1, BRCA1, RRM1 and TUBB3 to predict prognosis in patients with non-small cell lung cancer who received adjuvant chemotherapy. **Journal of Experimental & Clinical Cancer Research**, v. 31, n. 1, p. 25, 2012.

LEUNG, A. W. Y. et al. Combined Use of Gene Expression Modeling and siRNA Screening Identifies Genes and Pathways Which Enhance the Activity of Cisplatin When Added at No Effect Levels to Non-Small Cell Lung Cancer Cells In Vitro. **PLOS ONE**, v. 11, n. 3, p. e0150675, 2016.

LI, W. et al. Proteomics Analysis of Normal and Senescent NG108-15 Cells: GRP78 Plays a Negative Role in Cisplatin-Induced Senescence in the NG108-15 Cell Line. **PLoS ONE**, v. 9, n. 3, p. e90114, 2014a.

LI, W. et al. Cisplatin-induced senescence in ovarian cancer cells is mediated by GRP78. **Oncology Reports**, v. 31, n. 6, p. 2525–2534, 2014b.

LI, Z. et al. Predictive value of APE1, BRCA1, ERCC1 and TUBB3 expression in patients with advanced non-small cell lung cancer (NSCLC) receiving first-line platinum–paclitaxel chemotherapy. **Cancer Chemotherapy and Pharmacology**, v. 74, n. 4, p. 777–786, 2014c.

LIU, C.-Y. et al. Vimentin contributes to epithelial-mesenchymal transition cancer cell mechanics by mediating cytoskeletal organization and focal adhesion maturation. **Oncotarget**, v. 6, n. 18, p. 15966–15983, 2015a.

LIU, X. et al. Oncogenes associated with drug resistance in ovarian cancer. **Journal of Cancer Research and Clinical Oncology**, v. 141, n. 3, p. 381–395, 2015b.

LIZUKA, N. et al. Downregulation of intracellular nm23-H1 prevents cisplatin-induced DNA damage in oesophageal cancer cells: possible association with Na(+), K(+)-ATPase. **British journal of cancer**, v. 83, n. 9, p. 1209–15, 2000.

LU, H. et al. HSP27 Knockdown Increases Cytoplasmic p21 and Cisplatin Sensitivity in Ovarian Carcinoma Cells. **Oncology Research Featuring Preclinical and Clinical Cancer Therapeutics**, v. 23, n. 3, p. 119–128, 2016.

MARTIN, L. P.; HAMILTON, T. C.; SCHILDER, R. J. Platinum Resistance: The Role of DNA Repair Pathways. **Clinical Cancer Research**, v. 14, n. 5, p. 1291–1295, 2008.

MCCARROLL, J. A. et al. III-Tubulin Is a Multifunctional Protein Involved in Drug Sensitivity and Tumorigenesis in Non-Small Cell Lung Cancer. **Cancer Research**, v. 70, n. 12, p. 4995–5003, 2010.

MCDERMOTT, M. et al. In vitro Development of Chemotherapy and Targeted Therapy Drug-Resistant Cancer Cell Lines: A Practical Guide with Case Studies. **Frontiers in Oncology**, v. 4, 2014.

MHAIDAT, N. M. et al. GRP78 regulates sensitivity of human colorectal cancer cells to DNA targeting agents. **Cytotechnology**, v. 68, n. 3, p. 459–467, 2016.

NAKAGAWA, T. et al. Expression of copper-transporting P-type adenosine triphosphatase (ATP7B) correlates with cisplatin resistance in human non-small cell lung cancer xenografts. **Oncology Reports**, 1994.

NEJDL, L. et al. Mechanisms of Uptake and Interaction of Platinum Based Drugs in Eukaryotic Cells. In: **Platinum Metals in the Environment**. p. 401–415, 2015.

OISO, S. et al. Factors involved in the cisplatin resistance of KCP-4 human epidermoid carcinoma cells. **Oncology Reports**, v. 31, n. 2, p. 719–726,2014.

OJI, Y. et al. The translation elongation factor eEF2 is a novel tumor-associated antigen overexpressed in various types of cancers. **International Journal of Oncology**, 2014.

PISKAREVA, O. et al. The development of cisplatin resistance in neuroblastoma is accompanied by epithelial to mesenchymal transition in vitro. **Cancer Letters**, v. 364, n. 2, p. 142–155, 2015.

PUJOL, J. L. et al. Tumor-tissue and plasma concentrations of platinum during chemotherapy of non-small-cell lung cancer patients. **Cancer chemotherapy and pharmacology**, v. 27, n. 1, p. 72–5, 1990.

QI, K. et al. Id4 promotes cisplatin resistance in lung cancer through the p38 MAPK pathway. **Anti-cancer drugs**, v. 27, n. 10, p. 970–8, 2016.

Reduced Lung-Cancer Mortality with Low-Dose Computed Tomographic Screening. **New England Journal of Medicine**, v. 365, n. 5, p. 395–409, 2011.

ROSENBERG, B. et al. Platinum compounds: a new class of potent antitumour agents. **Nature**, v. 222, n. 5191, p. 385–6, 1969.

SCHRAMEK, D. et al. Direct in Vivo RNAi Screen Unveils Myosin IIa as a Tumor Suppressor of Squamous Cell Carcinomas. **Science**, v. 343, n. 6168, p. 309–313, 2014.

SEVE, P. Expression of Class III -Tubulin Is Predictive of Patient Outcome in Patients with Non-Small Cell Lung Cancer Receiving Vinorelbine-Based Chemotherapy. **Clinical Cancer Research**, v. 11, n. 15, p. 5481–5486, 2005.

SIDDIK, Z. H. Cisplatin: mode of cytotoxic action and molecular basis of resistance. **Oncogene**, v. 22, n. 47, p. 7265–7279, 2003.

SISTEMA ÚNICO DE SAÚDE. **Controle do Tabagismo**. Disponível em: <http://portalarquivos2.saude.gov.br/images/pdf/2015/maio/28/apresentacao-tabaco.pdf>. Acesso em: 18 dez. 2017.

STEWART, D. et al. Human tissue distribution of platinum after cis-diamminedichloroplatinum. **Cancer Chemotherapy and Pharmacology**, v. 10, n. 1, 1982.

STORR, S. J. et al. Calpain-2 expression is associated with response to platinum based chemotherapy, progression-free and overall survival in ovarian cancer. **Journal of Cellular and Molecular Medicine**, v. 16, n. 10, p. 2422–2428, 2012.

SUN, H.-G. et al. Clinical Value of Eukaryotic Elongation Factor 2 (eEF2) in Non-small Cell Lung Cancer Patients. **Asian Pacific Journal of Cancer Prevention**, v. 14, n. 11, p. 6533–6535, 2013.

TANG, S. et al. Identification Keratin 1 as a cDDP-resistant protein in nasopharyngeal carcinoma cell lines. **Journal of Proteomics**, v. 75, n. 8, p. 2352–2360, 2012.

TIAN, H. et al. High expression of AKR1C1 is associated with proliferation and migration of small-cell lung cancer cells. **Lung Cancer: Targets and Therapy**, p. 53, 2016.

TORRE, L. A. et al. Global cancer statistics, 2012. **CA: A Cancer Journal for Clinicians**, v. 65, n. 2, p. 87–108, 2015.

TRIVEDI, R. et al. The antioxidant protein PARK7 plays an important role in cell resistance to Cisplatin-induced apoptosis in case of clear cell renal cell carcinoma. **European Journal of Pharmacology**, v. 784, p. 99–110, 2016.

WANG, C. et al. Macrophage migration inhibitory factor promotes osteosarcoma growth and lung metastasis through activating the RAS/MAPK pathway. **Cancer Letters**, v. 403, p. 271–279, 2017a.

WANG, H. et al. 3-O-(Z)-coumaroyloleanolic acid overcomes Cks1b -induced chemoresistance in lung cancer by inhibiting Hsp90 and MEK pathways. **Biochemical Pharmacology**, v. 135, p. 35–49, 2017b.

WANG, Y.-F. et al. NM23-H1 expression of head and neck squamous cell carcinoma in association with the response to cisplatin treatment. **Oncotarget**, v. 5, n. 17, p. 7392–7405, 2014.

WEN, J. et al. Comparative proteomic analysis of the esophageal squamous carcinoma cell line EC109 and its multi-drug resistant subline EC109/CDDP. **International Journal of Oncology**, v. 36, n. 1, 2009.

WENG, S.-H. et al. Inhibition of thymidine phosphorylase expression by using an HSP90 inhibitor potentiates the cytotoxic effect of cisplatin in non-small-cell lung cancer cells. **Biochemical Pharmacology**, v. 84, n. 1, p. 126–136, 2012.

XIONG, Y.; HUANG, B.-Y.; YIN, J.-Y. Pharmacogenomics of platinum-based chemotherapy in non-small cell lung cancer: focusing on DNA repair systems. **Medical Oncology**, v. 34, n. 4, p. 48, 2017.

ZENG, H.-Z. et al. Proteomic Analysis Identified DJ-1 as a Cisplatin Resistant Marker in Non-Small Cell Lung Cancer. **International Journal of Molecular Sciences**, v. 12, n. 12, p. 3489–3499, 2011.

ZHANG, H. et al. miR-181c contributes to cisplatin resistance in non-small cell lung cancer cells by targeting Wnt inhibition factor 1. **Cancer Chemotherapy and Pharmacology**, 2017.

CURRICULUM VITÆ resumido

MARTELLO, C. L.; MARTELLO, CAROLINA LUMERTZ; MARTELLO, CAROLINA

1. DADOS PESSOAIS

Nome:

Carolina Lumertz Martello

Local e data de nascimento:

Porto Alegre, Rio Grande do Sul, Brasil, 12/10/1990

Endereço profissional:

Universidade Federal do Rio Grande do Sul, Centro de Biotecnologia

Avenida Bento Gonçalves, 9500 Prédio 43421 salas 206/204

91501-970, Porto Alegre, RS, Brasil

Telefone profissional:

(051) 33086070

E-mail:

carolinamartello1@gmail.com

2. FORMAÇÃO:

2015 - Atual

Mestrado em Biologia Celular e Molecular

Universidade Federal do Rio Grande do Sul, UFRGS, Porto Alegre, Brasil

Orientador: Dra. Karina Mariante Monteiro

Bolsista do: Conselho Nacional de Desenvolvimento Científico e Tecnológico

2010 – 2014

Graduação em Biotecnologia Molecular

Universidade Federal do Rio Grande do Sul, UFRGS, Porto Alegre, Brasil

3. ESTÁGIOS:

2014 – 2014

Estágio Curricular

Enquadramento Funcional: Estagiário

Carga horária: 20 h

Instituição: Laboratório de Genética Molecular (Hospital de Clínicas de Porto Alegre)

Surpervisor: Dra. Maria Luiza Saraiva Pereira

Resumo das atividades desenvolvidas:

- Diagnóstico de doenças.
- Cultivo celular de linhagem primária de pacientes.
- Sequenciamento de ácidos nucleicos.
- Análise de fragmentos por PCR Multiplex e TP-PCR.
- Discriminação alélica por PCR em tempo real.

2013 - 2014

Bolsista

Enquadramento Funcional: Estagiário - Iniciação Tecnológica

Carga horária: 20 h

Instituição: Laboratório de Genômica Estrutural e Funcional (Centro de Biotecnologia/UFRGS)

Orientador: Dr. Henrique Bunselmeyer Ferreira

Resumo das atividades desenvolvidas:

- Extração de ácidos nucleicos e técnica de PCR.
- Clonagem molecular e transformação bacteriana.
- Expressão e purificação de proteína recombinante.
- Imunização animal em camundongos e ensaio imunológico ELISA.

2012 – 2013

Graduando

Enquadramento Funcional: Estagiário – Iniciação Científica Voluntária

Carga horária: 20 h

Instituição: Laboratório de Genômica Estrutural e Funcional (Centro de Biotecnologia/UFRGS)

Orientador: Dr. Henrique Bunselmeyer Ferreira

Resumo das atividades desenvolvidas:

- Extração de ácidos nucleicos e técnica de PCR.
- Clonagem molecular e transformação bacteriana.
- Expressão e purificação de proteína recombinante.

2010 – 2011

Bolsista

Enquadramento Funcional: Estagiário – Iniciação Científica

Carga horária: 20 h

Instituição: Laboratório de Fisiologia Vegetal (Departamento de Botânica/UFRGS)

Orientador: Dra. Janette Palma Fett

Resumo das atividades desenvolvidas:

- Crescimento vegetal.
- Extração de ácidos nucleicos, clonagem celular e transformação bacteriana.

4. ARTIGOS COMPLETOS PUBLICADOS

4.1. Leal, Fernanda Munhoz dos Anjos; Virginio, Veridiana Gomes; **Martello, Carolina Lumertz**; Paes, Jéssica Andrade; Borges, Thiago J.; Jaeger, Natália; Bonorino, Cristina; Ferreira, Henrique Bunselmeyer. *Mycoplasma hyopneumoniae* and *Mycoplasma flocculare* differential domains from orthologous surface proteins induce distinct cellular immune responses in mice. Veterinary microbiology (Amsterdam. Print), V. 190, P. 50-57, 2016.

4.2. Reolon, Luciano Antonio; **Martello, Carolina Lumertz**; Schrank, Irene Silveira; Ferreira, Henrique Bunselmeyer. Survey of surface proteins from the pathogenic *Mycoplasma hyopneumoniae* strain 7448 using a biotin cell surface labeling approach. Plos One, V. 9, P. E112596, 2014.

4.3. **Martello, Carolina**; Leal, Fernanda; Virginio, Veridiana; Reolon, Luciano; Schrank, Irene; Zaha, Arnaldo; Ferreira, Henrique. Orthologous surface proteins from *Mycoplasma hyopneumoniae* and *Mycoplasma flocculare*: in silico comparison and heterologous expression of differential extracellular domains. Bmc Proceedings, V. 8, P. P157, 2014.

5. RESUMOS E TRABALHOS APRESENTADOS EM CONGRESSOS

5.1. **Martello, C. L.**; Dutra, C. S.; Cadore, N. A.; Silveira, H. B.; Monteiro, K. M. Nuclear and perinuclear proteome analysis of cisplatin-sensitive and -resistant human lung adenocarcinoma cells. 2015. (Apresentação de trabalho/Outra).

5.2. Dutra, C. S.; **Martello, C. L.**; Silveira, H. B.; Cadore, N. A.; Monteiro, K. M. Identification of newly synthesized proteins in human lung adenocarcinoma cells exposed to cisplatin. 2015. (Apresentação de trabalho/Outra).

5.3. **Martello, C. L.**; Leal, F. M. A.; Ferreira, H. B. Immunological evaluation in mice of a *Mycoplasma hyopneumoniae* recombinant protein produced in LPS producing and LPS-free *Escherichia coli* strains. 2014. (Apresentação de trabalho/Congresso).

5.4. Leal, F. M. A.; **Martello, C. L.**; Virginio, V. G.; Reolon, L. A.; Schranck, I. S.; Ferreira, H. B. Expression of differential extracellular domains of orthologous surface proteins from *Mycoplasma hyopneumoniae* and *Mycoplasma flocculare*. 2014. (Apresentação de trabalho/Congresso).

5.5. **Martello, C. L.**; Virginio, V. G.; Paes, J. A.; Zaha, A.; Ferreira, H. B. Antígenos recombinantes de *Mycoplasma hyopneumoniae* para formulações de vacinas contra a pneumonia enzoótica suína. 2014. (Apresentação de Trabalho/Outra).

5.6. Leal, F. M. A.; **Martello, C. L.**; Virginio, V. G.; Reolon, L. A.; Schranck, I. S.; Zaha, A.; Ferreira, H. B. *In silico* analyses of ortholog surface proteins from *Mycoplasma hyopneumoniae* and *Mycoplasma flocculare*. 2013. (Apresentação de trabalho/Congresso).

5.7. Paes, J. A.; Virginio, V. G.; **Martello, C. L.**; Bonotto, R. M.; Zaha, A.; Ferreira, H. B. Antígenos recombinantes de *Mycoplasma hyopneumoniae* para a formulação de vacinas baseadas em construções de DNA contra a pneumonia enzoótica suína. 2013. (Apresentação De Trabalho/Outra).

5.8. Bonotto, R. M.; Virginio, V. G.; Paes, J. A.; **Martello, C. L.**; Zaha, A.; Ferreira, H. B. Caracterização de proteínas recombinantes de *Mycoplasma hyopneumoniae* para a formulação de vacinas contra a pneumonia enzoótica suína. 2013. (Apresentação De Trabalho/Outra).

5.9. **Martello, C. L.**; Paloma K. Menguer; Felipe K. Ricachenevsky; Karina L. Lopes; Janette P. Fett. Análises sobre a família gênica VIT em plantas e caracterização dos genes OsVIT1 e OsVIT2 por meio de transformação de levedura. 2012. (Apresentação De Trabalho/Outra).

5.10. **Martello, C. L.**; Paloma K. Menguer; Felipe K. Ricachenevsky; Karina L. Lopes; Janette P. Fett. Análises sobre a família gênica VIT em plantas e caracterização dos genes OsVIT1 e OsVIT2 por meio de transformação de levedura. 2011. (Apresentação De Trabalho/Outra).